TECHNOVATORS

QUASI-ISOTROPIC VHF ANTENNA ARRAY DESIGN STUDY FOR THE INTERNATIONAL ULTRAVIOLET EXPLORER SATELLITE

Jeremy K. Raines, Ph.D., P.E.
Technovators
805 Langley Drive
Silver Spring, Maryland 20901

18 July 1975
Final Report

Prepared for
Goddard Space Flight Center
Greenbelt, Maryland 20771

TECHNICAL REPORT STANDARD TITLE PAGE

1. Report No.	2. Government Accession No.	3. Recipient's Catalog No.
Final		

4. Title and Subtitle	5. Report Date
QUASI-ISOTROPIC VHF ANTENNA ARRAY DESIGN STUDY FOR THE INTERNATIONAL ULTRAVIOLET EXPLORER SATELLITE	18 July 1975
	6. Performing Organization Code

7. Author(s)	8. Performing Organization Report No.
Jeremy K. Raines	7.18.75

9. Performing Organization Name and Address	10. Work Unit No.
Technovators 805 Langley Drive Silver Spring, Maryland 20901	
	11. Contract or Grant No. NAS5-22364
	13. Type of Report and Period Covered: Final

12. Sponsoring Agency Name and Address	14. Sponsoring Agency Code
C. Vanek, Code 724.1 Goddard Space Flight Center Greenbelt, Maryland 20771	

15. Supplementary Notes

16. Abstract

This report describes progress resulting from a 13-week study to design a quasi-isotropic VHF antenna array for the IUE satellite. Significant progress was made in two categories. First, a free space configuration was obtained that has no nulls deeper than -6.4 dbi in each of two orthogonal polarizations. Second, much work has been completed on a computer program named SOAP that analyzes the electromagnetic interaction between antennas and complicated conducting bodies, such as satellites.

17. Key Words Suggested by Author	18. Distribution Statement
Isotropic antennas Computer aided antenna analysis VHF antenna arrays Satellite antennas Electromagnetic field analysis	

19. Security Classif. (of this report)	20. Security Classif. (of this page)	21. No. of Pages	22. Price
Unclassified	Unclassified	106	

Preface

This report describes progress in the analysis and design of quasi-isotropic antennas on satellites. This progress results from a specific, 13-week task, to design a VHF array for the International Ultraviolet Explorer (IUE) satellite.

The initial design proposed is a combination of radial electric and magnetic dipoles. In free space, this array has no nulls deeper than -6.4 db with respect to an isotropic radiator. This condition obtains for both E_θ and E_ϕ field components separately. It also obtains for the frequencies 148.98 MHz and 136.86 MHz separately.

The design has at least two significant advantages. First, the arrangement of the array elements is compatible with the structure of the IUE satellite. Second, the magnetic and electric dipoles tend to be independent controls over the E_θ and E_ϕ field components, respectively, especially at points in or near the horizontal plane ($\theta = 90°$). This feature allows flexibility in adjusting the array.

The initial design may be modified to compensate for interference from the satellite structure. To this end, much original work has been completed on a computer program named SOAP (Satellite Omnipurpose Antenna Program.) SOAP is an interactive computer program that allows the user to simulate virtually any metallic structure with a combination of cylinders, plates, and wires, by means of relatively simple commands. Similarly, he may position magnetic and electric dipole sources anywhere about the structure, and with any orientation. SOAP then computes the resultant electromagnetic field. Due to a novel hybrid approach, SOAP promises to be faster, easier to use, and more versatile than previous attempts at such a program.

SOAP is now producing preliminary results. The present contract ended before SOAP could be completed, however, and therefore the preliminary results are not conclusive. Many novel algorithms have already been implemented, and there appear to be no theoretical obstacles to implementing the remaining ones. It is recommended that this be done.

It is also recommended that the proposed design be modelled, tested, and modified experimentally. This should be done in conjunction with continued analytic investigationsusing SOAP.

Table of Contents

List of Symbols

E = electric field, volts/meter

F = either electric or magnetic field

H = magnetic field, amps/meter

k = wave number = 2π/(wave length)

p_e = electric dipole moment, amp-meters

p_m = magnetic dipole moment, volt-meters

ϵ = permittivity of free space = 8.854185×10^{-12} farads/meter

η = impedance of free space = 376.7304 ohms

μ = permeability of free space = $4\pi \times 10^{-7}$ henrys/meter

ω = radian frequency = 2π x frequency

1. Introduction.

This report describes the results of a 13-week study to design a quasi-isotropic VHF antenna array for the International Ultraviolet Explorer (IUE) satellite.

The objective was to synthesize a radiation pattern with no nulls deeper than -10 db with respect to an isotropic radiator. This was to obtain for each of two orthogonal polarizations of the electromagnetic field. It was also to obtain for each of two frequencies, 148.93 MHz and 136.86 MHz. Finally, it was to obtain when the solar panels were folded against the main body of the satellite, and when the panels were extended. Toward this design objective, significant progress was made in two categories.

First, a fundamental configuration has been derived for quasi-isotropic radiation in each of the two orthogonal field components E_θ and E_ϕ. The array is described in detail in Section 4, including plots of the radiation pattern. To be brief, it is a ring of radial electric and magnetic dipoles, appropriately phased. The diameter of the ring is one-half wave length at the highest frequency. The array is broad band and radiates a quasi-isotropic pattern at all lower frequencies as well. The ring geometry is well suited for positioning the array about a central mast or cylinder. Because the elements of the array are radially-directed, interaction with the mast is minimized. It is possible that this design achieves the objective. The reasons are discussed in Section 7.

Second, much work has been completed on a computer program that analyzes the interaction between antennas and complicated conducting bodies, such as satellites, aircraft, and ships. The program is named SOAP (Satellite Omnipurpose Antenna Program). The electromagnetic principles upon which SOAP is based are formulated in Section 3. The way in which the IUE satellite structure is modelled for analysis by SOAP is described in Section 5. A brief description of how to use SOAP is the subject of Section 6. Finally, some preliminary results of using SOAP, in the form of radiation patterns, are collected in the Appendix.

Though much original work has been completed, some work still remains in the development of SOAP. One recommendation of this report is that this work be continued. SOAP promises to be a very powerful and useful design tool for communications problems on satellites, aircraft, ships, and other complicated structures.

2. Survey of Previous Efforts.

2.1. The Realizability of Isotropic Radiators.

The published limitations on realizable isotropic radiators are few and not overly restrictive. For an antenna at the origin of a spherical coordinate system, Mathis submitted a proof that it is impossible to produce a radiation pattern depending only upon the distance from the origin [12, 13]. Either the direction and/or the magnitude of the field must fluctuate with the angular coordinates (θ and ϕ). Mathis did not estimate how small this fluctuation could be, however.

Over ten years later, Woodward investigated the patterns produced by radiators distributed about a ring of vanishingly small radius [15]. Rings of tangentially-directed and longitudinally-directed dipoles were superimposed, and the resultant pattern considered in detail. That pattern was described by the following formulas:

$$F_\theta = j\left[\sqrt{1.875 P_A}\,\sin^2\theta \pm \sqrt{0.75(1-P_A)}\,\cos\theta\, e^{j\beta}\right] \tag{2.1}$$

$$F_\varphi = \sqrt{0.75(1-P_A)}\, e^{j\beta} \tag{2.2}$$

where: P_A = fraction of the total power radiated by the longitudinally-directed elements.

β = phase difference between the current in the two rings.

In each ring, the current is assumed to vary according to $e^{\pm j\varphi}$.

Woodward evaluated these formulas for many combinations of P_A and β, and displayed the results in graphical form. In many cases, the fluctuation of either field component was within only several decibels of a constant. In addition, he showed that for $P_A = 0.27$ and $\beta = 90^\circ$, the radiated power density, $|F_\theta|^2 + |F_\phi|^2$, was within 0.6 decibel of a constant.

Though the results of Woodward are reassuring, they are derived from an abstract situation. That is, the distribution of dipoles about the ring is continuous (an infinite number of dipoles) and the ring is vanishingly small. It is not clear how the results must be modified to include a limited number of elements arranged about a ring comparable in radius to a wave length.

In addition, Woodward did not distinguish between electric and magnetic dipoles. The elements in his arrays were either one or the other, but not both.

This report will describe a quasi-isotropic array consisting of a finite number of elements arranged about a ring approximately one-half wave length in diameter. Some of the elements are electric dipoles, and some are magnetic.

2.2. Radiation from Antennas on Satellites.

When an antenna or array is mounted on an irregularly-shaped platform, such as a satellite, the radiation pattern is distorted from what it had been when the array was in free space. Predicting this distortion is a problem of current research, and there are many rival approaches. A representative survey is attempted in this section.

Formulas in terms of well known functions have been obtained in a number of simple or special cases. In 1943, Carter published formulas for the radiation patterns of elemental dipoles near a cylinder [3] . The cylinder was perfectly conducting and infinitely long. In 1951, Lucke extended the results of Carter to include elliptical as well as circular cylinders [11]. In 1970, Kravtsova considered the curious case of elemental dipoles near two intersecting cylinders [9] .

Geometries that were less manageable analytically, nonetheless yielded formulas that, while approximate, were as accurate as experimental measurements. In 1958, Knight treated the radiation pattern of dipoles near a mast of triangular cross section [16] . His procedure was as follows. If radiation from the dipole is incident, without obstruction, at a point on the mast, then the current induced there is approximated by:

$$\vec{J}_s = 2\hat{n} \times \vec{H}^i \qquad (2.3)$$

where: $\vec{J}_s$ = induced surface current density.

$\hat{n}$ = outward normal from the mast.

$\vec{H}^i$ = incident magnetic field.

This induced current contributes to the net radiation pattern by means of the well known retarded potentials from electromagnetic theory. If radiation from the dipole is not incident without obstruction (i.e. part of the mast blocks the straight-line path between the source and the point of observation), then the diffraction formulas due to Schelkunoff may be used [19] .

Like his predecessors, Knight limited himself to masts that were infinite in length.

With the advent of high-speed computers, numerical techniques were investigated for treating more complicated geometries. In one popular approach, the structure is replaced, for computational purposes, by a cage, mesh, or grid of wires. Hence, the name "wire grid model". The wire grid structure is analyzed rigorously by solving a lengthy integro-differential equation for the current on every filament of wire. The current is then used to calculate the radiation pattern by means of well known retarded potential functions from electromagnetic theory. This procedure was applied to some satellite structures by Albertsen et al [1, 2].

The wire grid model has severe limitations, both practical and theoretical. From a practical point of view, structures of even modest complexity exhaust the storage of even the most modern computers. This is because there are so many wire filaments, and the currents on all must be resolved simultaneously. This leads to operations on matrices with orders of several hundreds. These large matrices not only tax the storage capacity of computers, but they ultimately destroy all accuracy. This is because the precision of the matrix elements rapidly becomes inadequate for numerical operations, such as matrix inversion. Needless to say, while this approach may be marginally useful for analysis, it will not likely result in a fast, interactive program suitable for design tasks.

The mathematical exactness and complexity of the wire grid model might be warranted, if the physical foundations were as rigorous. Unfortunately, this is not the case, and there are unresolved weaknesses and contradictions. Some of these were investigated by Forgan [5]. He reports that the diameter of the wire used in the model may significantly affect the results. Yet there is no rational basis for selecting one diameter over another. Also, in the wire grid model of a closed conducting surface, there is no assurance that the field inside will vanish, as it must in actual fact. For example, the wire grid approach cannot distinguish between a spherical radiator and a spherical resonant cavity.

The many wire filaments and the associated high-order matrices of the wire grid model are avoided in an approach discussed by Kouyoumijian [18] and by Albertsen et al [1]. It is called the geometric theory of diffraction (GTD). By this method, the well known formulas describing reflection and diffraction at optical frequencies are extended to the electromagnetic field at lower frequencies by adding high-order terms. This has been successful when structures are large compared to a wave length and not in the near field of the radiation sources.

These requirements exclude many practical situations, including satellites with VHF antennas.

The approach developed here draws from the work of Knight to account for reflection from surfaces and diffraction by edges. New types of calculations will be added, such as reradiation by parasitic wires. Also, magnetic dipole sources are treated as well as electric ones. Thus, all anticipated electromagnetic phenomena are considered. The high speed computer is utilized, so that a great variety of shapes and sizes may be modelled, using combinations of finite cylinders and finite ribbons (i.e. rectangular plates). At the same time, since the cumbersome wire grid model is not used, the computer responds quickly, facilitating an interactive program well suited to design tasks.

3. Formulation of the Present Approach.

3.1. Fundamental Radiating Elements.

There are six fundamental types of electromagnetic sources with which to synthesize a radiation pattern. Three are electric dipoles in the x, y, and z directions. The remaining three are magnetic dipoles in the x, y, and z directions. In practice, electric dipoles may be realized by exciting current along a straight wire which is parallel to the desired direction. Magnetic dipoles may be realized by exciting current on a circular loop of wire which is normal to the desired direction.

The strength of a radiation source is proportional to its dipole moment. The electric dipole moment of a short, straight wire is given by the formula:

$$p_e = I\ell \text{ amp-meters} \qquad (3.1)$$

where: I = current on the wire

ℓ = length of the wire

The magnetic dipole moment of a small circular wire loop is given by the formula:

$$p_m = j\omega\mu IA \text{ volt-meters} \qquad (3.2)$$

where: I = current on the wire

A = area of the loop

The formulas for the electromagnetic field radiated by each of the six types of sources are not commonly found in the literature. Usually, only those for the z-directed electric dipole are given. Also, they are usually written in terms of a spherical coordinate system with the dipole at the origin.

In the following subsections, explicit formulas will be presented for the electromagnetic field of each of the six fundamental sources. They will be expressed in rectangular coordinates. These are the most convenient for computational purposes. If it is desired to convert the rectangular field components (F_x , F_y , F_z) to spherical ones (F_r , F_θ , F_ϕ), the following formulas may be used:

$$F_r = F_z \cos\theta + \left(F_x \cos\phi + F_y \sin\phi \right) \sin\theta$$

$$F_\theta = \left(F_x \cos\phi + F_y \sin\phi \right) \cos\theta - F_z \sin\theta$$

$$F_\phi = F_y \cos\phi - F_x \sin\phi \qquad (3.3)$$

where: F = either electric field E or magnetic field H.

3.1.1. Elementary Electric Dipoles.

The formulas for the field of the z-directed electric dipole are obtained in a straight-forward, if tedious, manner. If the well known results published in spherical coordinates are converted to rectangular ones, there results:

$$E_x = \frac{Pez}{4\pi r} e^{-jkr} \left(\frac{zx}{r^2}\right)\left(j\omega\mu + \frac{3\eta}{r} - \frac{j3}{\omega\epsilon r^2}\right)$$

$$E_y = \frac{Pez}{4\pi r} e^{-jkr} \left(\frac{zy}{r^2}\right)\left(j\omega\mu + \frac{3\eta}{r} - \frac{j3}{\omega\epsilon r^2}\right)$$

$$E_z = \frac{Pez}{4\pi r} e^{-jkr} \left[2\left(\frac{z}{r}\right)^2\left(\frac{\eta}{r} - \frac{j}{\omega\epsilon r^2}\right)\right.$$

$$\left. - \left(\frac{x^2+y^2}{r^2}\right)\left(j\omega\mu + \frac{\eta}{r} - \frac{j}{\omega\epsilon r^2}\right)\right]$$

$$H_x = -\frac{Pez}{4\pi r} e^{-jkr} \left(\frac{y}{r}\right)\left(jk + \frac{1}{r}\right)$$

$$H_y = \frac{Pez}{4\pi r} e^{-jkr} \left(\frac{x}{r}\right)\left(jk + \frac{1}{r}\right)$$

$$H_z = 0 \qquad (3.4)$$

The formulas for the field of the x-directed electric dipole are quickly obtained by a cyclical transformation of the coordinates (x, y, z) according to the following rules:

$$x \longrightarrow -z$$

$$y \longrightarrow y$$

$$z \longrightarrow x$$

Thus obtain:

$$E_x = \frac{P_{ex}}{4\pi r} e^{-jkr}\left[2\left(\frac{x}{r}\right)^2\left(\frac{\eta}{r} - \frac{j}{\omega\epsilon r^2}\right) - \left(\frac{z^2+y^2}{r^2}\right)\left(j\omega\mu + \frac{\eta}{r} - \frac{j}{\omega\epsilon r^2}\right)\right]$$

$$E_y = \frac{P_{ex}}{4\pi r} e^{-jkr}\left(\frac{xy}{r^2}\right)\left(j\omega\mu + \frac{3\eta}{r} - \frac{j3}{\omega\epsilon r^2}\right)$$

$$E_z = \frac{P_{ex}}{4\pi r} e^{-jkr}\left(\frac{xz}{r^2}\right)\left(j\omega\mu + \frac{3\eta}{r} - \frac{j3}{\omega\epsilon r^2}\right)$$

$$H_x = 0$$

$$H_y = -\frac{P_{ex}}{4\pi r} e^{-jkr}\left(\frac{z}{r}\right)\left(jk + \frac{1}{r}\right)$$

$$H_z = \frac{P_{ex}}{4\pi r} e^{-jkr}\left(\frac{y}{r}\right)\left(jk + \frac{1}{r}\right) \qquad (3.5)$$

The transformations for obtaining the field of the y-directed electric dipole from the z-directed one are:

$$x \longrightarrow x$$

$$y \longrightarrow -z$$

$$z \longrightarrow y$$

Thus obtain:

$$E_x = \frac{P_{ey}}{4\pi r} e^{-jkr} \left(\frac{yx}{r^2}\right)\left(j\omega\mu + \frac{3\eta}{r} - \frac{3}{j\omega\epsilon r^2}\right)$$

$$E_y = \frac{P_{ey}}{4\pi r} e^{-jkr} \left[2\left(\frac{y}{r}\right)^2\left(\frac{1}{r} - \frac{j}{\omega\epsilon r^2}\right) - \left(\frac{x^2+z^2}{r^2}\right)\left(j\omega\mu + \frac{\eta}{r} - \frac{j}{\omega\epsilon r^2}\right)\right]$$

$$E_z = \frac{P_{ey}}{4\pi r} e^{-jkr} \left(\frac{yz}{r^2}\right)\left(j\omega\mu + \frac{3\eta}{r} - \frac{3}{j\omega\epsilon r^2}\right)$$

$$H_x = \frac{P_{ey}}{4\pi r} e^{-jkr} \left(\frac{z}{r}\right)\left(jk + \frac{1}{r}\right)$$

$$H_y = 0$$

$$H_z = -\frac{P_{ey}}{4\pi r} e^{-jkr} \left(\frac{x}{r}\right)\left(jk + \frac{1}{r}\right) \quad (3.6)$$

3.1.2. Elementary Magnetic Dipoles.

The formulas for the fields of the magnetic dipoles are quickly obtained by applying the duality transformations to the formulas for electric dipoles. Those transformations are:

$$p_e \rightarrow p_m$$
$$E \rightarrow H$$
$$H \rightarrow -E$$
$$\epsilon \rightarrow \mu$$
$$\mu \rightarrow \epsilon$$
$$\eta \rightarrow \frac{1}{\eta}$$

Thus obtain, for the z-directed magnetic dipole:

$$E_x = \frac{p_{mz}}{4\pi r} e^{-jkr} \left(\frac{y}{r}\right)\left(jk + \frac{1}{r}\right)$$

$$E_y = -\frac{p_{mz}}{4\pi r} e^{-jkr} \left(\frac{x}{r}\right)\left(jk + \frac{1}{r}\right)$$

$$E_z = 0 \qquad (3.7)$$

$$H_x = \frac{p_{mz}}{4\pi r} e^{-jkr} \left(\frac{zx}{r^2}\right)\left(j\omega\epsilon + \frac{3}{\eta r} - \frac{j3}{\omega\mu r^2}\right)$$

$$H_y = \frac{p_{mz}}{4\pi r} e^{-jkr} \left(\frac{zy}{r^2}\right)\left(j\omega\epsilon + \frac{3}{\eta r} - \frac{j3}{\omega\mu r^2}\right)$$

$$H_z = \frac{p_{mz}}{4\pi r} e^{-jkr} \left[2\left(\frac{z}{r}\right)^2\left(\frac{2}{\eta r} - \frac{j2}{\omega\mu r^2}\right) - \left(\frac{x^2+y^2}{r^2}\right)\left(j\omega\epsilon + \frac{1}{\eta r} - \frac{j}{\omega\mu r^2}\right)\right]$$

For the x-directed magnetic dipole:

$$E_x = 0$$

$$E_y = \frac{P_{mx}}{4\pi r} e^{-jkr} \left(\frac{z}{r}\right)\left(jk + \frac{1}{r}\right)$$

$$E_z = \frac{-P_{mx}}{4\pi r} e^{-jkr} \left(\frac{y}{r}\right)\left(jk + \frac{1}{r}\right) \qquad (3.8)$$

$$H_x = \frac{P_{mx}}{4\pi r} e^{-jkr} \left[2\left(\frac{x}{r}\right)^2 \left(\frac{1}{\eta r} - \frac{j}{\omega \mu r^2}\right) - \left(\frac{z^2+y^2}{r^2}\right)\left(j\omega\epsilon + \frac{1}{\eta r} - \frac{j}{\omega \mu r^2}\right)\right]$$

$$H_y = \frac{P_{mx}}{4\pi r} e^{-jkr} \left(\frac{xy}{r^2}\right)\left(j\omega\epsilon + \frac{3}{\eta r} - \frac{j3}{\omega \mu r^2}\right)$$

$$H_z = \frac{P_{mx}}{4\pi r} e^{-jkr} \left(\frac{xz}{r^2}\right)\left(j\omega\epsilon + \frac{3}{\eta r} - \frac{j3}{\omega \mu r^2}\right)$$

For the y-directed magnetic dipole:

$$E_x = \frac{-P_{my}}{4\pi r} e^{-jkr} \left(\frac{z}{r}\right)\left(jk + \frac{1}{r}\right)$$

$$E_y = 0$$

$$E_z = \frac{P_{my}}{4\pi r} e^{-jkr} \left(\frac{x}{r}\right)\left(jk + \frac{1}{r}\right) \qquad (3.9)$$

$$H_x = \frac{P_{my}}{4\pi r} e^{-jkr} \left(\frac{yx}{r^2}\right)\left(j\omega\epsilon + \frac{3}{\eta r} - \frac{j3}{\omega\mu r^2}\right)$$

$$H_y = \frac{P_{my}}{4\pi r} e^{-jkr} \left[2\left(\frac{x}{r}\right)^2\left(\frac{1}{\eta r} - \frac{j}{\omega\mu r^2}\right) - \left(\frac{x^2+z^2}{r^2}\right)\left(j\omega\epsilon + \frac{1}{\eta r} - \frac{j}{\omega\mu r^2}\right)\right]$$

$$H_z = \frac{P_{my}}{4\pi r} e^{-jkr} \left(\frac{yz}{r^2}\right)\left(j\omega\epsilon + \frac{3}{\eta r} - \frac{j3}{\omega\mu r^2}\right)$$

At great distances, the electric field radiated by a magnetic dipole is of the form:

$$E = \frac{jkp_m}{4\pi r} e^{-jkr} f(\theta, \phi)$$

In contrast, the electric field radiated by an electric dipole is of the form:

$$E = \frac{j\omega\mu p_e}{4\pi r} e^{-jkr} f(\theta, \phi)$$

It is evident that to produce electric fields of comparable magnitude, a magnetic dipole moment must be η times stronger, numerically, than an electric dipole moment.

3.2. Fundamental Interference Phenomena.

If any of the six fundamental radiators are located near a conducting body, surface, or wire, then the formulas of sections 3.1.1. and 3.1.2., while necessary, are not sufficient to describe the electromagnetic field. Additional formulas and algorithms are needed. These account for the four fundamental interference phenomena: shielding by surfaces, reflection by surfaces, diffraction by edges, and reradiation by parasitic wires.

3.2.1. Shielding by Surfaces.

Shielding, or blocking, by a surface may be described entirely in geometric terms. To be brief, if a body or surface obstructs the straight-line path between a source and the point of observation, then that point is shielded from that source by that body or surface. If shielding occurs between a fundamental source and a point of interest, then there is no contribution to the electromagnetic field from the formulas of subsections 3.1.1. or 3.1.2.

Whether or not shielding occurs is determined by specialized formulas that depend upon the size, shape, orientation, and location of the conductor. There are too many such formulas, and they are too complicated to make listing them here worthwhile.

The computer program SOAP, being developed as part of this contract, includes such formulas for finite cylinders, and for rectangular plates. These bodies may be of arbitrary size, shape, orientation, and location. Furthermore, the cylinders and plates may be combined arbitrarily to construct a variety

of additional geometries. These were sufficient to describe the IUE satellite. For other satellites and other structures, SOAP can be expanded to account for other fundamental shapes, such as spheres and triangles.

3.2.2. Reflection by Surfaces.

If a point on the surface of a conductor is not shielded from a fundamental source, then that source excites an electric surface current density at that point. Following the work of Knight [16], the formula for the surface current density is:

$$\vec{J}_s = 2\hat{n} \times \vec{H} \qquad (3.10)$$

where: $\hat{n}$ = outward normal from the surface.

$\vec{H}$ = magnetic field radiated by the fundamental source according the formulas in subsections 3.1.1. and 3.1.2.

These surface current densities in turn determine new elementary electric dipoles according to the formula:

$$\vec{p}_e = A\vec{J}_s \qquad (3.11)$$

where: A = area of the region enclosing the point of observation.

To ensure accuracy of this last formula, the surface of a conductor must be divided into non-overlapping regions of area A, each much smaller than a square wave length.

The new elementary electric dipoles contribute to the electromagnetic field according to the formulas in subsections 3.1.1. and 3.1.2. This contribution is called the reflected field. It is subject to the other fundamental interference phenomena, such as shielding.

The computer program SOAP evaluates the surface current densities, the resulting electric dipole moments, and the reflected field, taking into account the effect of shielding.

3.2.3. Diffraction by Edges.

If a point of observation is shielded from a source, the contribution to the electromagnetic field from that source may still be significant. This is due to the phenomena of diffraction by which electromagnetic waves may propagate around wedges and behind cylinders.

The formulas describing this phenomena are relatively complicated, but they are available in scattered literature. Unfortunately, the present contract ended before diffraction phenomena could be programmed into SOAP. There is no reason why this cannot be done, however.

3.2.4. Reradiation by Parasitic Wires.

If all but one of the dimensions of a surface are very small compared to a wave length, then that surface may nonetheless give rise to a significant reflected field. This phenomena is not evident in the formulas of subsection 3.2.2. A different set of formulas apply. Like the formulas for diffraction, they are relatively complicated, but available in scattered literature. Unfortunately, these formulas could not be programmed into SOAP before the present contract ended. This would certainly be a worthwhile effort for the future, however.

4. Initial Design for Array.

In the interests of simplicity, the array was initially designed to operate in free space. It was noted, however, that this array would be relocated to the IUE satellite. Therefore, the following constraints were immediately considered:

1. The array must be of a size and shape so as to fit within available space around the satellite.

2. The elements of the array should be spaced as distant as possible from as many of the satellite structures as possible. This will tend to reduce interference from the satellite.

3. The elements should not interfere with the functioning parts of the satellite, such as the solar panels, the optical telescope, or the rocket thrusters.

4. The radiating properties of the array should be sufficiently broad band so as to allow operation at two discrete frequencies, 148.98 MHz and 136.86 MHz.

5. As many elements as possible should influence the radiation pattern independently, so that adjustment of the array is not unduly complicated.

It was decided that a ring of dipoles approximately half way up the optical telescope would be relatively isolated from the complicated satellite structure. The number and type of elements, and the diameter of the ring were next to be determined.

Combinations of tangential magnetic and electric dipoles were considered. It was determined that the diameter of the ring would approach that of the telescope, however. While this would not adversely affect the radiation efficiency of the magnetic dipoles, that of the electric dipoles would be greatly reduced. Also, the close proximity to the telescope would tend to emphasize interference from shielding.

Next, combinations of radial magnetic and electric dipoles were considered. The chief disadvantage of the tangential case, the close proximity to the telescope, was mitigated. The ring diameter in the radial case was one-half wave length at 148.98 MHz. This same diameter proved satisfactory also at 136.86 MHz.

In addition, the magnetic elements tended to influence E_θ independently, while the electric elements influenced E_ϕ independently. This was increasingly the case as θ approached 90°.

The design is shown in Fig. 4.1. It is seen that the phases of the magnetic dipole moments are 45° out of step from those of the electric dipole moments. Other relative phases (0°, 90°, and 135°) were also investigated, with inferior results.

It is also seen that the magnitudes of the magnetic dipole moments are η (about 377) times those of the electric dipole moments. When this result is translated into power distribution, however, it is found that the magnetic and electric dipoles radiate equal amounts. This is shown in the following calculation:

The magnitude of the electric dipole moments is specified to be:

$$|p_e| = |I|\ell = \text{const.} \tag{4.1}$$

The magnitude of the magnetic dipole moments is specified to be:

$$|p_m| = \omega\mu |I| A = \eta \times \text{const.} \tag{4.2}$$

Solving for the current magnitude for the electric dipoles:

$$|I| = \text{const.}/\ell \tag{4.3}$$

Similarly, the current magnitude for the magnetic dipoles is:

$$|I| = \frac{\eta \times \text{const.}}{\omega\mu A} = \frac{\text{const.}}{kA} \tag{4.4}$$

The radiation resistance of a short electric dipole is:

$$R = \frac{\eta}{6\pi}(k\ell)^2 \tag{4.5}$$

The radiation resistance of a small circular loop is:

$$R = \frac{\eta}{6\pi}(k^2A)^2 \tag{4.6}$$

Therefore, the power radiated by each electric dipole is:

$$P = \frac{1}{2}|I|^2 R$$

$$= \frac{1}{2}\left(\frac{\text{const.}}{\ell}\right)^2 \frac{\eta}{6\pi}(k\ell)^2$$

$$= \frac{\eta}{12\pi}(k \cdot \text{const})^2$$

The power radiated by each magnetic dipole is:

$$P = \frac{1}{2}|I|^2 R$$

$$= \frac{1}{2}\left(\frac{\text{const.}}{kA}\right)^2 \frac{\eta}{6\pi}(k^2A)^2$$

$$= \frac{\eta}{12\pi}(k \cdot \text{const})^2$$

Thus, magnetic and electric sources radiate equal amounts of power, despite the significant numerical difference in their dipole moments.

The radiation pattern, as calculated by the computer program SOAP, is shown in Figs. 4.2-4.15.

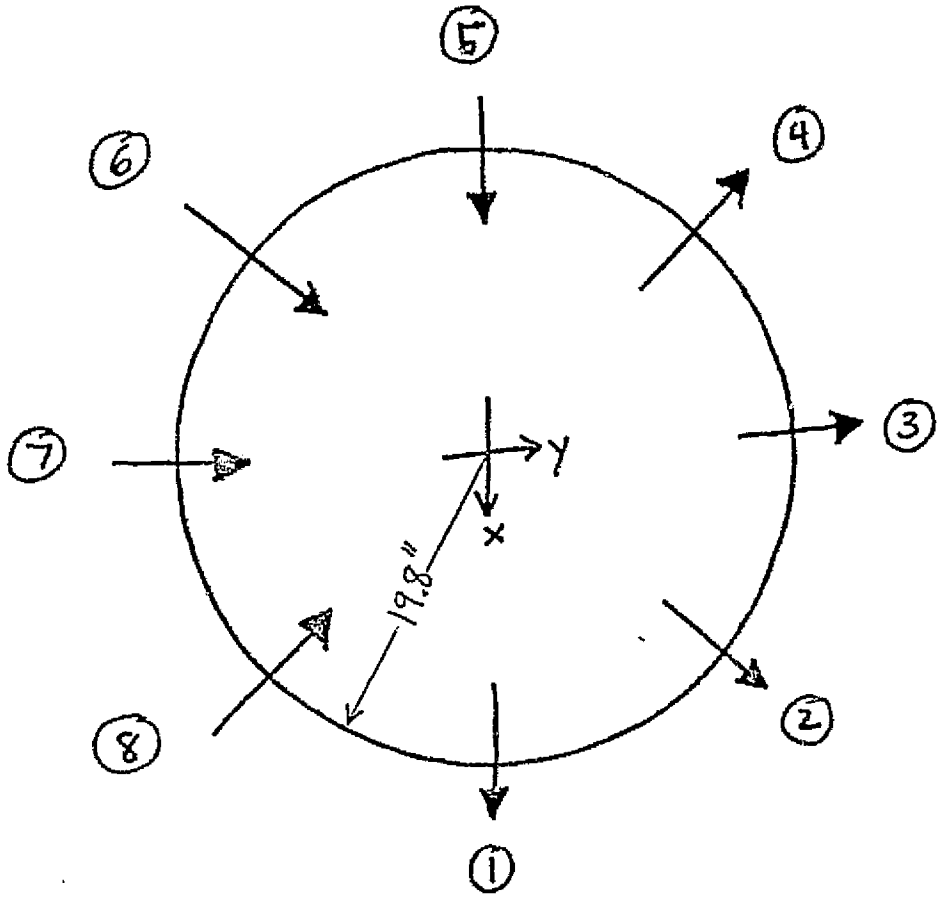

ELEMENT NUMBER	TYPE	DIPOLE MOMENT MAGNITUDE	PHASE
1	E	1	0°
2	M	η	45°
3	E	1	90°
4	M	η	135°
5	E	1	0°
6	M	η	45°
7	E	1	90°
8	M	η	135°

Fig. 4.1. Initial quasi-isotropic antenna array design

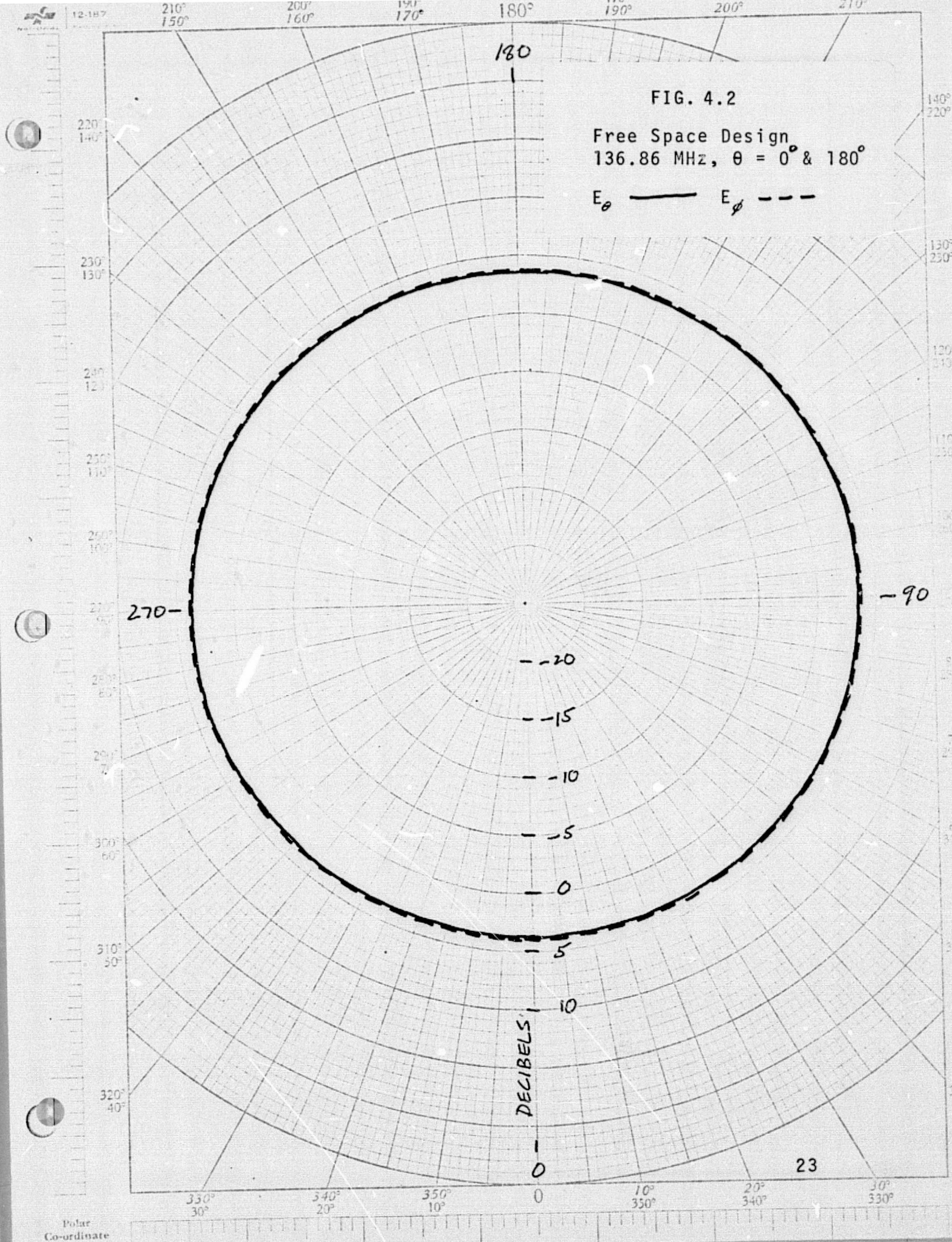
FIG. 4.2
Free Space Design
136.86 MHz, θ = 0° & 180°
E_θ ——— E_ϕ - - -
180
270
90
-20
-15
-10
-5
0
5
10
DECIBELS
0
23

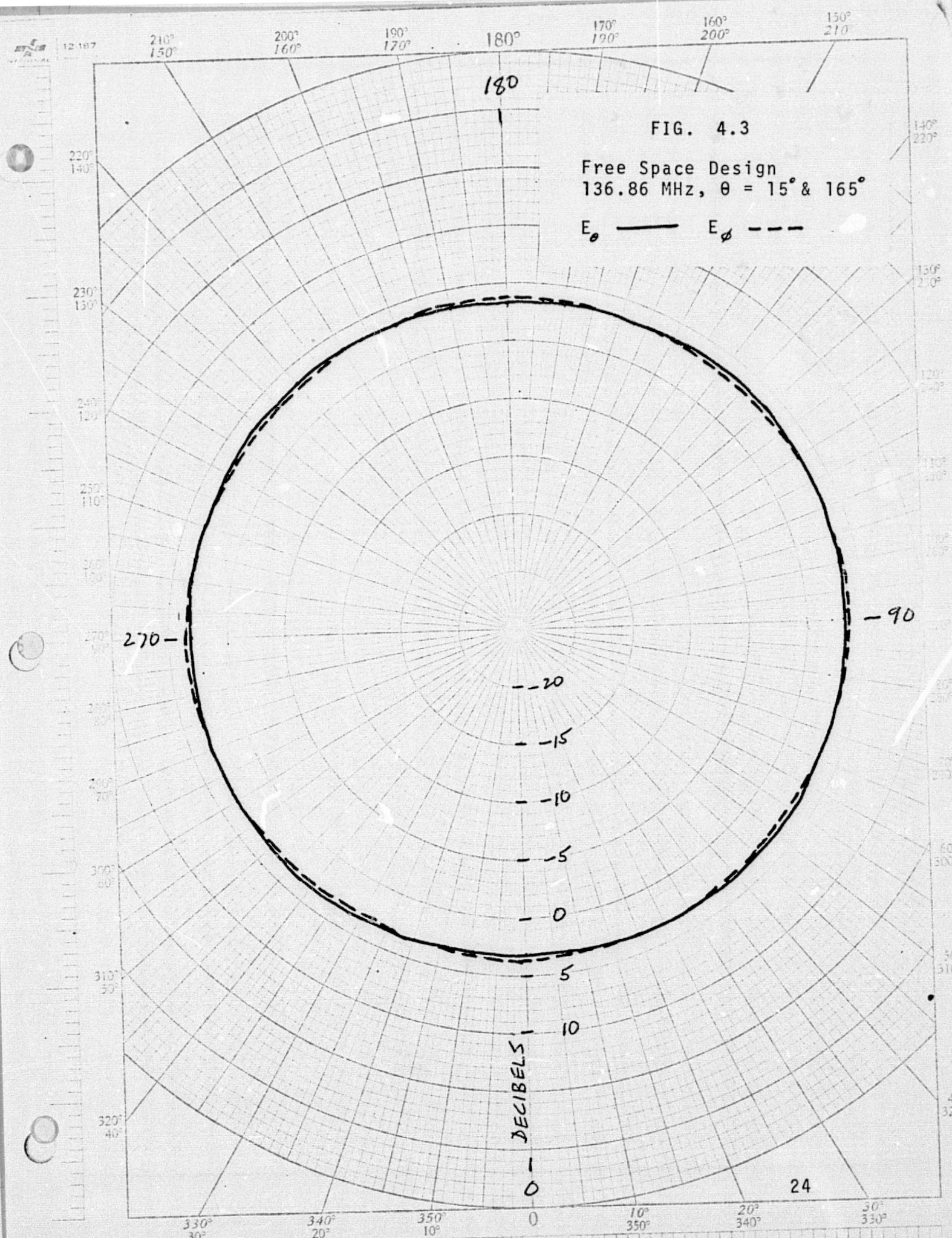

FIG. 4.3

Free Space Design
136.86 MHz, θ = 15° & 165°

E_θ ——— E_ϕ - - -

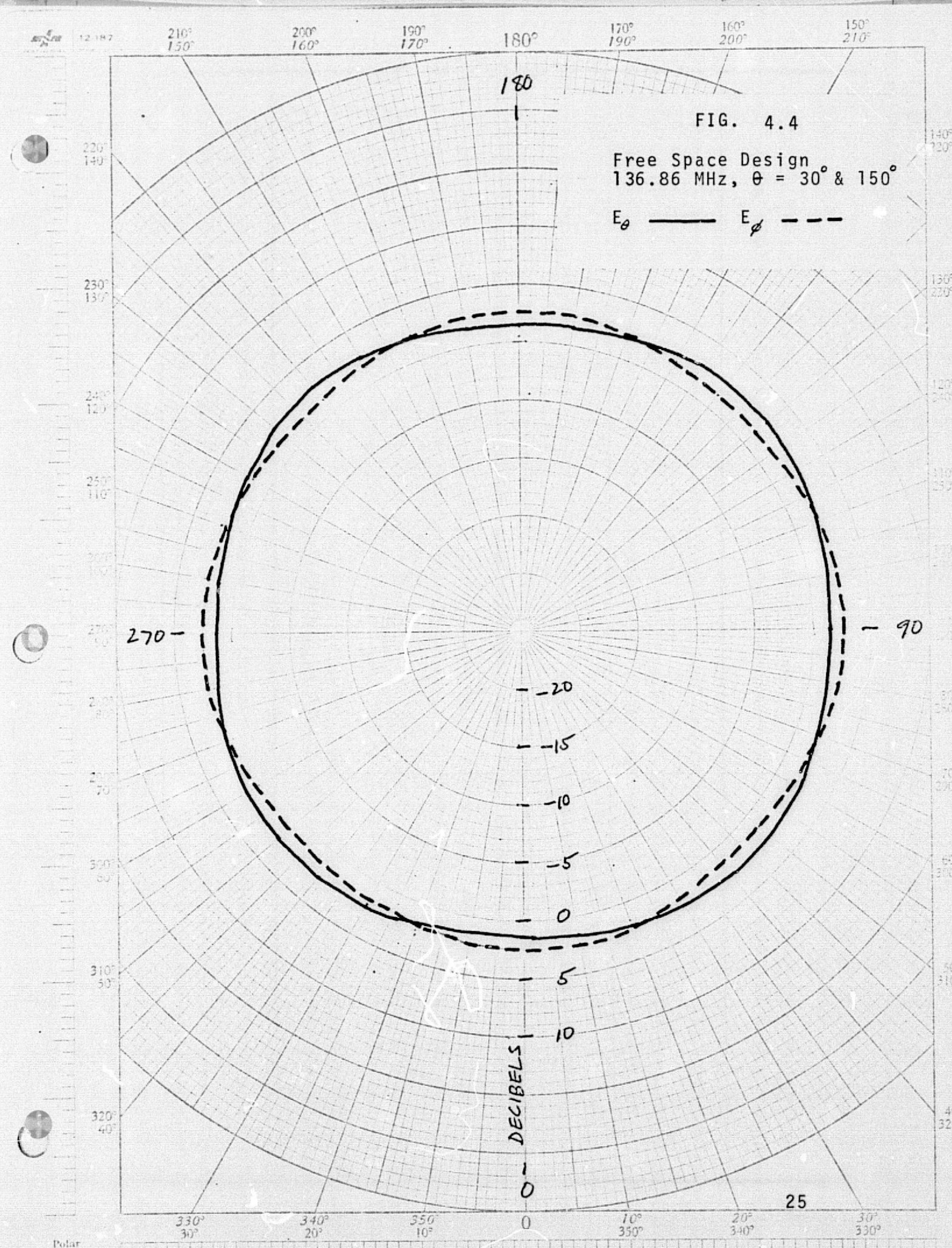

FIG. 4.4

Free Space Design
136.86 MHz, θ = 30° & 150°

E_θ ——— E_ϕ - - -

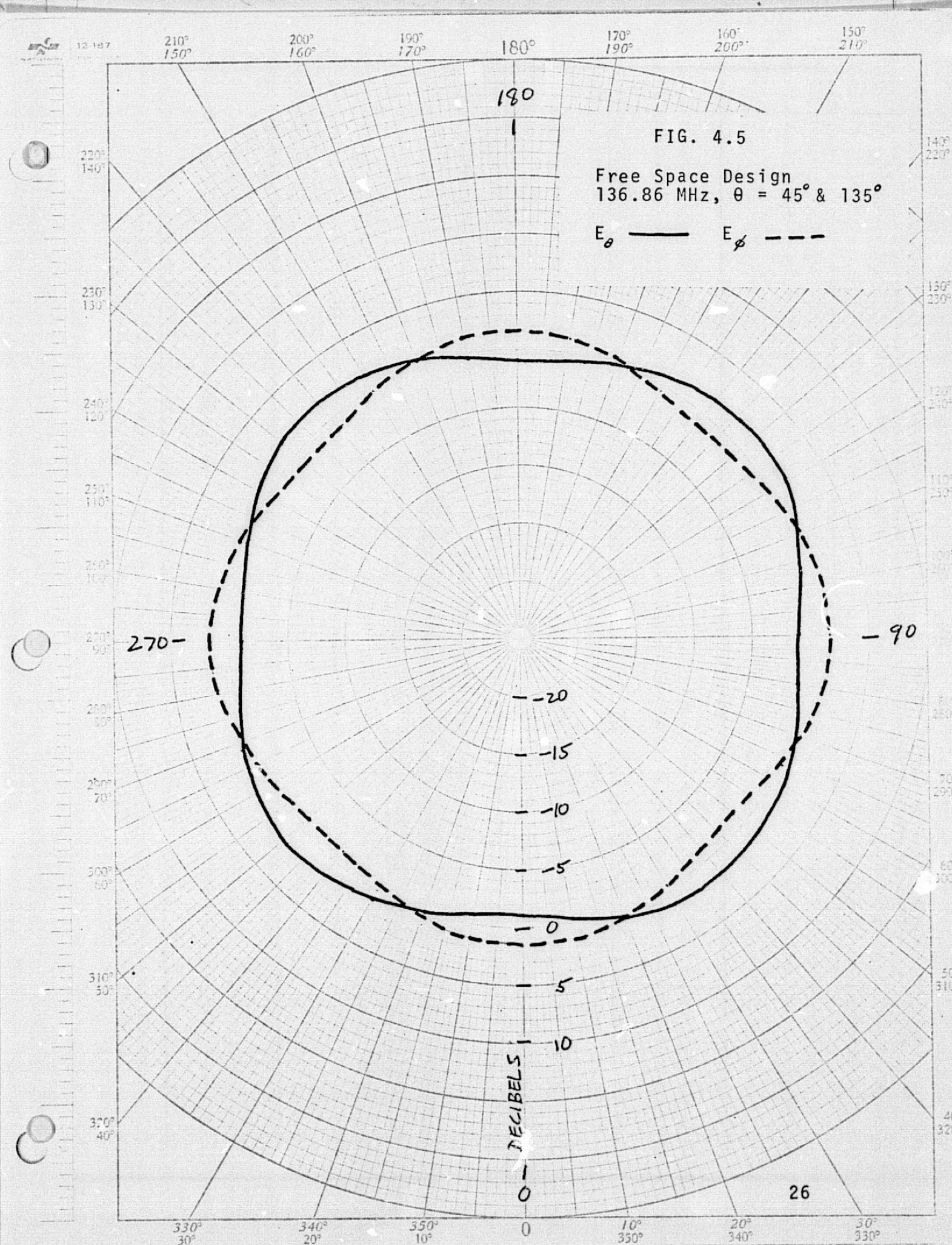

FIG. 4.5

Free Space Design
136.86 MHz, θ = 45° & 135°

E_θ ——— E_ϕ - - -

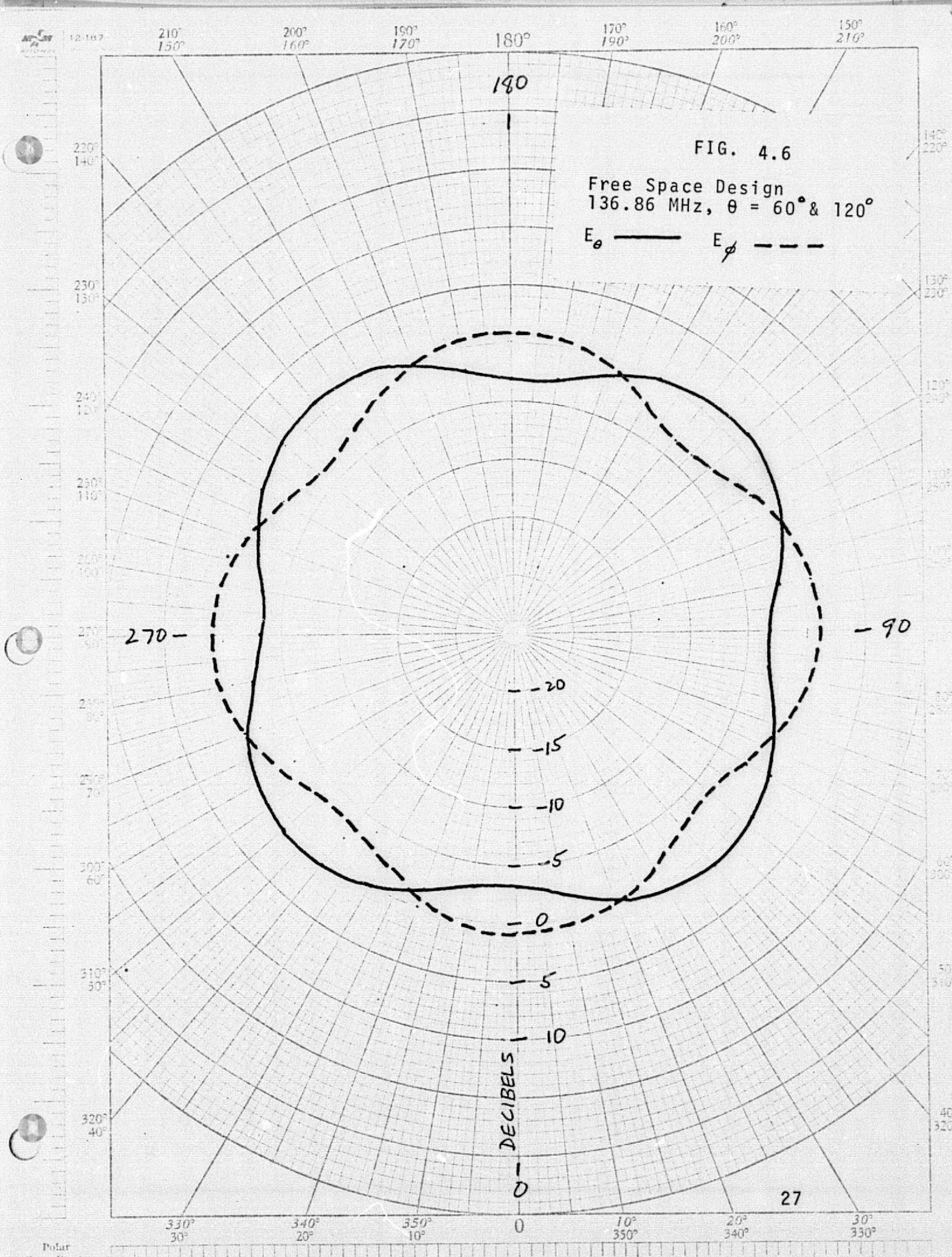
FIG. 4.6
Free Space Design
136.86 MHz, θ = 60° & 120°
E_θ ——— E_ϕ – – –
180°
140
270
90
-20
-15
-10
-5
0
-5
-10
DECIBELS
0
27

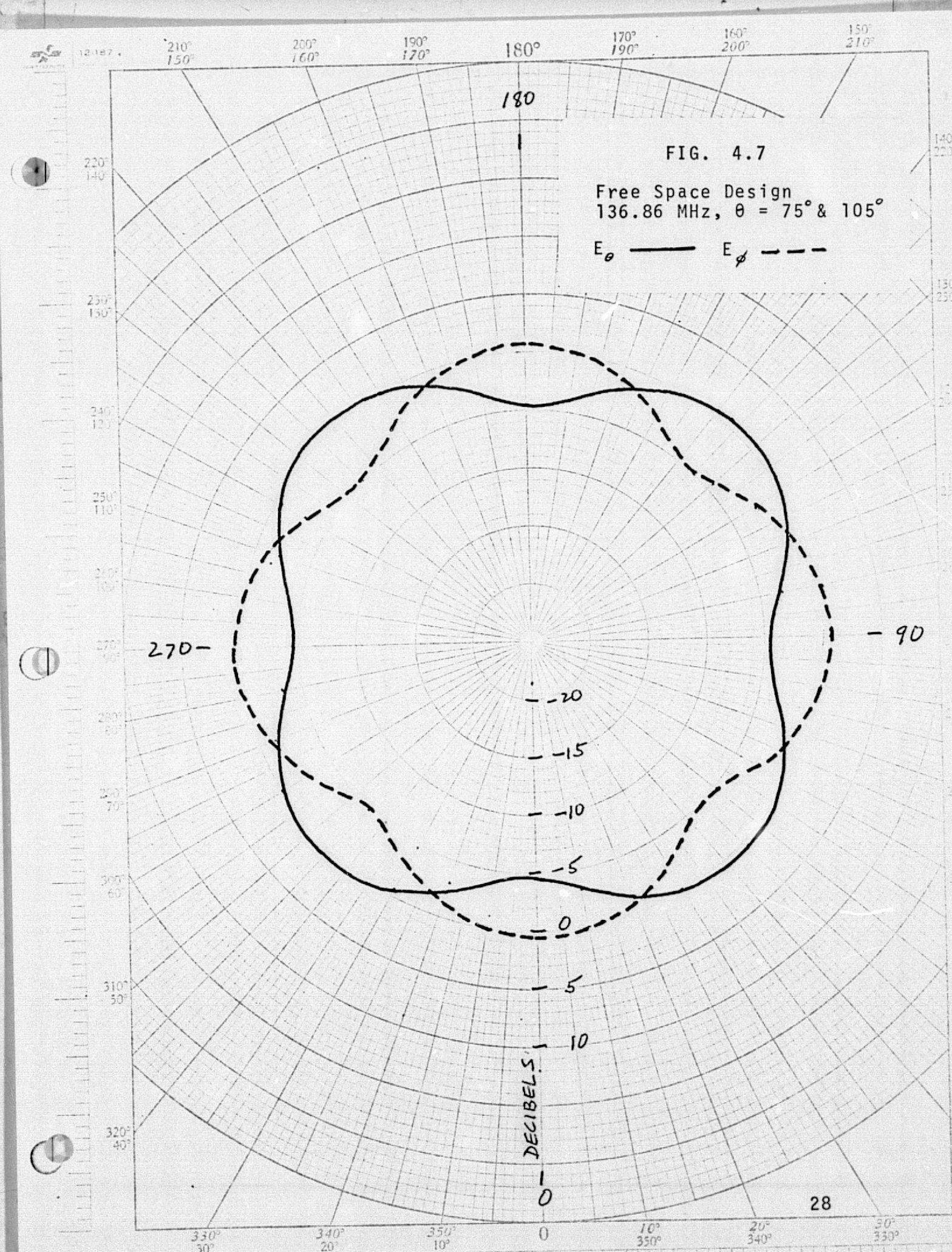

FIG. 4.7

Free Space Design
136.86 MHz, θ = 75° & 105°

E_θ ——— E_ϕ - - -

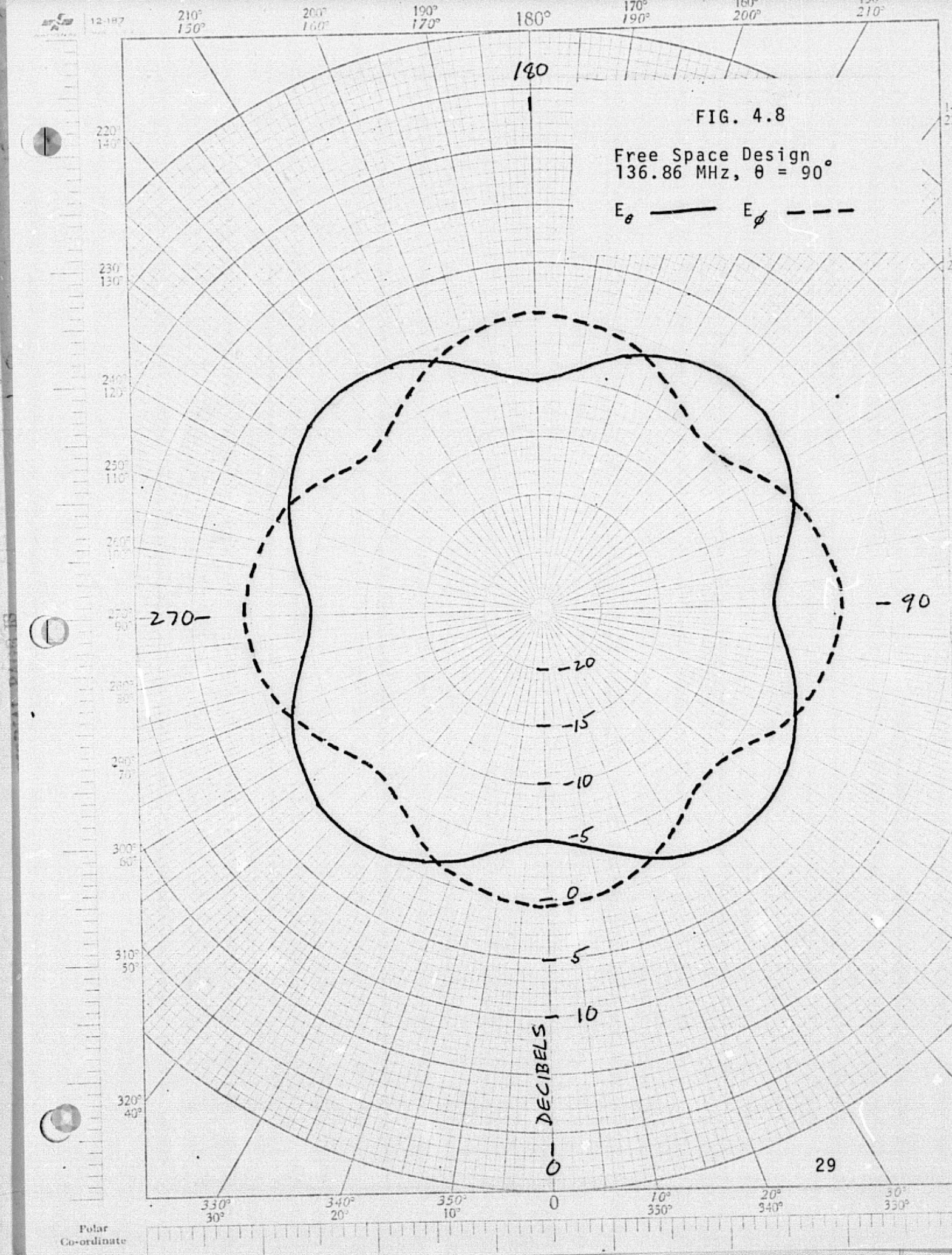

FIG. 4.8

Free Space Design
136.86 MHz, $\theta = 90°$

E_θ ——— E_ϕ - - -

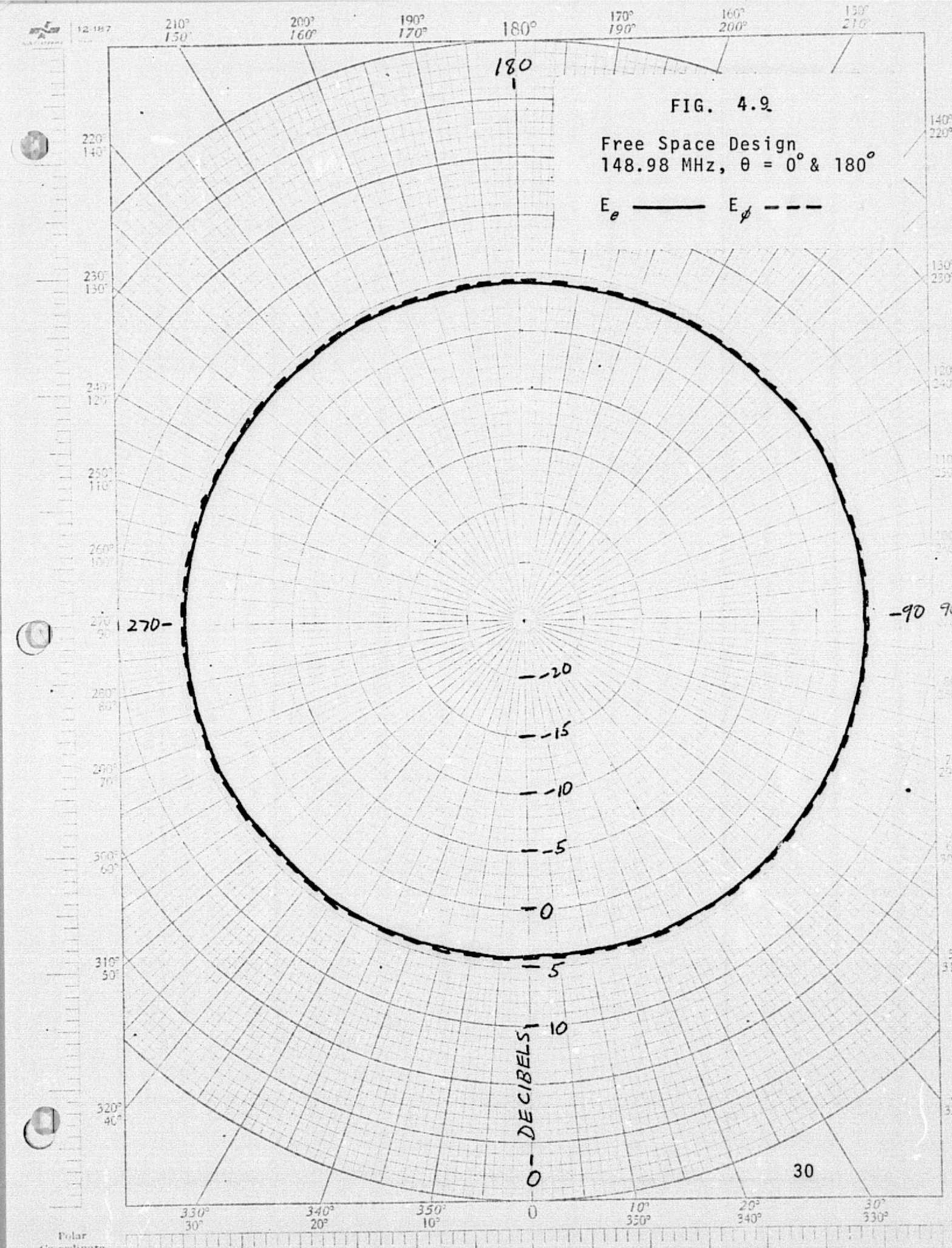

FIG. 4.9

Free Space Design
148.98 MHz, $\theta = 0^\circ$ & 180°

E_θ ——— E_ϕ - - -

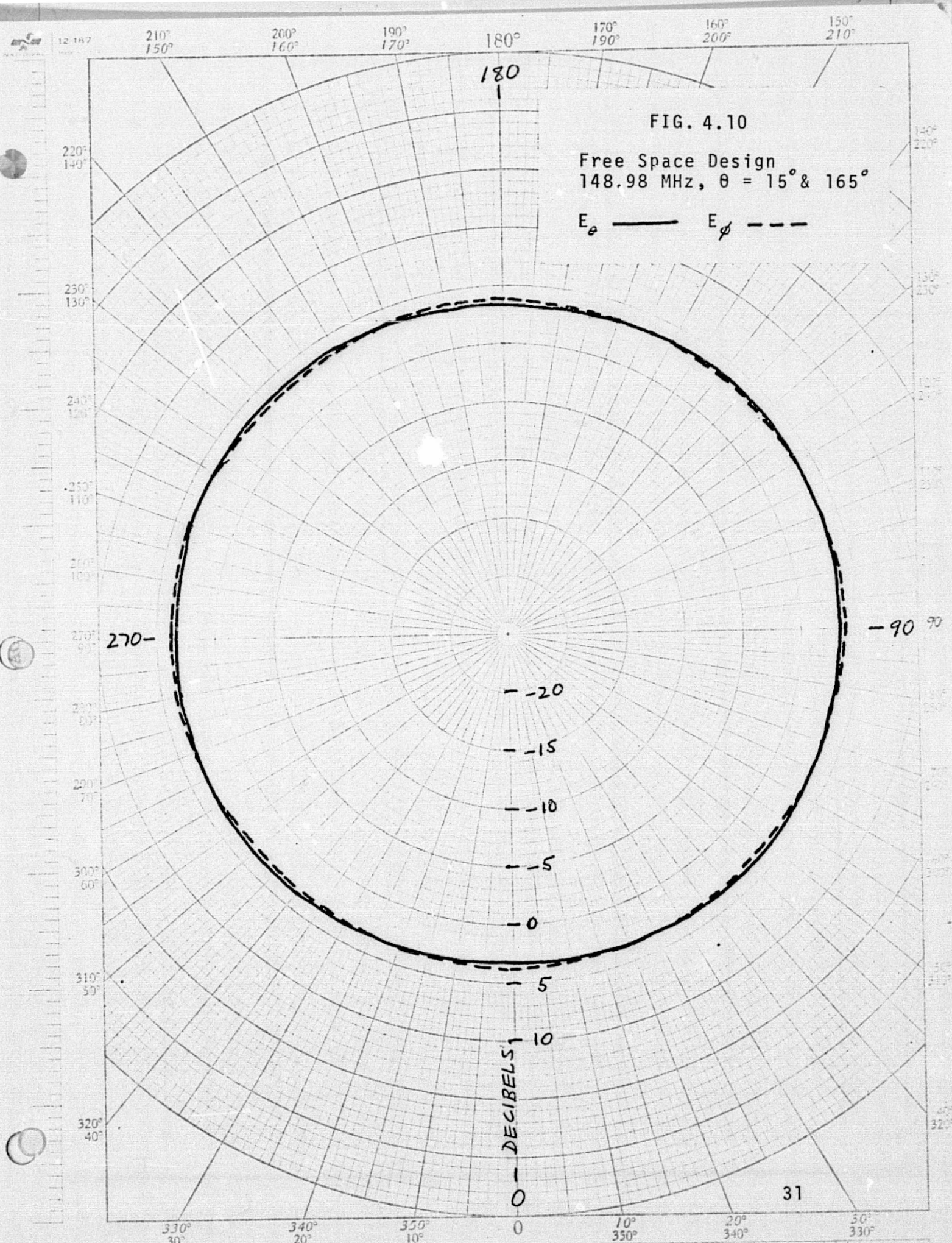

FIG. 4.10

Free Space Design
148.98 MHz, θ = 15° & 165°

E_θ ——— E_ϕ - - -

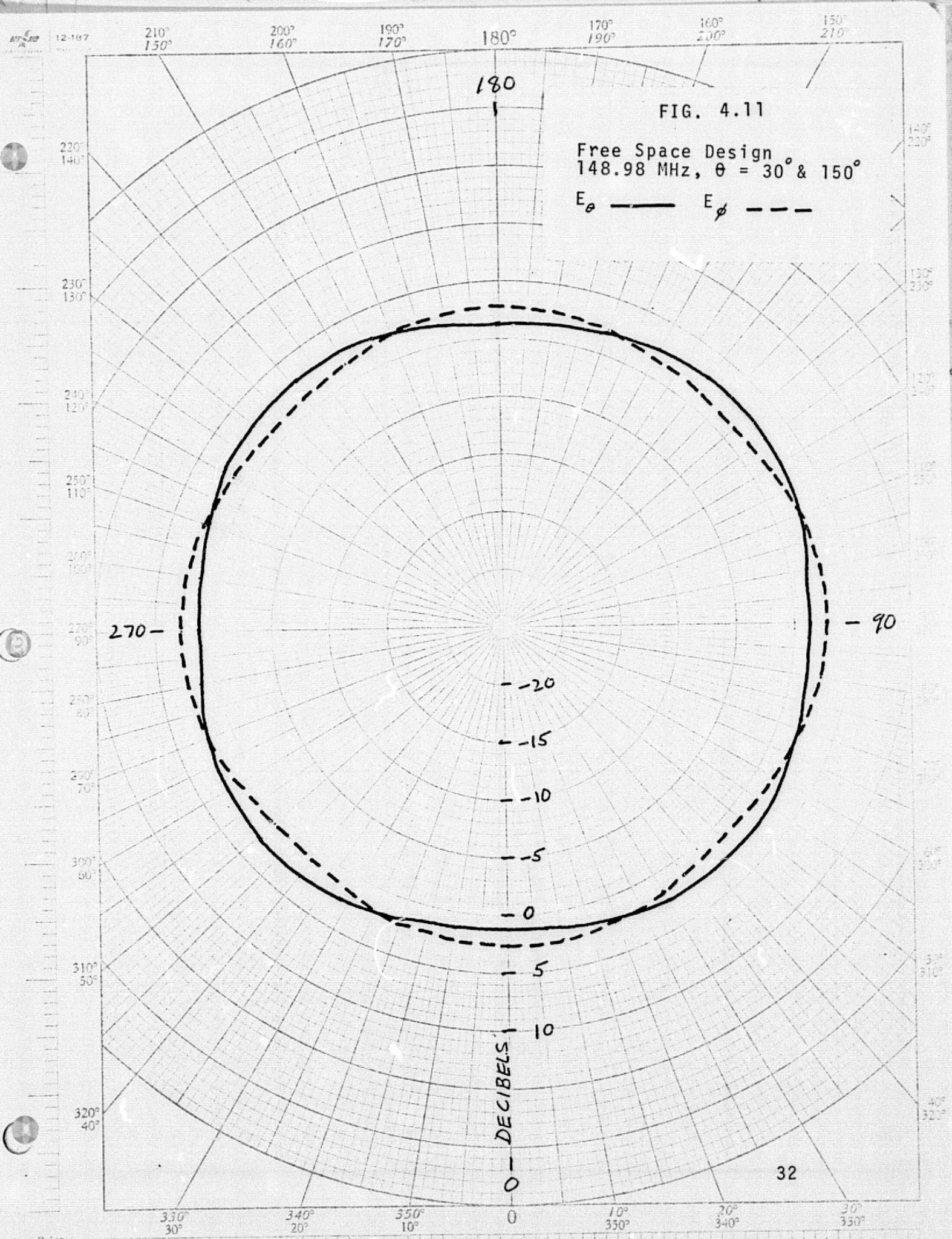
FIG. 4.11
Free Space Design
148.98 MHz, θ = 30° & 150°
E_θ —— E_ϕ - - -
180
270
90
0
-20
-15
-10
-5
0
5
10
0 - DECIBELS
32

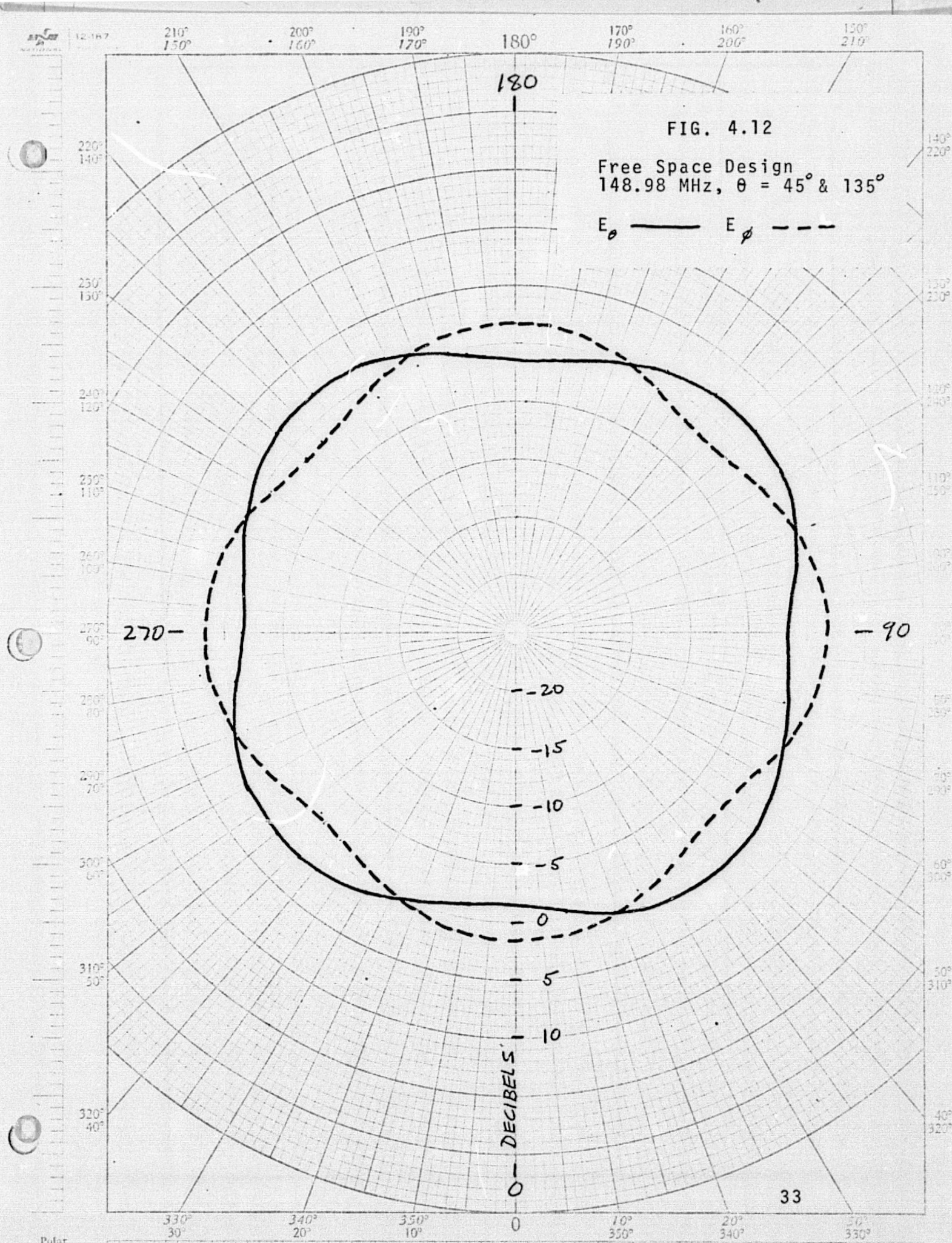

FIG. 4.12

Free Space Design
148.98 MHz, $\theta = 45^\circ$ & 135°

E_θ ——— E_ϕ - - -

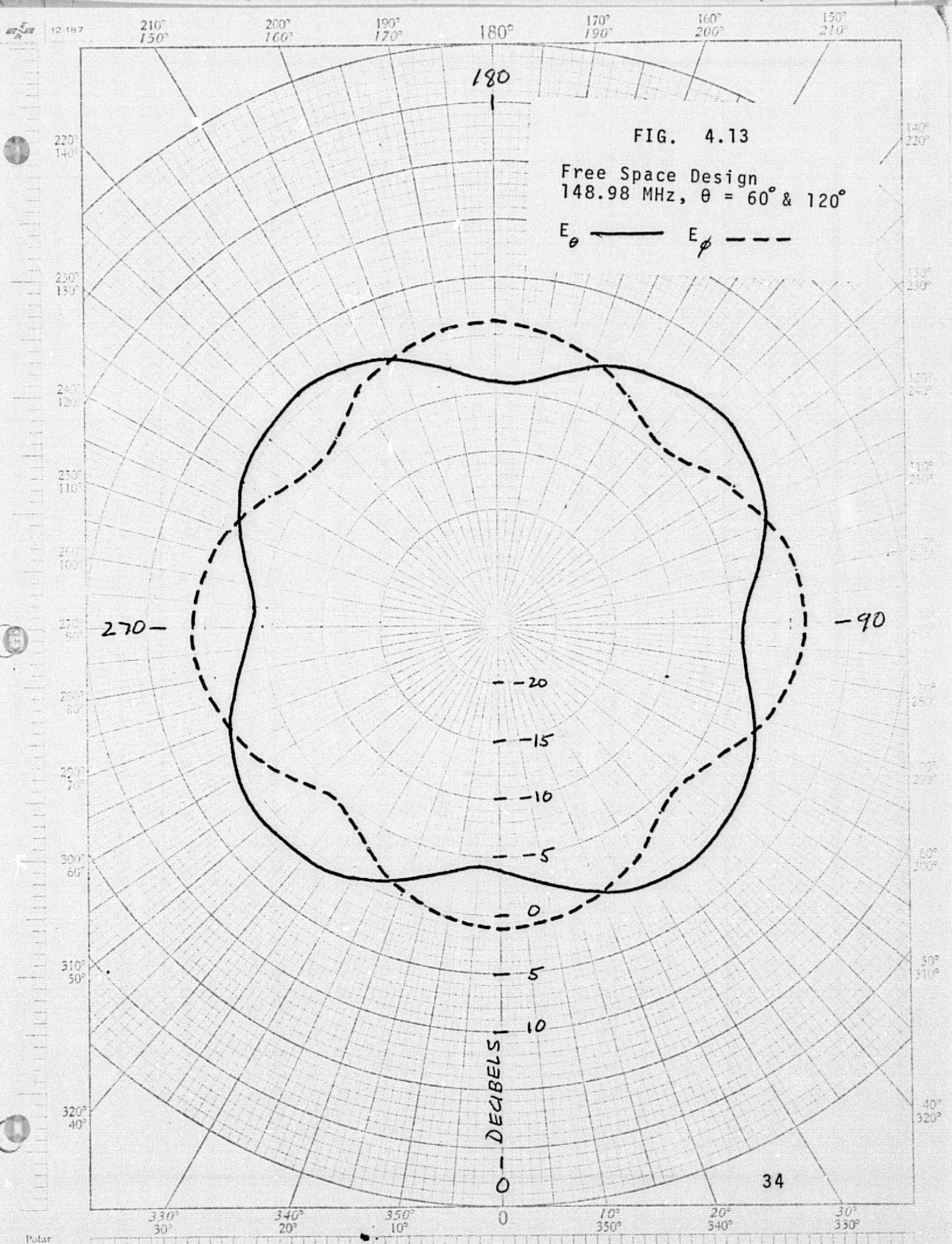

FIG. 4.13

Free Space Design
148.98 MHz, $\theta = 60^\circ$ & 120°

E_θ ——— E_ϕ - - -

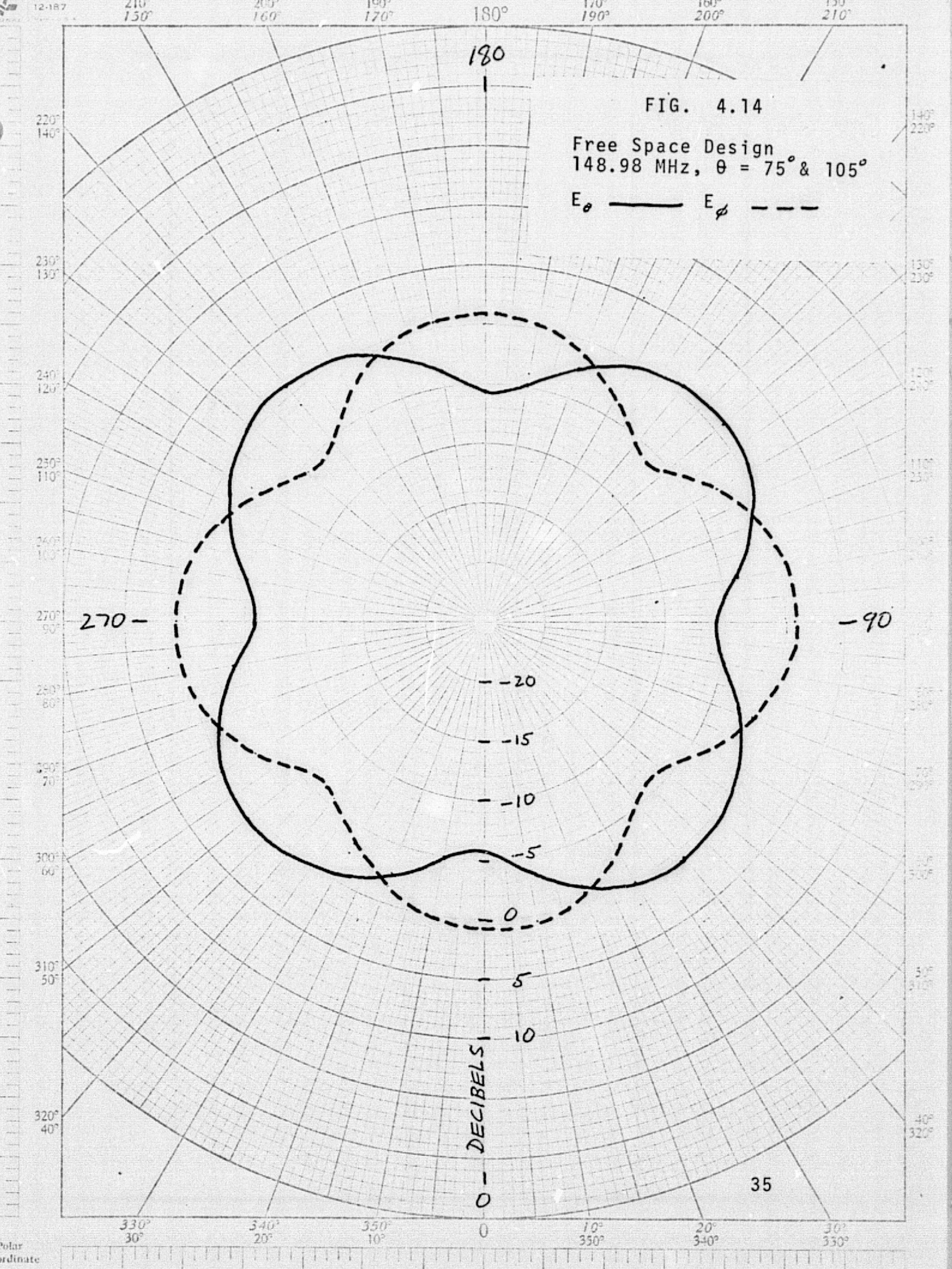

FIG. 4.14

Free Space Design
148.98 MHz, θ = 75° & 105°

E_θ ——— E_ϕ - - -

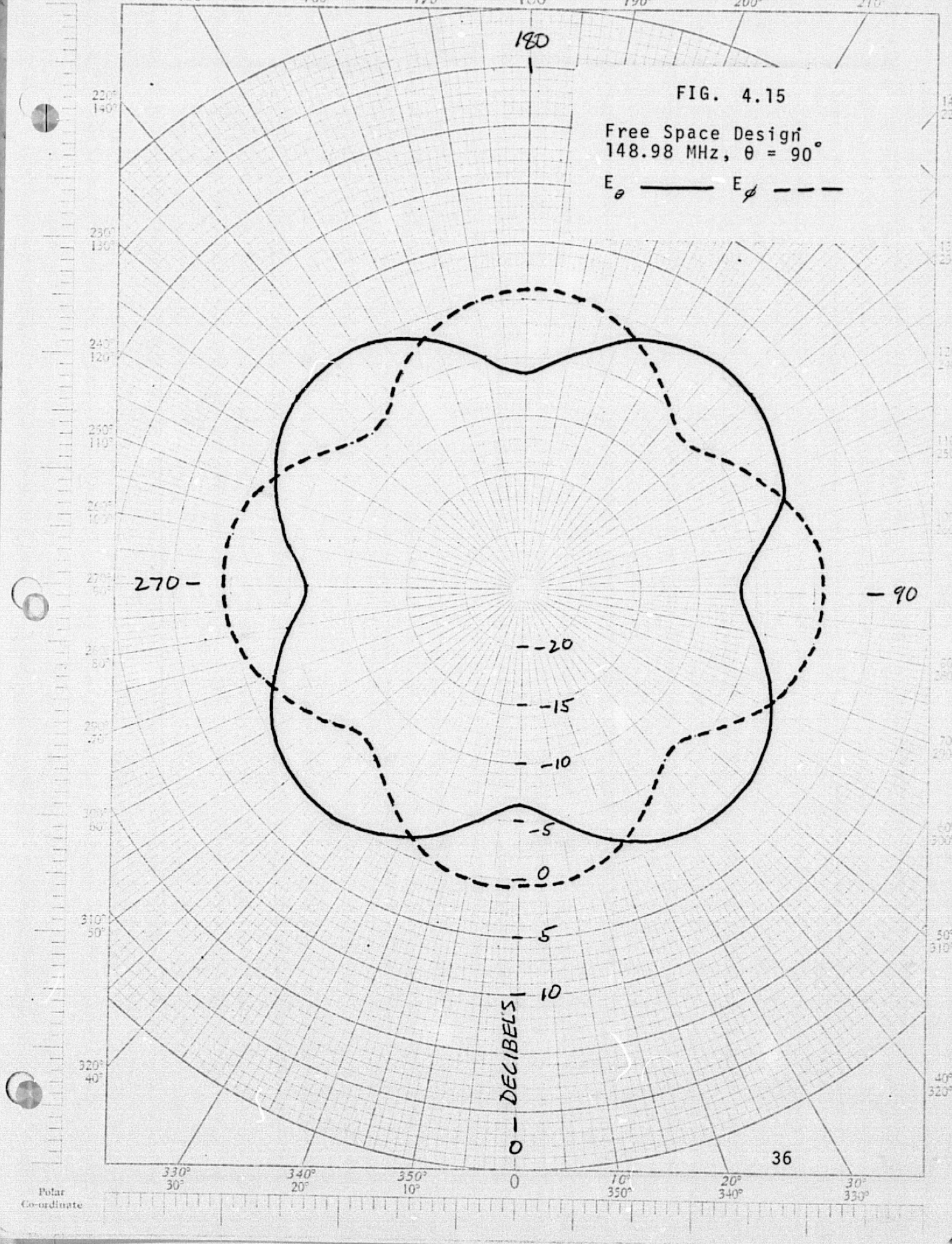

FIG. 4.15

Free Space Design
148.98 MHz, $\theta = 90^\circ$

E_θ ——— E_ϕ - - -

Polar Co-ordinate

5. Analytic Model of the IUE Satellite.

The initial array design described in Section 4 is a suitable starting point for further investigation, either experimental or analytic. For analytic investigations, a computational model is required. A mathematical description of the IUE satellite, which can be readily extended to include other satellites and structures, was developed. It is described in the present section.

5.1. Geometric Considerations.

Figs. 5.1-5.2 show how the IUE satellite may be regarded as a combination of circular cylinders and rectangular plates. Two situations are depicted, one in which the solar panels are folded, and the other in which they are extended.

Each cylinder and plate is uniquely and completely described by certain information depicted in Figs. 5.3-5.4. There are eight items of information for a cylinder. They are:

1. radius
2. height
3. location of center (x, y, z)
4. components of longitudinal direction vector (ℓ_x , ℓ_y , ℓ_z)

There are eleven items of information for a plate. They are:

1. length
2. width
3. location of center (x, y, z)
4. components of normal direction vector (n_x , n_y , n_z)
5. components of lengthwise direction vector (t_x , t_y , t_z)

These items of information were determined by making measurements on a life-sized model of the IUE satellite at the Goddard Space Flight Center. They are listed in Figs. 5.5-5.6.

As discussed in subsection 3.2.1., this information is necessary and sufficient for calculating the effects of interference by shielding.

The computer program SOAP does the shielding calculation automatically, once the geometric description of the cylinders and plates is provided in a data file.

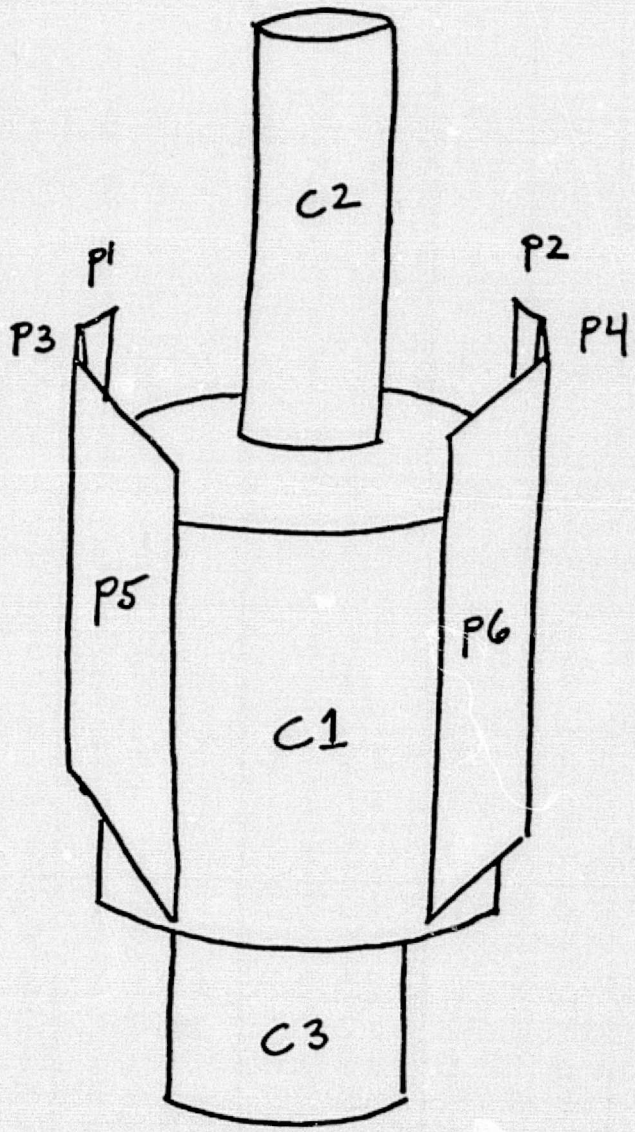

Fig. 5.1. The IUE satellite may be modelled by three circular cylinders (C1,C2, and C3) and six rectangular plates (P1 through P6). In this view, the solar panels are folded against the body of the satellite.

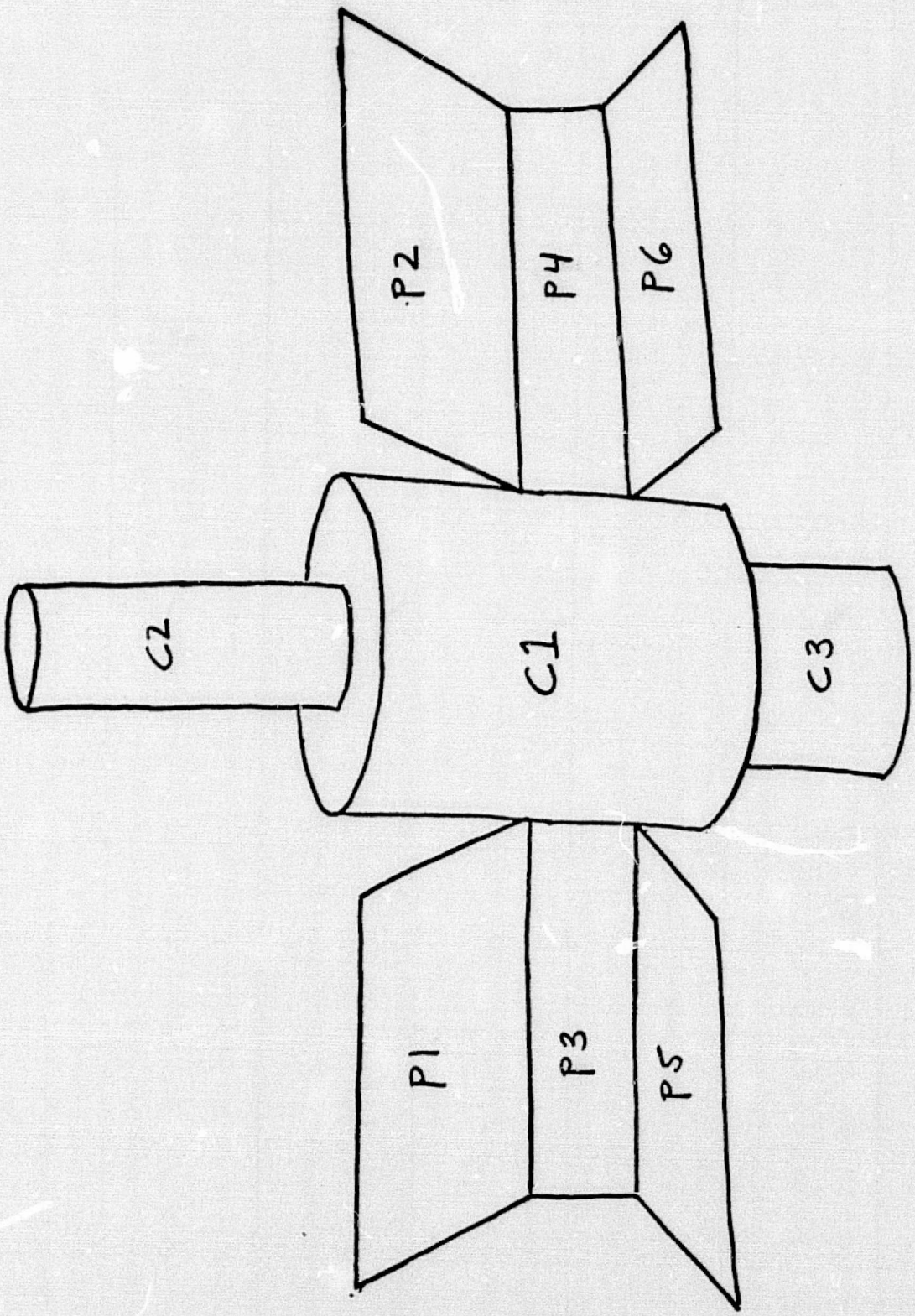

Fig. 5.2. Model of the IUE satellite with the solar panels extended.

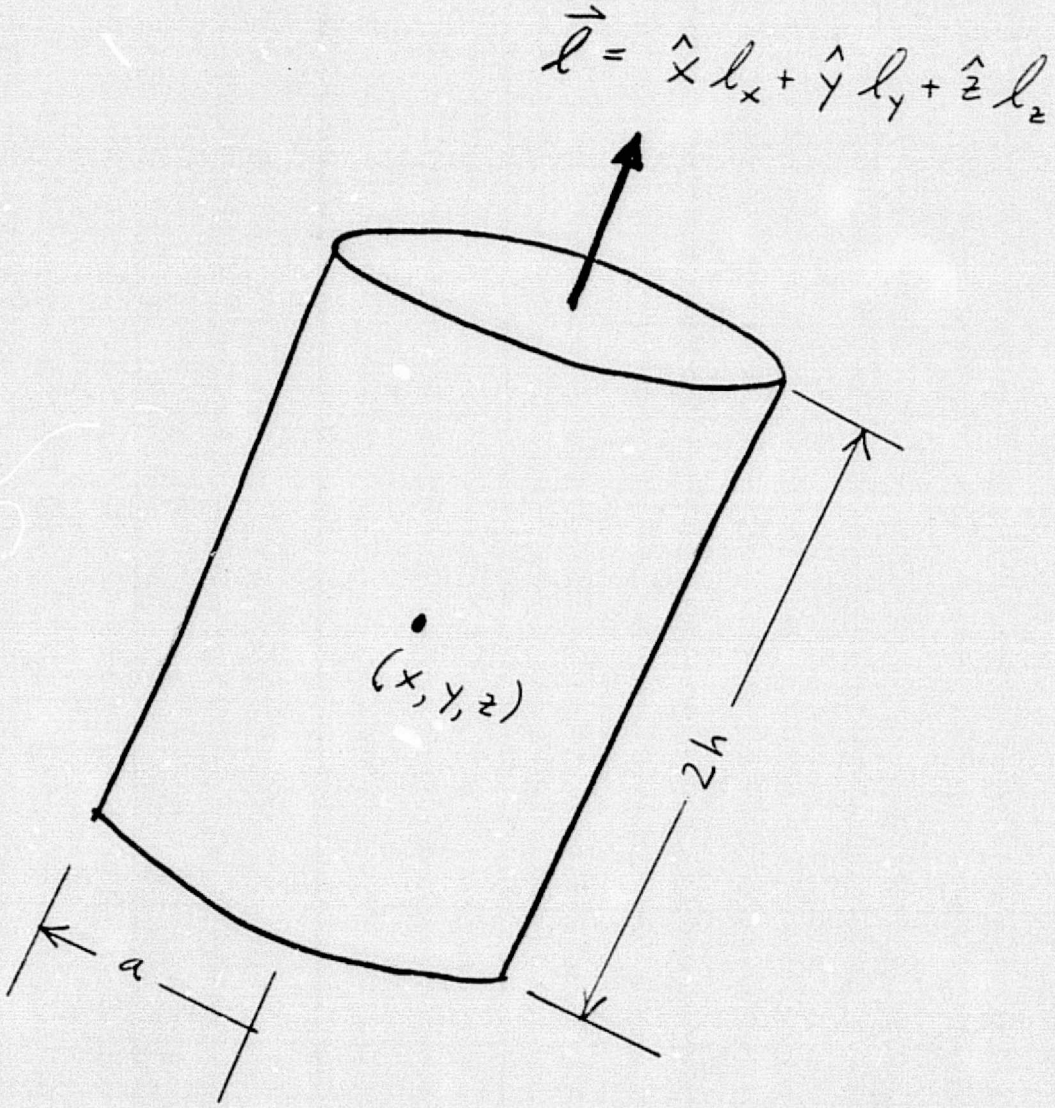

Fig. 5.3. The information necessary and sufficient to describe the size, shape, location, and orientation of a circular cylinder.

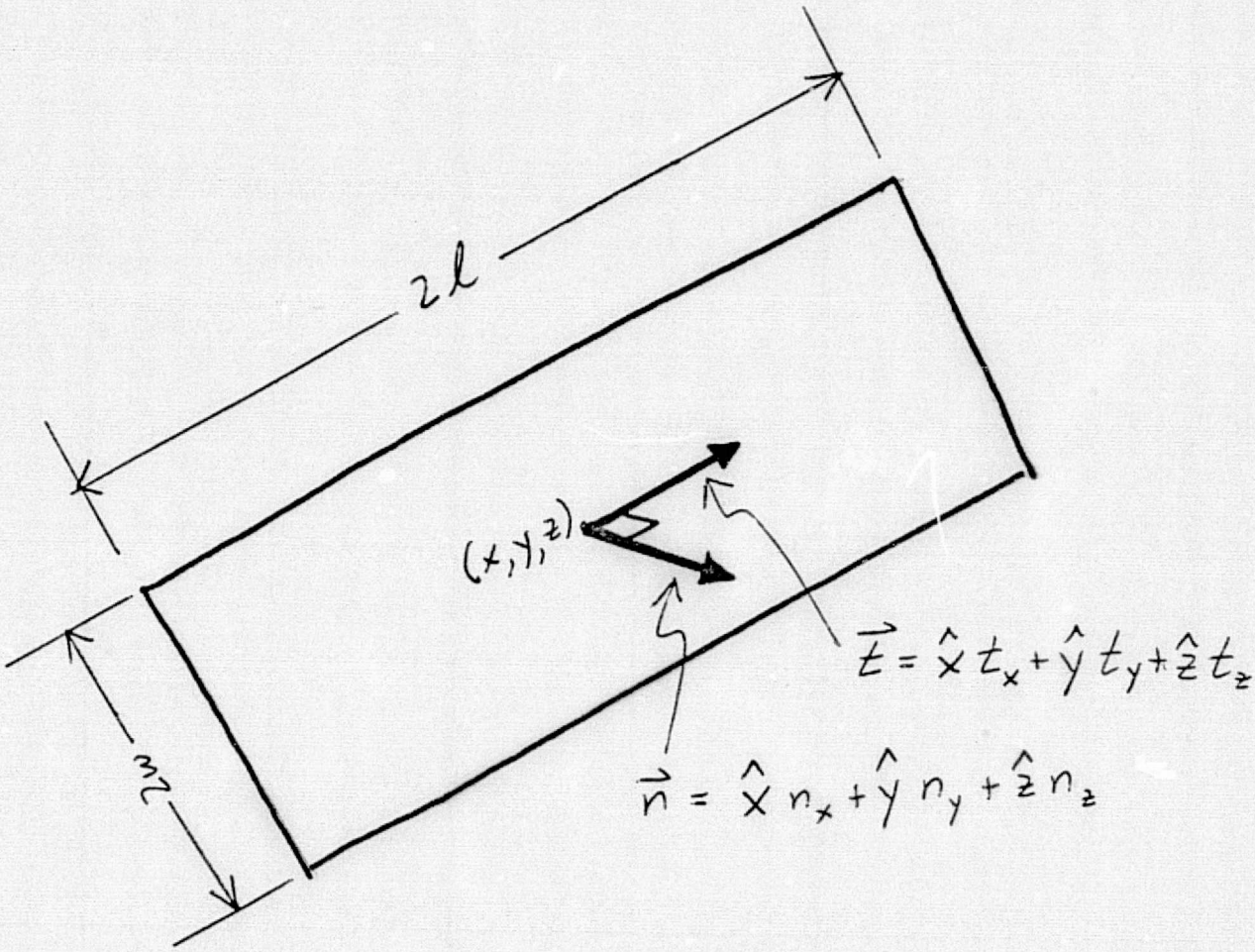

Fig. 5.4. The information necessary and sufficient to describe the size, shape, location, and orientation of a rectangular plate.

	C1	C2	C3
radius (inches)	27.69	12.5	17.688
height (inches)	61.75	59.625	29.25
location of center (inches)	0 0 0	0 0 60.685	0 0 -45.5
components of longitudinal direction vector	0 0 1	0 0 1	0 0 1

Fig. 5.5. Information necessary and sufficient to describe those parts of the IUE satellite modelled by circular cylinders.

	P1	P3	P5	P2	P4	P6
length (inches)	61	61	61	61	61	61
width (inches)	27	18.75	27	27	18.75	27
location of center (inches)	1.64 -58.19 21.094	0 -58.19 0	15.469 -58.19 -14.531	1.64 58.19 21.094	0 58.19 0	15.469 58.19 -14.531
component of normal direction vector	10 0 -4	13 0 5	2 0 4	10 0 -4	13 0 5	2 0 4
components of lengthwise direction vector	0 1 0	0 1 0	0 1 0	0 1 0	0 1 0	0 1 0

Fig. 5.6. Information necessary and sufficient to model solar panels on IUE satellite, when they are extended.

	P1	P3	P5	P2	P4	P6
length (inches)	61	61	61	61	61	61
width (inches)	27	18.75	27	27	18.75	27
location of center (inches)	-16.685 -19.34 30.5	0 -27.69 30.5	16.685 -19.34 30.5	-16.685 19.34 30.5	0 27.69 30.5	16.685 19.34 30.5
components of normal direction vector	1 1 0	0 1 0	-1 1 0	1 -1 0	0 -1 0	-1 -1 0
components of lengthwise direction vector	0 0 1	0 0 1	0 0 1	0 0 1	0 0 1	0 0 1

Fig. 5.7. Information necessary and sufficient to model solar panels on IUE satellite, when they are folded.

5.2. Electromagnetic Considerations.

Besides shielding, it is also necessary to compute the current induced on the surface of the satellite, either by reflection or diffraction. To that end, the surface is divided into non overlapping areas, each much smaller than a square wave length. This is shown in Fig. 5.8. The areas are well suited to the techniques described in subsection 3.2.2. for the calculation of the reflected field. Each area is uniquely and completely described by seven items of information. They are:

1. area
2. location of center (x, y, z)
3. components of outward normal vector (n_x , n_y , n_z)

The computer program SOAP calculates the reflected field automatically, including the effect of shielding, once the information describing the areas is provided in a data file.

Since there are many such areas, an auxiliary computer program was written to create the data file automatically. The program is called SUDS. Information describing a plate is provided, and SUDS automatically divides it into areas and writes the necessary information into the file. It may then be read by SOAP.

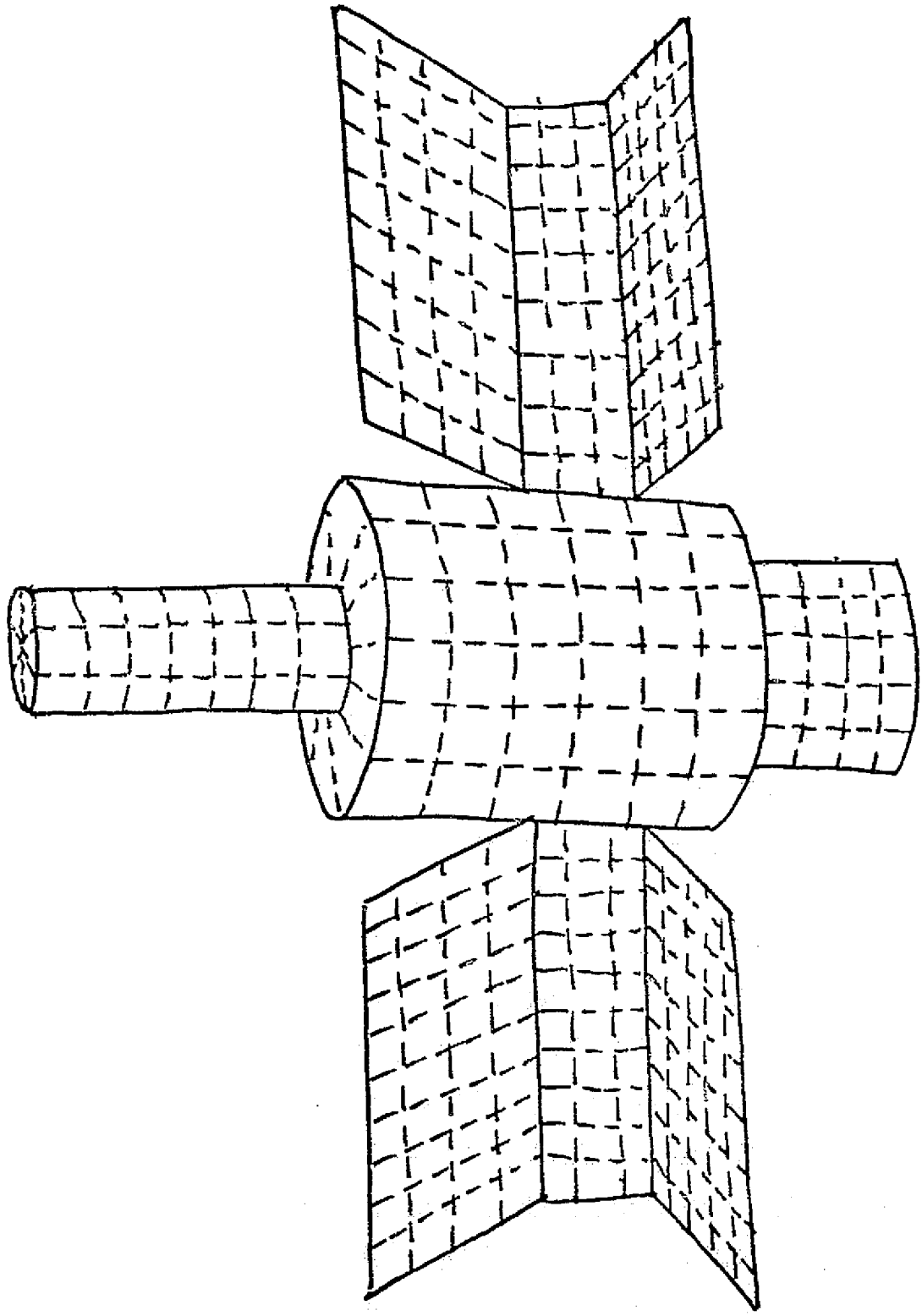

Fig. 5.8. For purposes of computing the current induced on the surface of the satellite, either by reflection or by diffraction, the cylinders and plates are divided into non-overlapping areas, each much smaller than a square wavelength.

6. An Interactive Computer Program.

Significant progress has been made in developing an original computer program named SOAP (Satellite Omnipurpose Antenna Program). SOAP calculates the electromagnetic field radiated by electric and magnetic dipoles in the presence of conducting cylinders and plates. Compared to previous efforts described in the literature [1, 5], it is faster, requires less storage, and is more versatile. With continued development, it will become a powerful design tool.

6.1. Present Capabilities.

At present, SOAP is operational on a Honeywell 1648 computer. The program may be conveniently accessed from a time-sharing terminal. The 1648 is a 16-bit machine, and it is slow and offers modest storage compared to most other time-sharing computers. This is a tribute to the speed and efficiency of SOAP. Since SOAP is a FORTRAN program, it can be easily transferred to a more powerful computer for increased speed and more complicated problems.

In its present form, SOAP incorporates all of the formulas for the six fundamental sources, described in Section 3.1. It also incorporates formulas and algorithms for two of the four fundamental interference phenomena, shielding and reflection. The present contract ended before the remaining two phenomena could be programmed.

A typical run by SOAP is shown as Figs. 6.1-6.2. A description of the run is as follows: Before running SOAP, the user prepares a data file containing this information:

1. frequency in MHz
2. the number of circular cylinders
3. description of each cylinder, as discussed in Section 5.1.
4. number of rectangular plates
5. description of each plate, as discussed in Section 5.1.
6. the number of sources
7. description of each source (location, direction, electric or magnetic, amplitude and phase of dipole moment)
8. the number of areas for computing current induced on surface of satellite
9. description of each area, as discussed in Section 5.2

When SOAP is run, it first asks the user for the name of the

data file. (In Fig. 6.1, see the message NAME INPUT FILE!) It then reads the data automatically as it is needed. SOAP displays as output the frequency and the description of the sources (TABULATION OF DIPOLE SOURCE DATA).

Next, SOAP asks the user to name an output data file (NAME OUTPUT FILE!) SOAP will store the calculated values of the electromagnetic field in this file for convenient use after the run. For example, such data might be used as input to a plotting program.

Next, SOAP asks a series of self-explanatory questions concerning how the answers are to be tabulated and for what points of observation. Then, SOAP begins calculating and displays the results at the terminal, as well as writing them into the output data file.

After displaying all of the electromagnetic field calculations, SOAP prints the RMS (root-mean-square) electric field. This is the field intensity that would have been radiated uniformly had the array been truly isotropic. SOAP has been calculating the RMS field all along, according to the following formula:

$$E_{rms} = \sqrt{\frac{\Delta\theta \cdot \Delta\phi}{4\pi} \sum_{\theta=0}^{\pi} \sum_{\phi=0}^{2\pi} |E(\theta,\phi)|^2 \sin\theta} \qquad (6.1)$$

where: $\Delta\theta$ = incremental step in θ

$\Delta\phi$ = incremental step in ϕ

Finally, SOAP asks the user if he wishes to go back and calculate the field at some additional points of interest (ANOTHER TABULATION?) or do a new run starting from the very beginning (START OVER AGAIN?)

6.2. Recommendations for Extending Capabilities.

For SOAP to be a credible design tool, it is essential to incorporate the remaining two fundamental interference phenomena.

It may be desirable to incorporate other shapes in addition to circular cylinders and rectangular plates. The new shapes might include spheres, cones, and triangular plates.

Since SOAP is a fast program and requires relatively little storage, it would be reasonable to add some design algorithms. Such algorithms would perturb source parameters in order to synthesize a prescribed radiation pattern.

```
NAME INPUT FILE ! TRY01


FREQUENCY=     136.860 MEGAHERTZ

          TABULATION OF DIPOLE SOURCE DATA

DIRECTION      TYPE          LOCATION                AMPLITUDE     PHASE

    X           E       19.80    0.00   56.00          1.00         0.00
    X           M       14.00   14.00   56.00          0.71        45.00
    Y           M       14.00   14.00   56.00          0.71        45.00
    Y           E        0.00   19.80   56.00          1.00        90.00
    X           M      -14.00   14.00   56.00         -0.71       135.00
    Y           M      -14.00   14.00   56.00          0.71       135.00
    X           E      -19.80    0.00   56.00          1.00         0.00
    X           M      -14.00  -14.00   56.00          0.71        45.00
    Y           M      -14.00  -14.00   56.00          0.71        45.00
    Y           E        0.00  -19.80   56.00          1.00        90.00
    X           M       14.00  -14.00   56.00         -0.71       135.00
    Y           M       14.00  -14.00   56.00          0.71       135.00


NAME OUTPUT FILE ! DUMP
```

Fig. 6.1. Example of the output to a time-sharing terminal during a run of SOAP.

```
TABULATE FIELD IN HORIZ.(1) OR VERT.(2) SLICES? ! 1


FIELD IN VOLTS/METER(1) OR DECIBELS(2)? ! 1


RANGE IN FEET ! 100

THETA IN DEGREES (START,STOP,STEP) ! 0,180,15

BEARING IN DEGREES (START,STOP,STEP) ! 0,355,5


TABULATION FOR THETA=    0.00 DEGREES
BEARING          ETHETA                EPHI                PHASE DIFFERENCE

  0.00       0.836783E 01        0.836786E 01        -0.900001E 02
  5.00       0.836783E 01        0.836786E 01        -0.900001E 02
 10.00       0.836783E 01        0.836786E 01        -0.900001E 02
 15.00       0.836783E 01        0.836786E 01        -0.900000E 02
 20.00       0.836783E 01        0.836786E 01        -0.900000E 02
 25.00       0.836782E 01        0.836786E 01        -0.900000E 02
 30.00       0.836783E 01        0.836786E 01        -0.900000E 02
 35.00       0.836783E 01        0.836786E 01
 40.00       0.836783E 01        0.836786E
 45.00       0.836783E 01        0.836
 50.00       0.836783E 01
 55.00       0.836783E
 60.00       0.
 65.00
 70
                                 0.762215E 01        0.900000E 02
                                 0.762215E 01        0.900000E 02
                 0.762216E 01    0.762216E 01        0.900000E 02
                 0.762216E 01    0.762216E 01        0.900000E 02
345.00           0.762215E 01    0.762215E 01        -0.270000E 03
350.00           0.762215E 01    0.762216E 01        -0.270000E 03
355.00           0.762215E 01    0.762215E 01        -0.270000E 03


RMS ETHETA   0.539124E 01 VOLTS/METER
RMS EPHI     0.537850E 01 VOLTS/METER
RMS EFIELD   0.537987E 01 VOLTS/METER


ANOTHER TABULATION? (1=YES,0=NO) ! 0


START OVER AGAIN? (1=YES,0=NO) ! 0
```

Fig. 6.2. Continued output from SOAP.

7. Discussion of Results.

The initial design described in Section 4 may be a satisfactory final design as well. There are a number of reasons to expect this. Three of them are:

1. The radial direction of each of the array elements is particularly fortunate. For, each has a minimum in the direction of the telescope. Thus, interference in the form of reflection from that structure is less than in the case of either tangentially or longitudinally directed elements. The dominant form of interference is shielding, and it is likely that diffraction reduces the effects of this significantly.

2. In his 1943 paper concerning the radiation patterns of dipoles around cylinders [3], Carter states that "a substantially circular pattern may be obtained with four dipoles when the radius of the array is less than 0.14 wave length." This statement refers to an array of radial electric dipoles, fed in phase rotation. In the design proposed for the IUE satellite the dipoles are radial and also fed in phase rotation. The radius of the telescope is 0.158 wave length at 148.98 MHz, which means the pattern may not be "substantially circular" but sufficiently so to meet the desired specifications.

3. Though the remaining structure of the IUE satellite also interferes with the free space radiation pattern, the effect of diffraction may, in general, negate the effects of shielding and reflection. Because there was insufficient time to program the diffraction phenomena, SOAP is presently unable to substantiate this, however.

In its present form, SOAP can calculate the effects of shielding and reflection. As an exercise, the initial design was modified in an attempt to reduce these two forms of interference. The modified design is shown as Fig. 7.1.

The corresponding radiation patterns are collected in the Appendix. It is seen that, with the solar panels folded, there are occasional nulls in the E_θ radiation pattern that are deeper than -10 db with respect to an isotropic radiator. These nulls do not subtend an angle greater than 6°. It is very possible, therefore, that they are filled by diffraction.

With the panels extended, the nulls are more frequent, deeper, and subtend wider angles. This is increasingly true for θ sufficiently great so that the panels shield the sources. Therefore, it is very possible that these nulls are also filled by diffraction.

For θ greater than about 163°, all the sources are shielded by the main body of the satellite. Therefore, in its present form, SOAP calculates zero field, and so radiation plots for the horizontal slices $\theta = 165^\circ$ & 180° are not included. It is again likely,

however, that, in fact, this region of space is illuminated by diffraction phenomena.

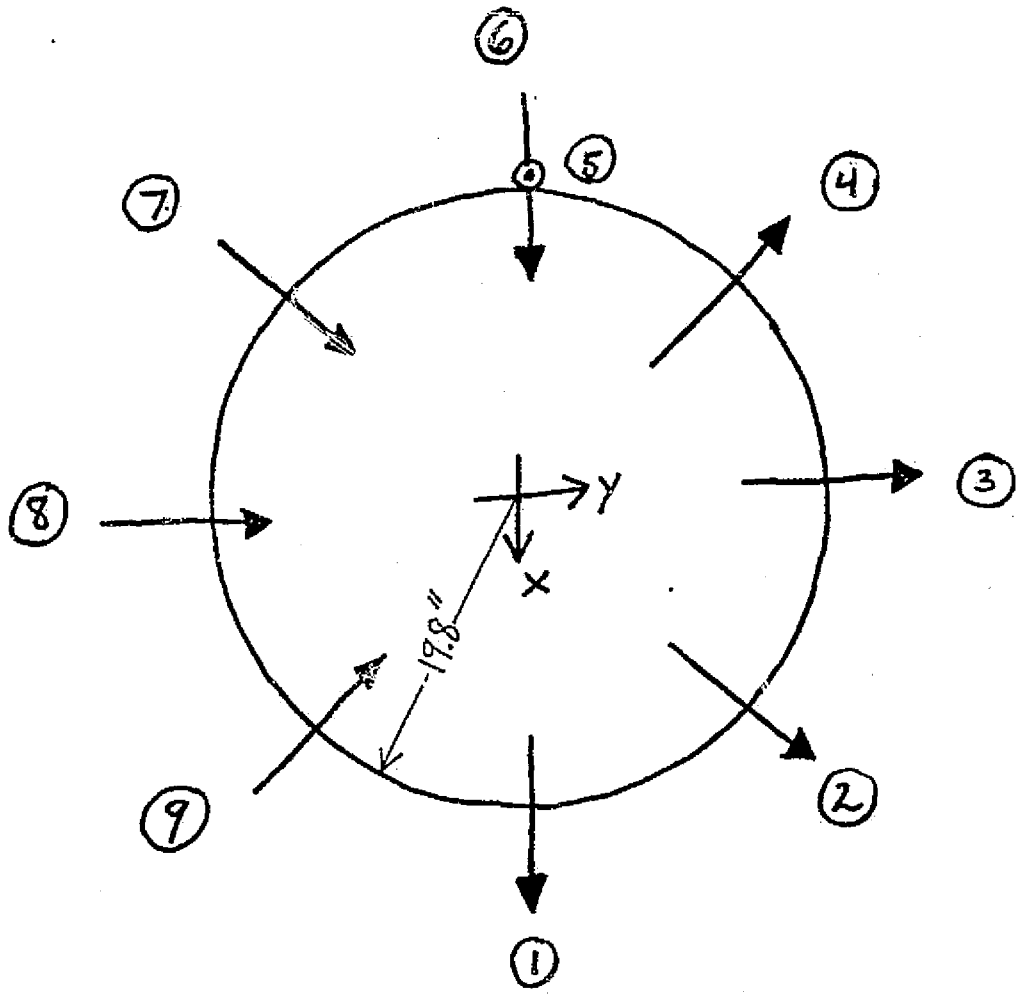

ELEMENT NUMBER	TYPE	DIPOLE MOMENT MAGNITUDE	PHASE
1	E	1	0°
2	M	η	45°
3	E	1	90°
4	M	η	135°
5	E	1	0°
6	E	1	0°
7	M	η	22°
8	E	1	90°
9	M	η	135°

Fig. 7.1. Modified quasi isotropic array for IUE satellite, designed using SOAP. The effects of shielding and reflection are reduced in this configuration. It is still tentative, however, because the effect of diffraction has not been calculated.

8. Recommendations for Future Action.

Significant progress has been made in the design and analysis of satellite antenna arrays. To build on that progress, the following activities are recommended for the future.

1. It is recommended that the design proposed in Section 4 be evaluated experimentally.

2. It is also recommended that the physical realization of the individual array elements be studied in further detail. The goal of the study should be to predict the input impedance of each element so that phasing and power dividing networks may be conveniently designed. Techniques for improving the impedance, such as folding and loading, should be explored so that the array may be made as small and as light in weight as possible.

3. It is strongly recommended that development of the computer program SOAP be continued. Many original algorithms have already been implemented. Subroutines for the interference phenomena of diffraction by edges and reradiation by parasitic wires should be added. SOAP promises to be a very powerful and useful design tool that is significantly faster, more efficient, and more versatile than similar programming efforts. It is estimated that the new subroutines could be incorporated in another 13 weeks, assuming the same rate of progress as during the present study.

9. New Technology.

The following original developments are disclosed.

9.1. Quasi-Isotropic Dual Polarization Ring Array.

The design described in Section 4 has not appeared elsewhere in the literature, and it likely qualifies as an invention. A concise description of the invention follows.

The array consists of eight elements, directed radially outward, and equally spaced around a circle. The elements alternate in type between electric and magnetic. The phases progress in steps of 45 degrees, starting from 0. The radius of the circle is one-quarter wavelength at the highest frequency of interest. The array retains its pattern for all lower frequencies.

The unique features of the array are: that no null is deeper than -6.4 db with reference to an isotropic radiator; that this is true for each of the two orthogonal field components E_θ and E_ϕ separately; that the magnetic elements tend to control the component E_θ independently, and that the electric elements tend to control the component E_ϕ independently; and that the ring geometry of the array is well suited to the placement of a cylinder or mast through its center.

9.2. Satellite Omnipurpose Antenna Program (SOAP).

A FORTRAN computer program featuring many original algorithms has been developed. The purpose of the program is to compute the electromagnetic field of any combination of electric and magnetic dipoles in the presence of any combination of conducting plates and cylinders. The latter combination is intended to simulate a satellite, space craft, aircraft, ship, land vehicle, etc.

10. Appendices: Plots of Radiation Patterns.

These patterns correspond to the array shown as Fig. 7.1. This array is not necessarily superior to that described in Section 4. It was investigated as part of the development of the computer program SOAP. The investigation cannot be conclusive until subroutines for diffraction phenomena are added to SOAP.

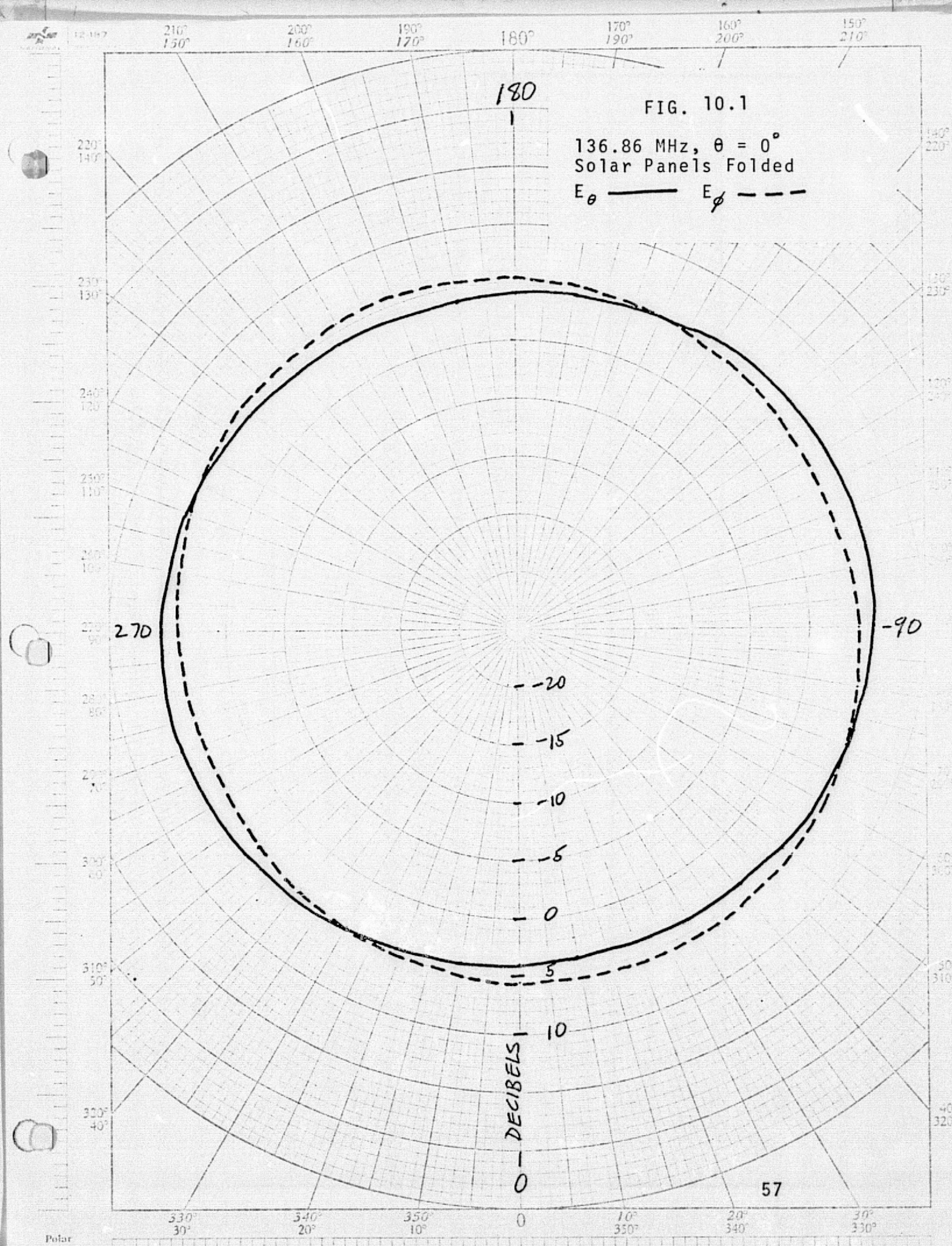
FIG. 10.1
136.86 MHz, θ = 0°
Solar Panels Folded
E_θ —— E_ϕ - - -
180
270
-90
0
-20
-15
-10
-5
0
5
10
0 - DECIBELS
Polar

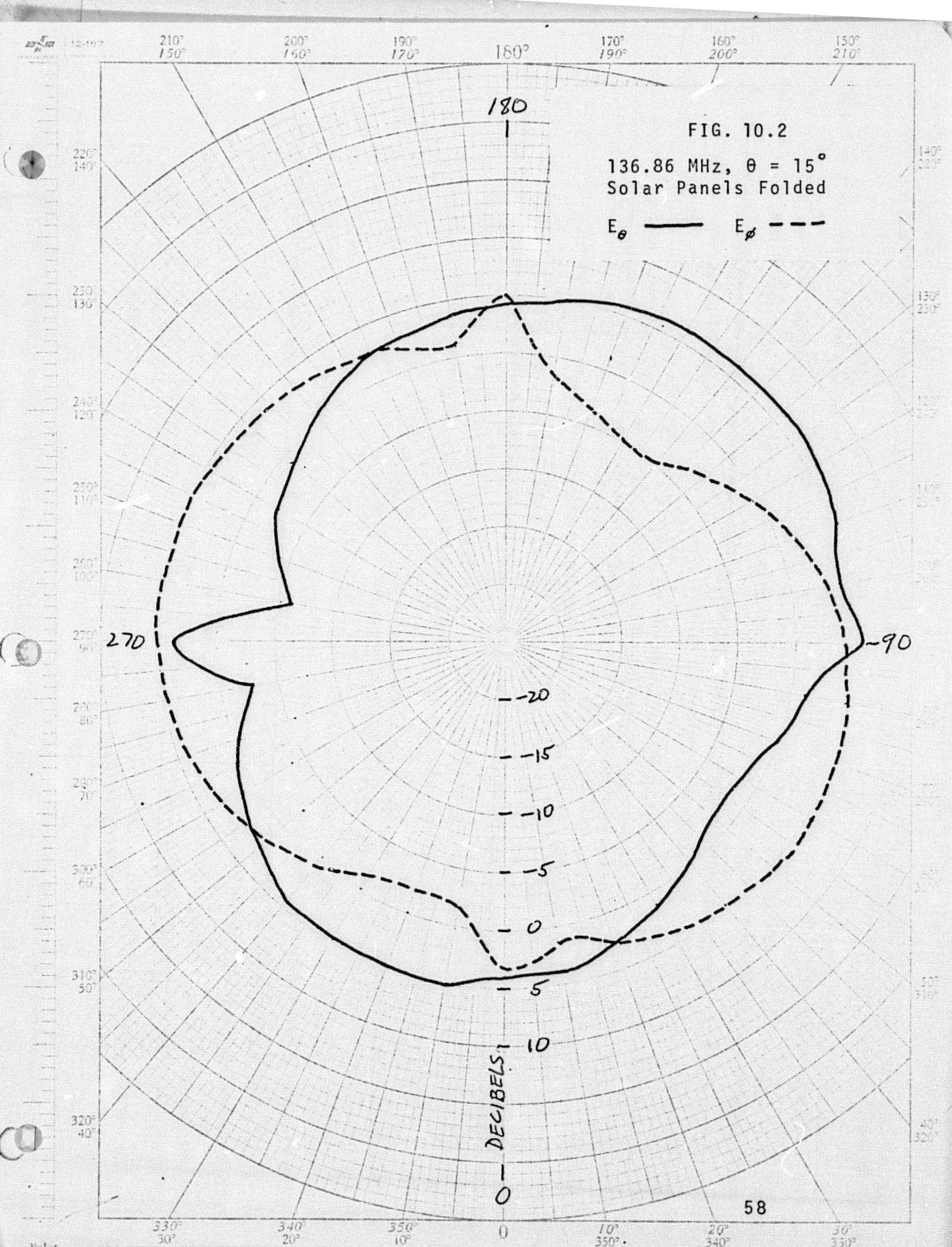

FIG. 10.2

136.86 MHz, θ = 15°
Solar Panels Folded

E_θ ——— E_ϕ - - -

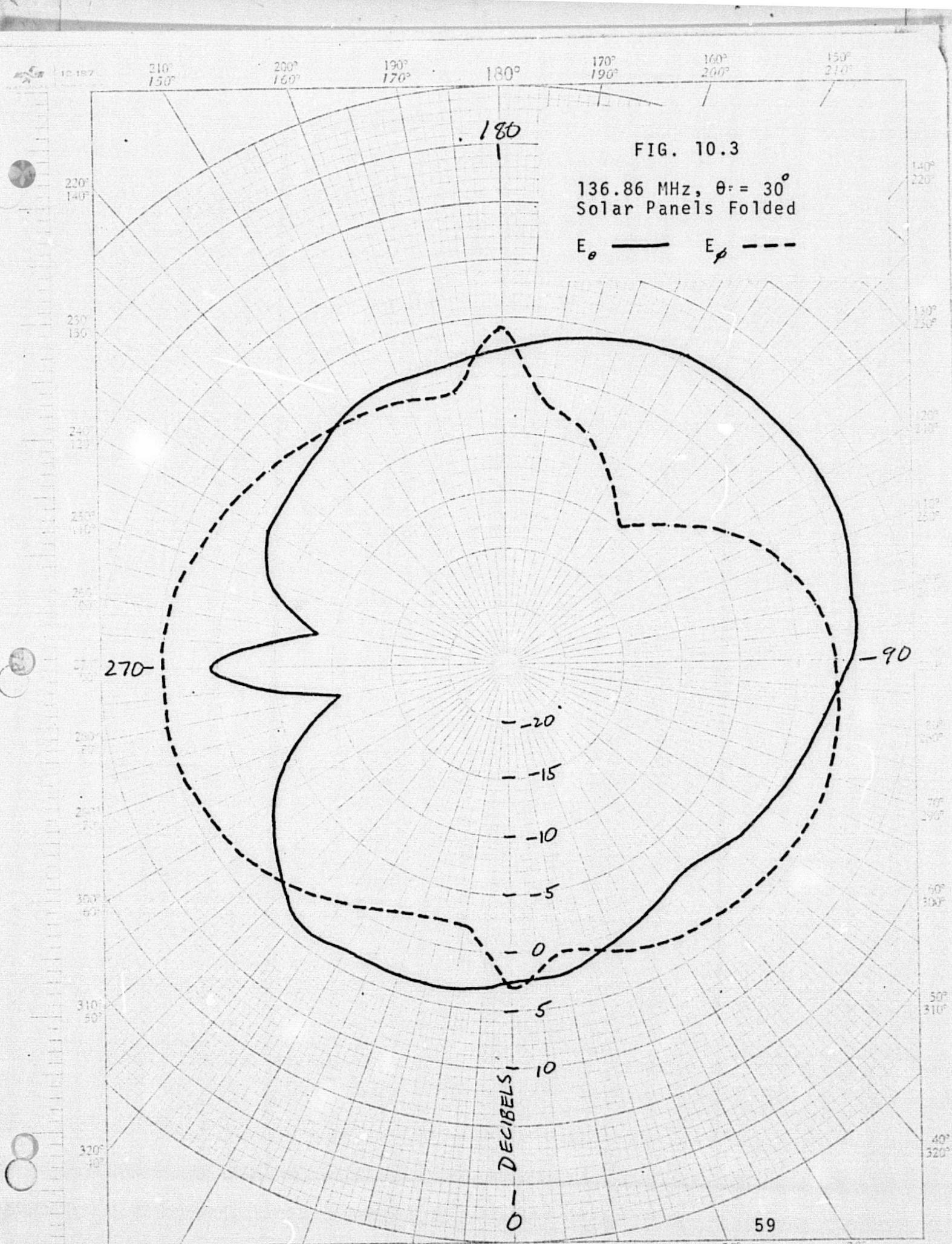

FIG. 10.3

136.86 MHz, $\theta = 30^{\circ}$
Solar Panels Folded

E_θ ——— E_ϕ - - -

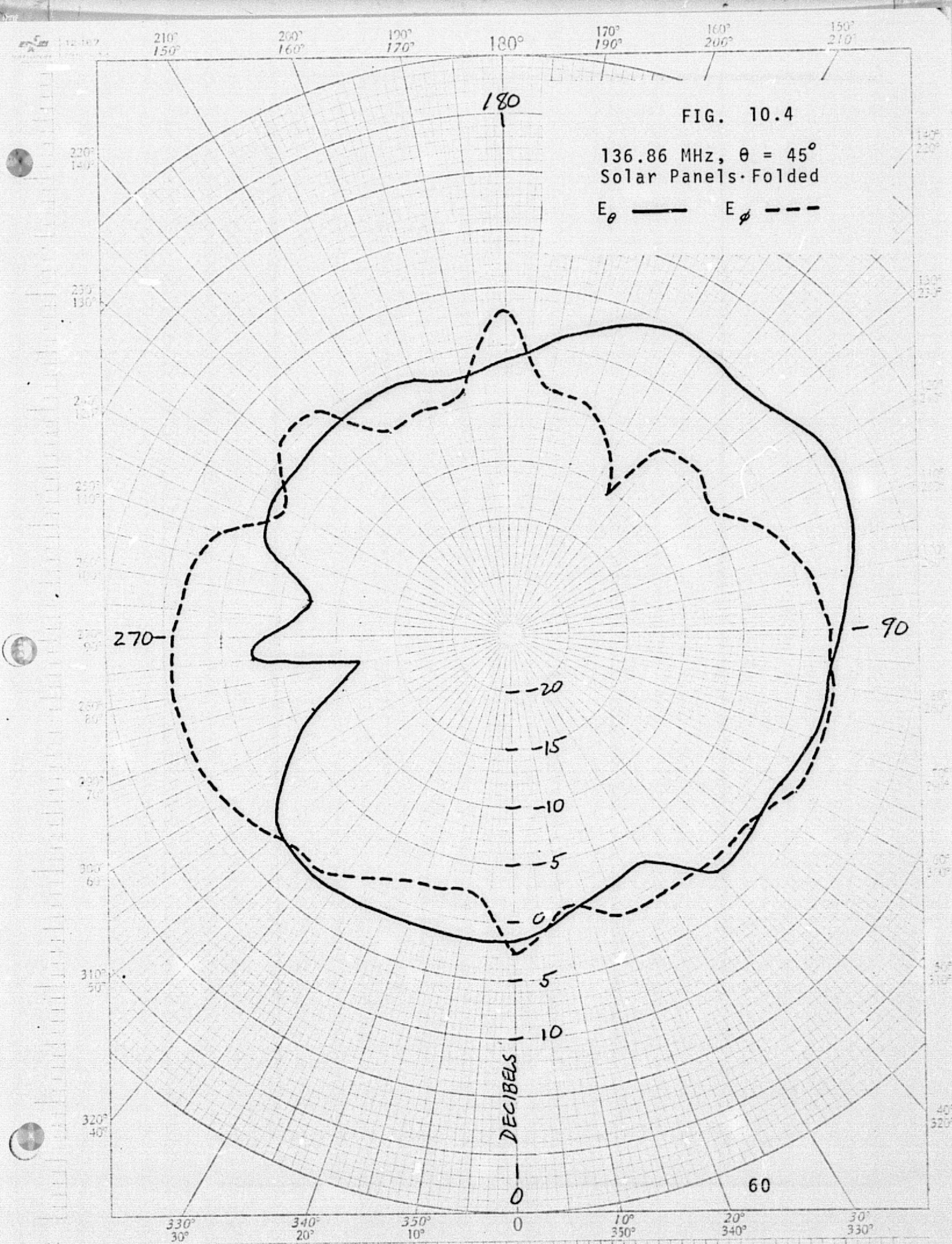
FIG. 10.4
136.86 MHz, θ = 45°
Solar Panels Folded
E_θ —— E_ϕ - - -
180
270
90
60
0
-20
-15
-10
-5
0
-5
-10
DECIBELS

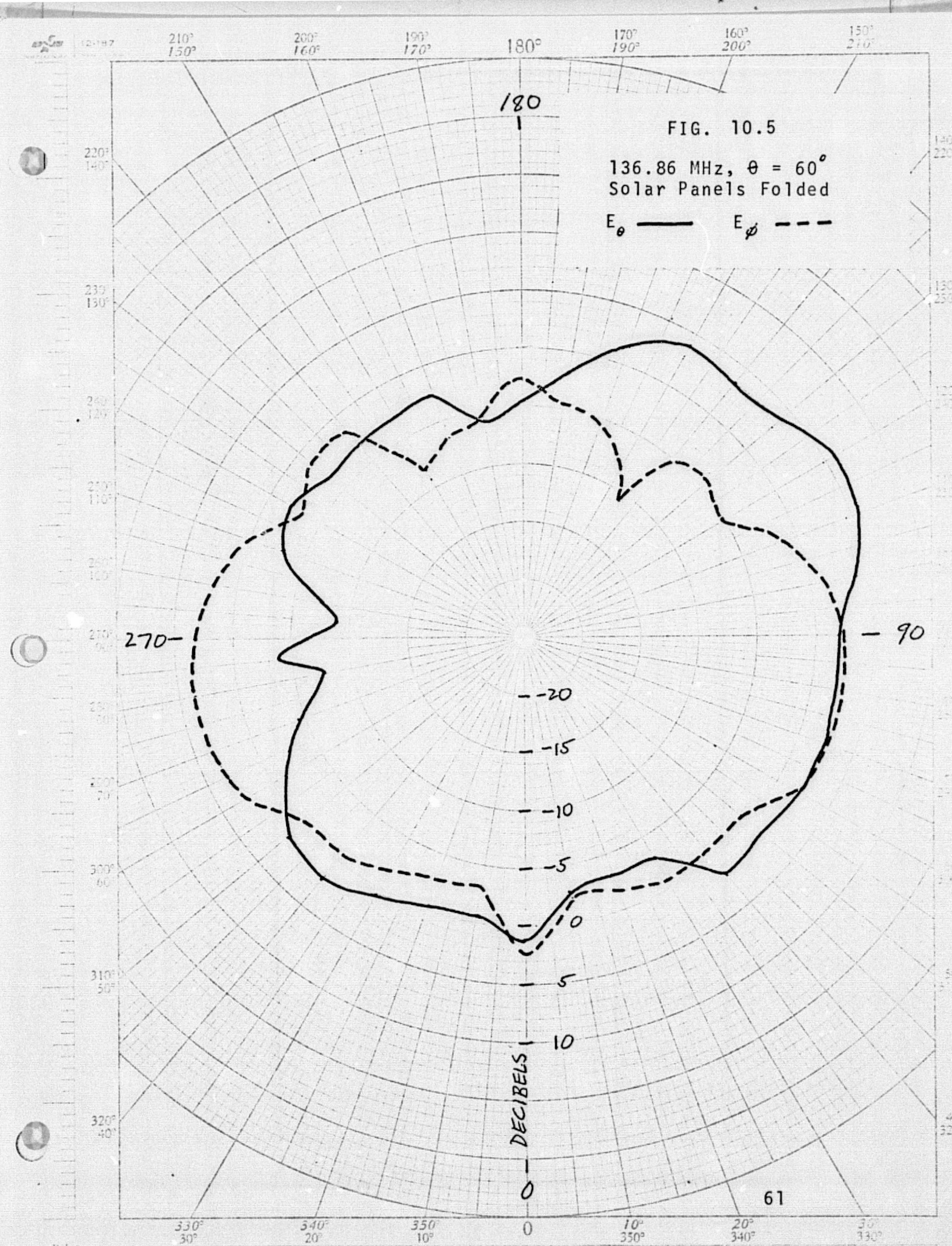

FIG. 10.5

136.86 MHz, $\theta = 60^{\circ}$
Solar Panels Folded

E_{θ} ——— E_{ϕ} - - -

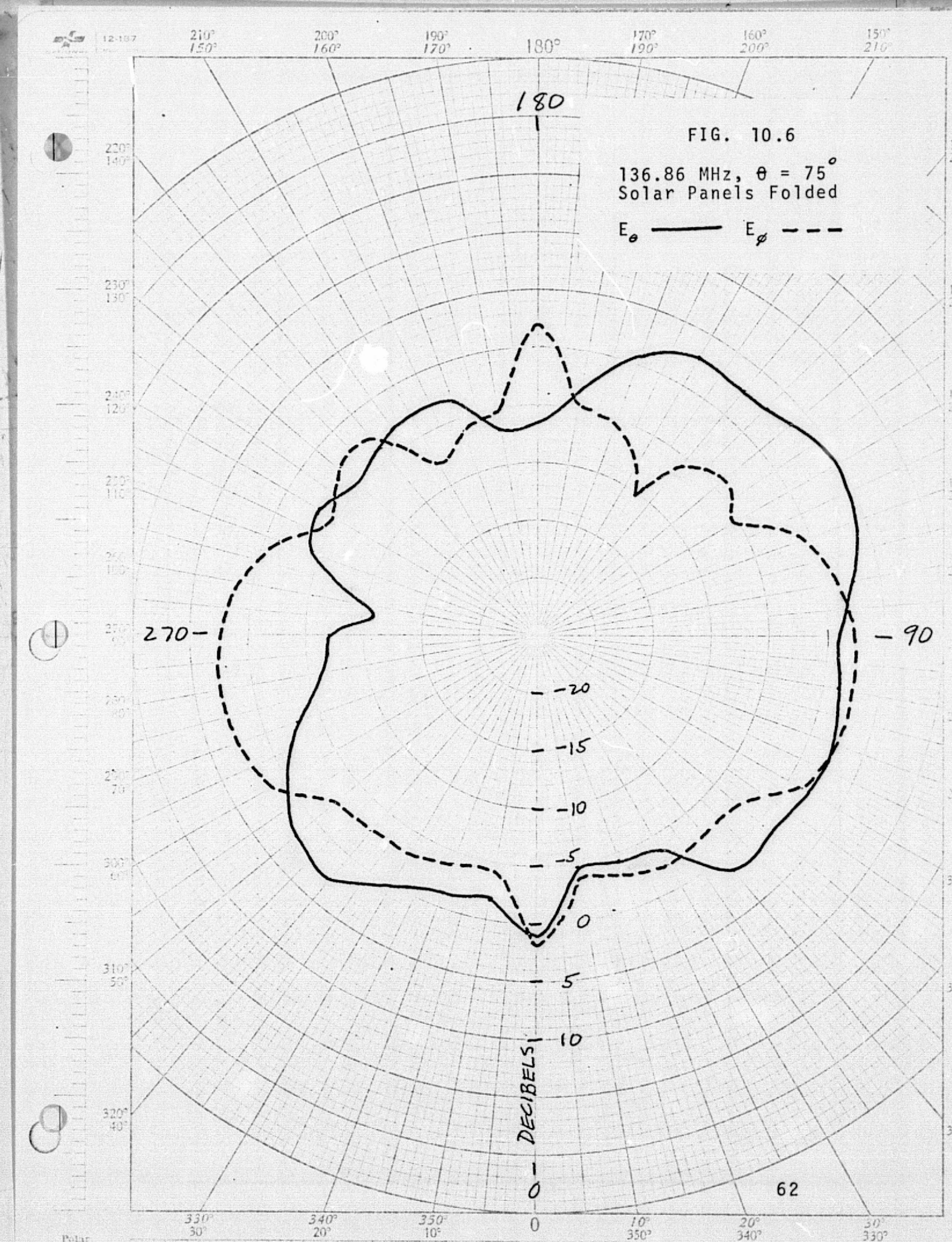
180
270
90
0
-20
-15
-10
-5
0
5
10
DECIBELS
FIG. 10.6
136.86 MHz, θ = 75°
Solar Panels Folded
E_θ ——— E_ϕ - - -

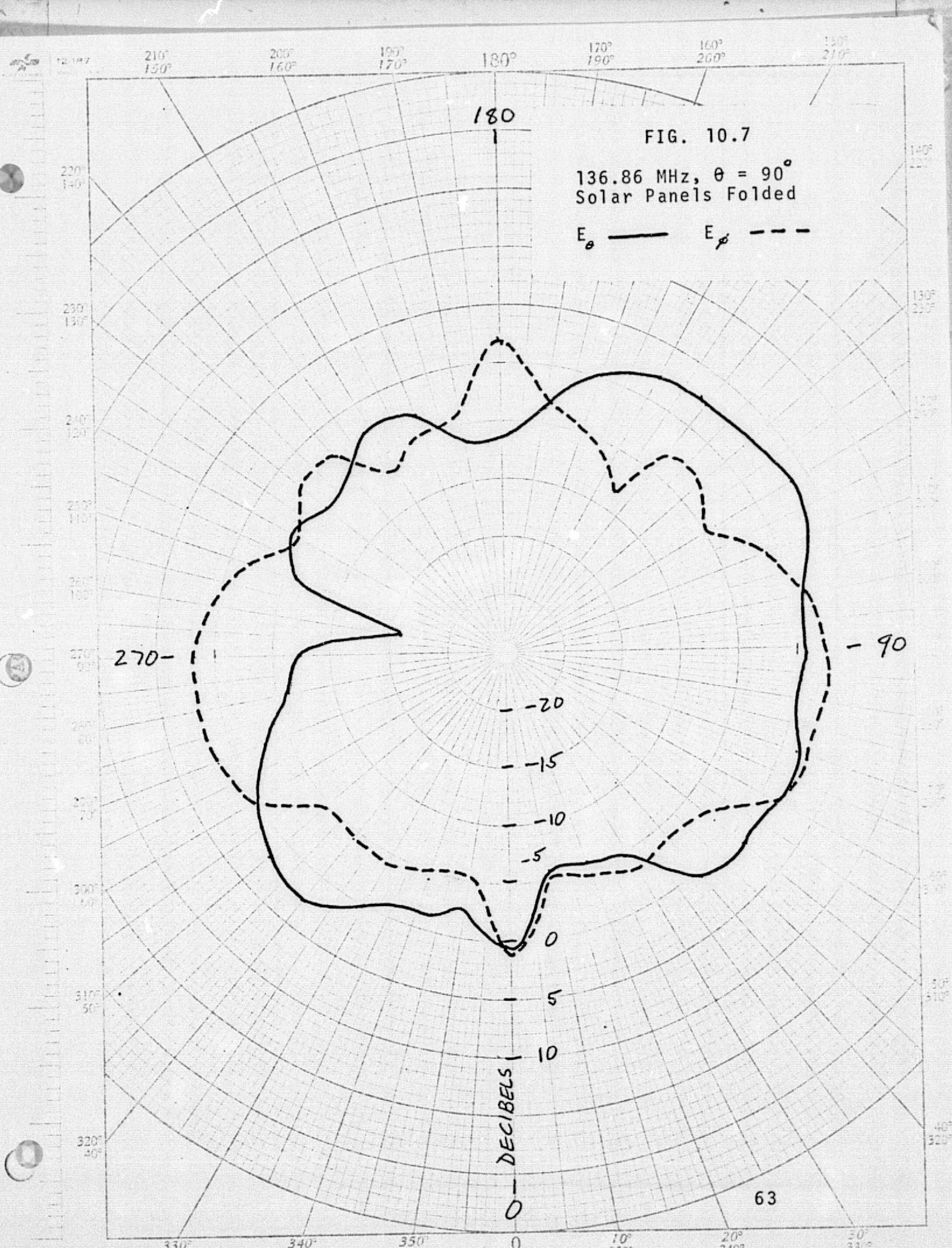

FIG. 10.7

136.86 MHz, $\theta = 90^{\circ}$
Solar Panels Folded

E_{θ} ——— E_{ϕ} - - -

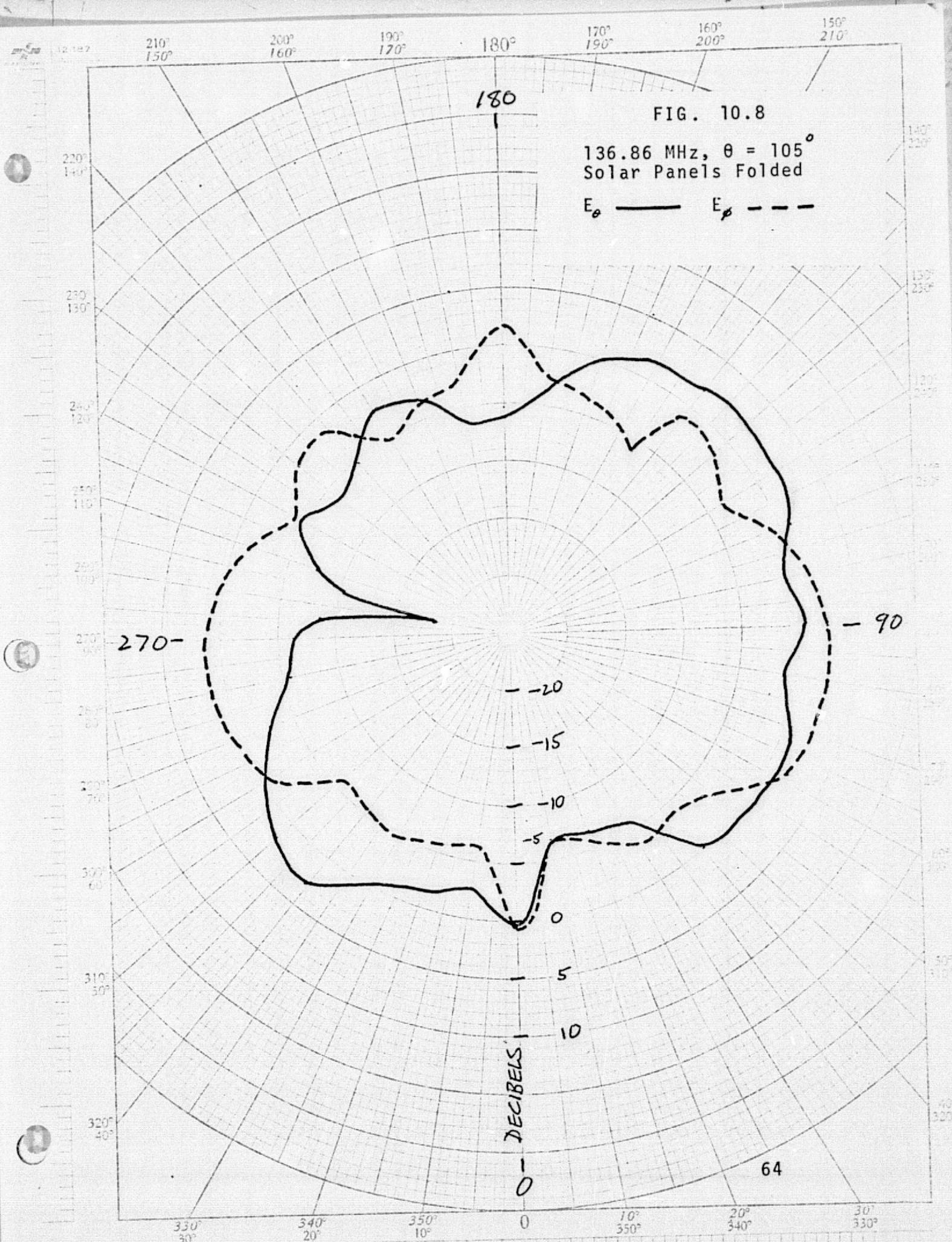
FIG. 10.8
136.86 MHz, θ = 105°
Solar Panels Folded
E_θ ——— E_ϕ - - -
180
270
90
-20
-15
-10
-5
0
5
10
DECIBELS
0
64

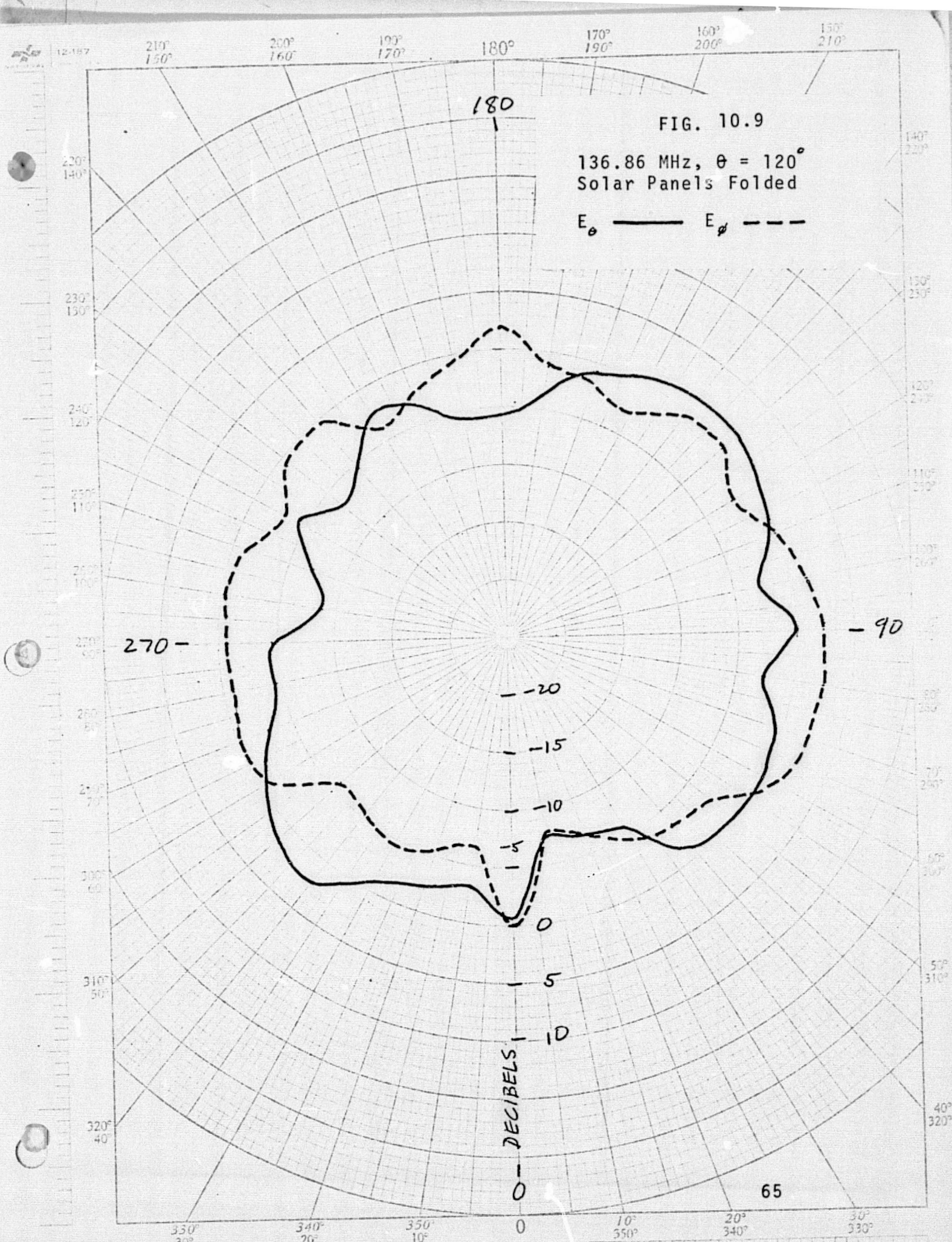

FIG. 10.9

136.86 MHz, $\theta = 120^{\circ}$
Solar Panels Folded

E_{θ} ——— E_{ϕ} - - -

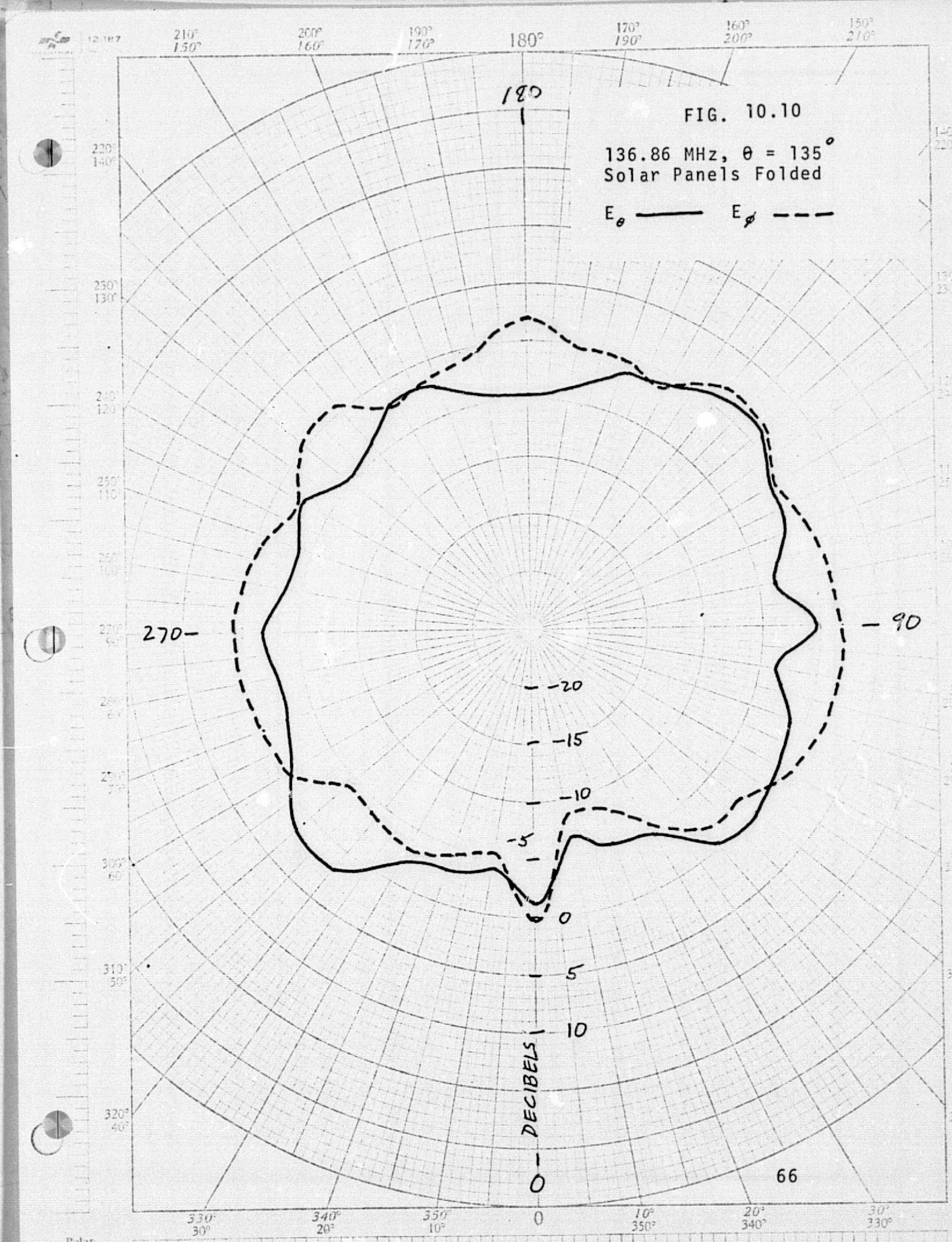
FIG. 10.10
136.86 MHz, θ = 135°
Solar Panels Folded
E_θ ——— E_ϕ - - -
180
270
90
-20
-15
-10
-5
0
5
10
DECIBELS
66

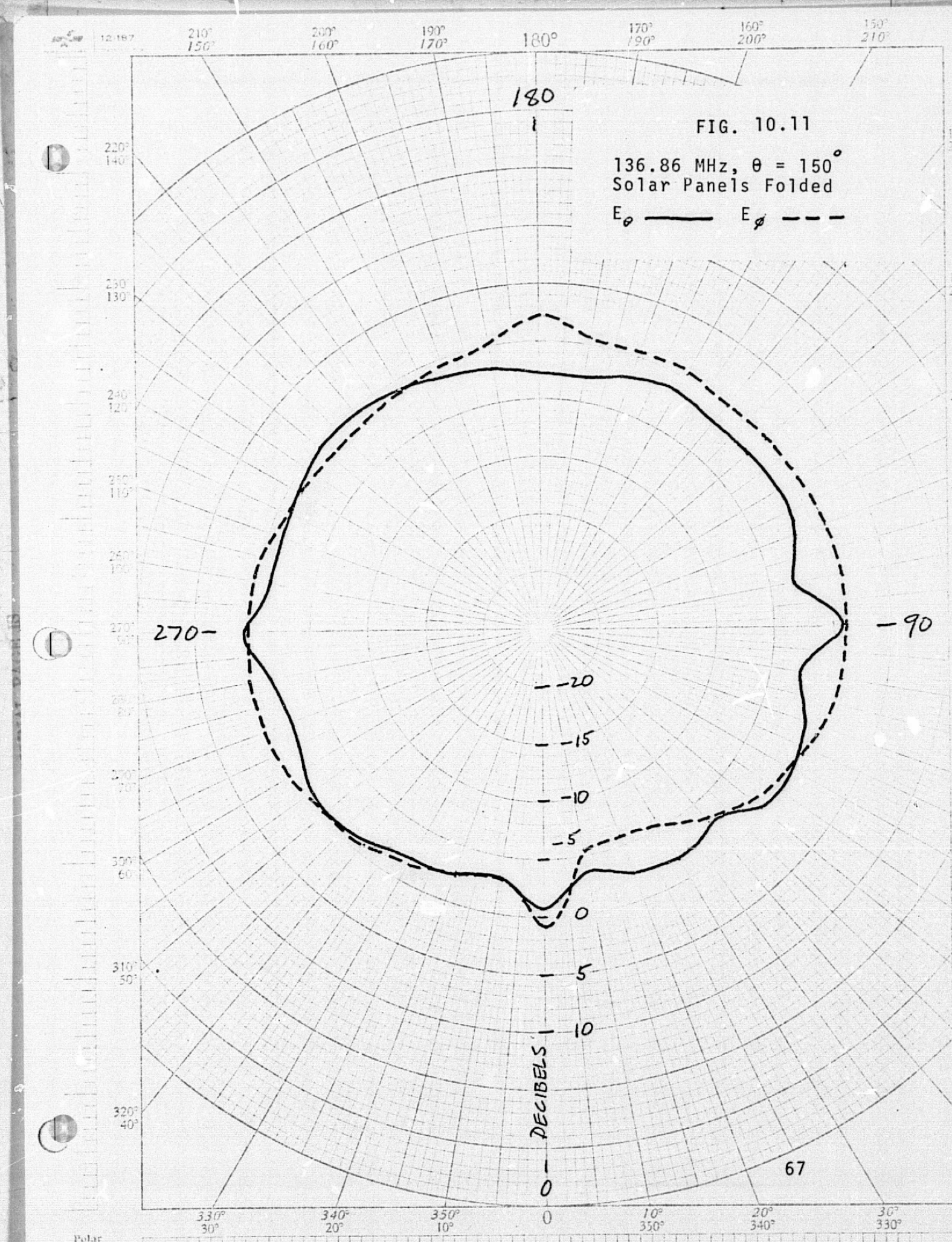

FIG. 10.11

136.86 MHz, θ = 150°
Solar Panels Folded

E_θ ——— E_ϕ - - -

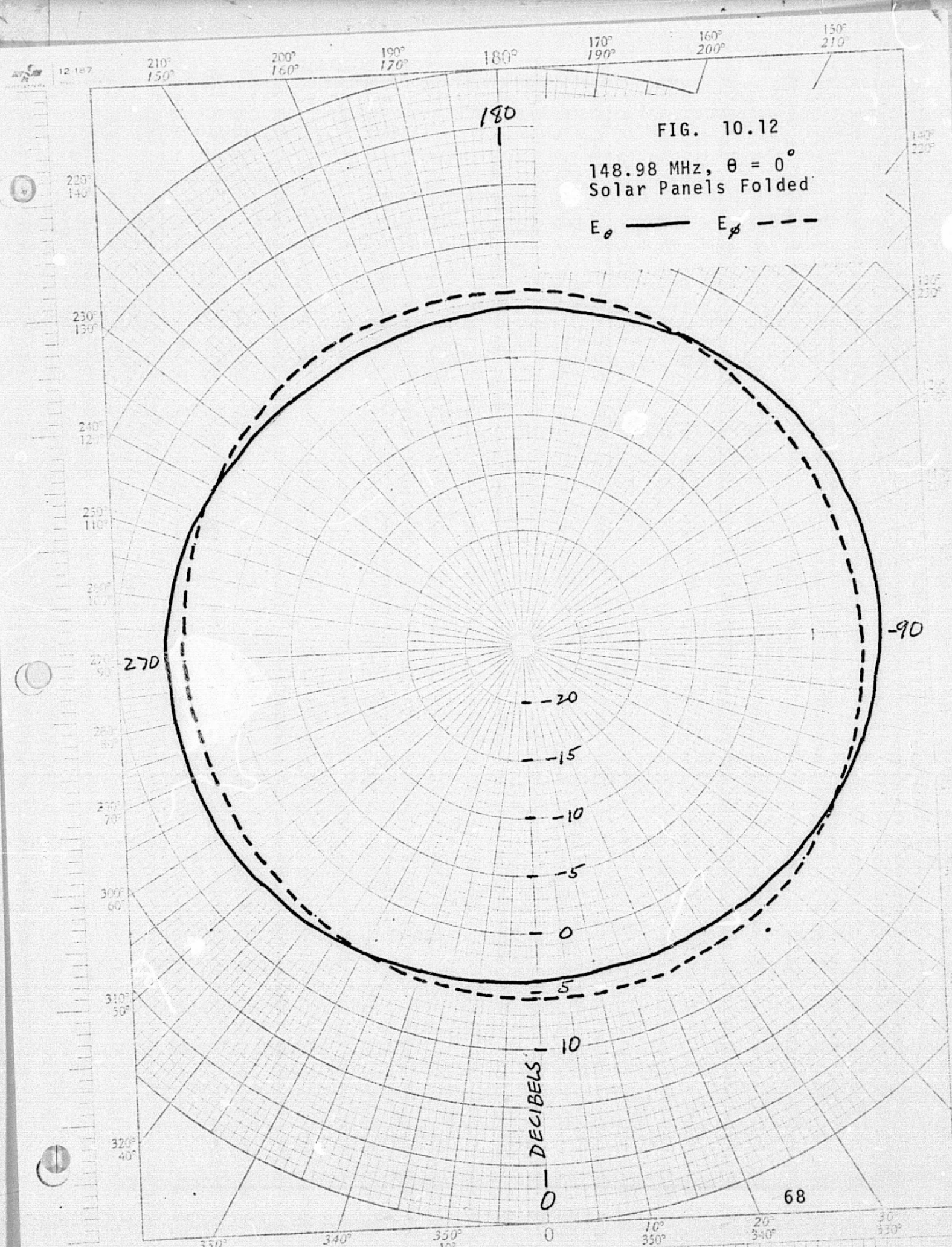

FIG. 10.12

148.98 MHz, $\theta = 0^{\circ}$
Solar Panels Folded

E_{θ} ——— E_{ϕ} - - -

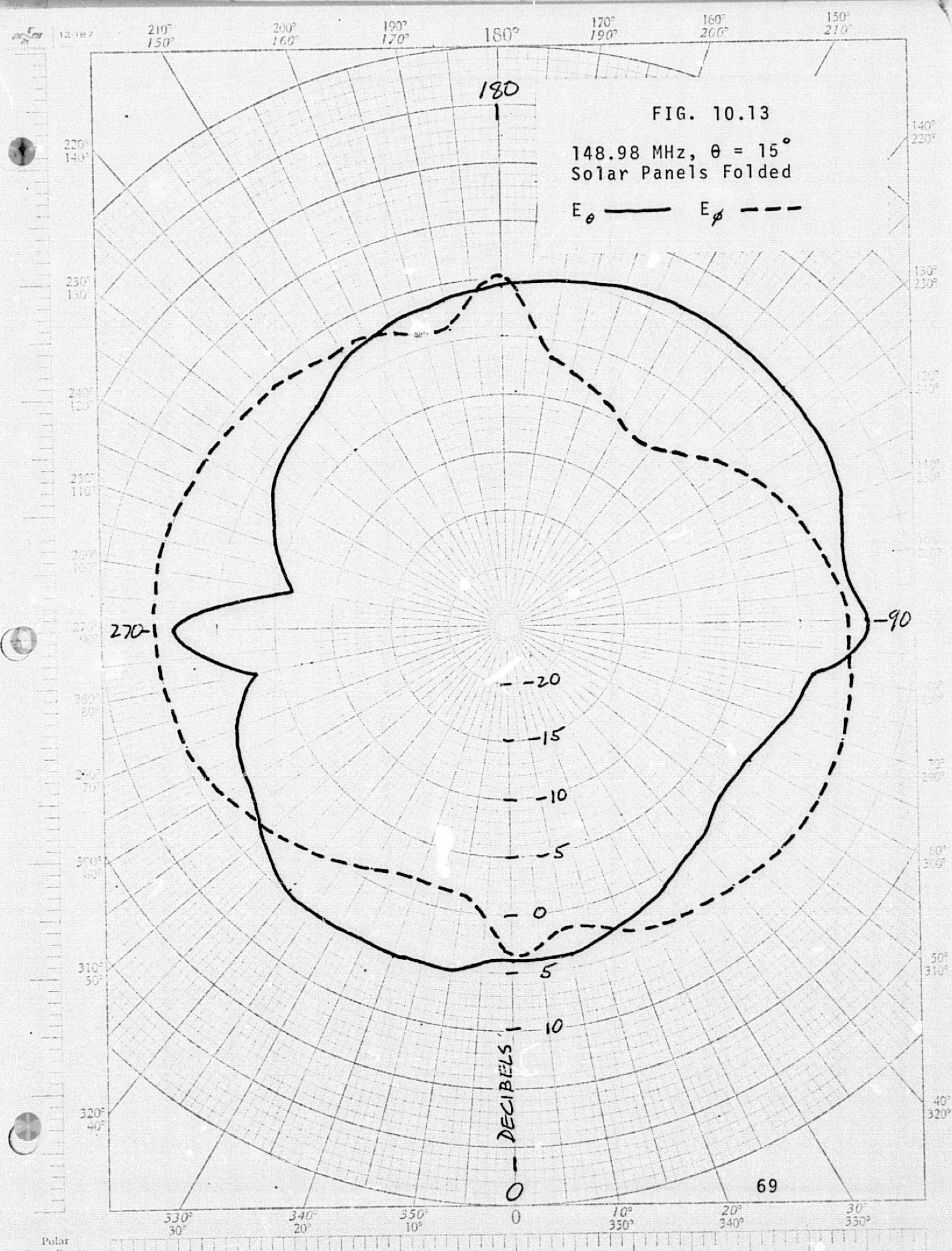
180
270
90
0
-20
-15
-10
-5
0
5
10
DECIBELS
FIG. 10.13
148.98 MHz, θ = 15°
Solar Panels Folded
E_θ —— E_ϕ - - -

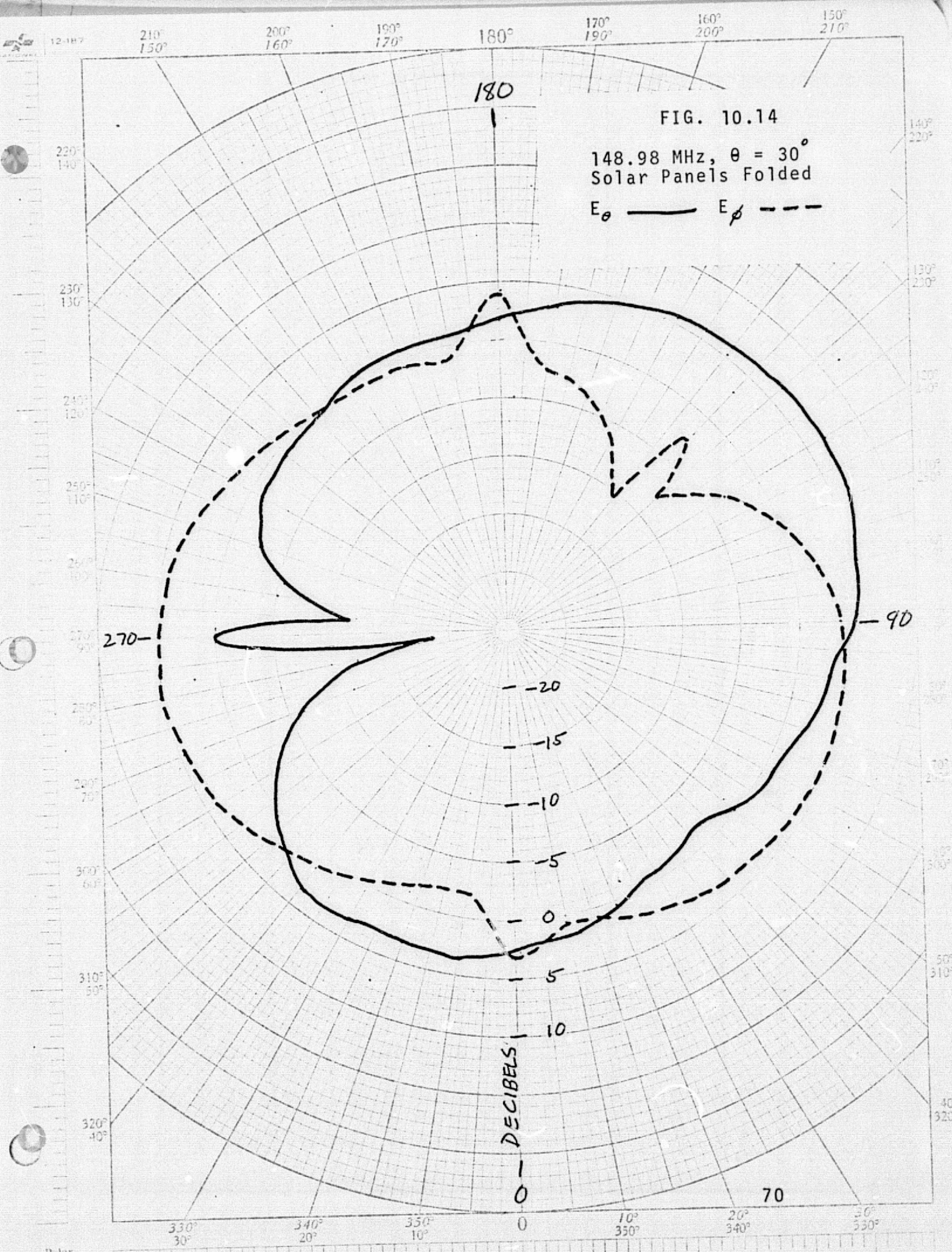
FIG. 10.14
148.98 MHz, θ = 30°
Solar Panels Folded
E_θ —— E_ϕ - - -
180
90
270
0
70
-20
-15
-10
-5
0
5
10
DECIBELS

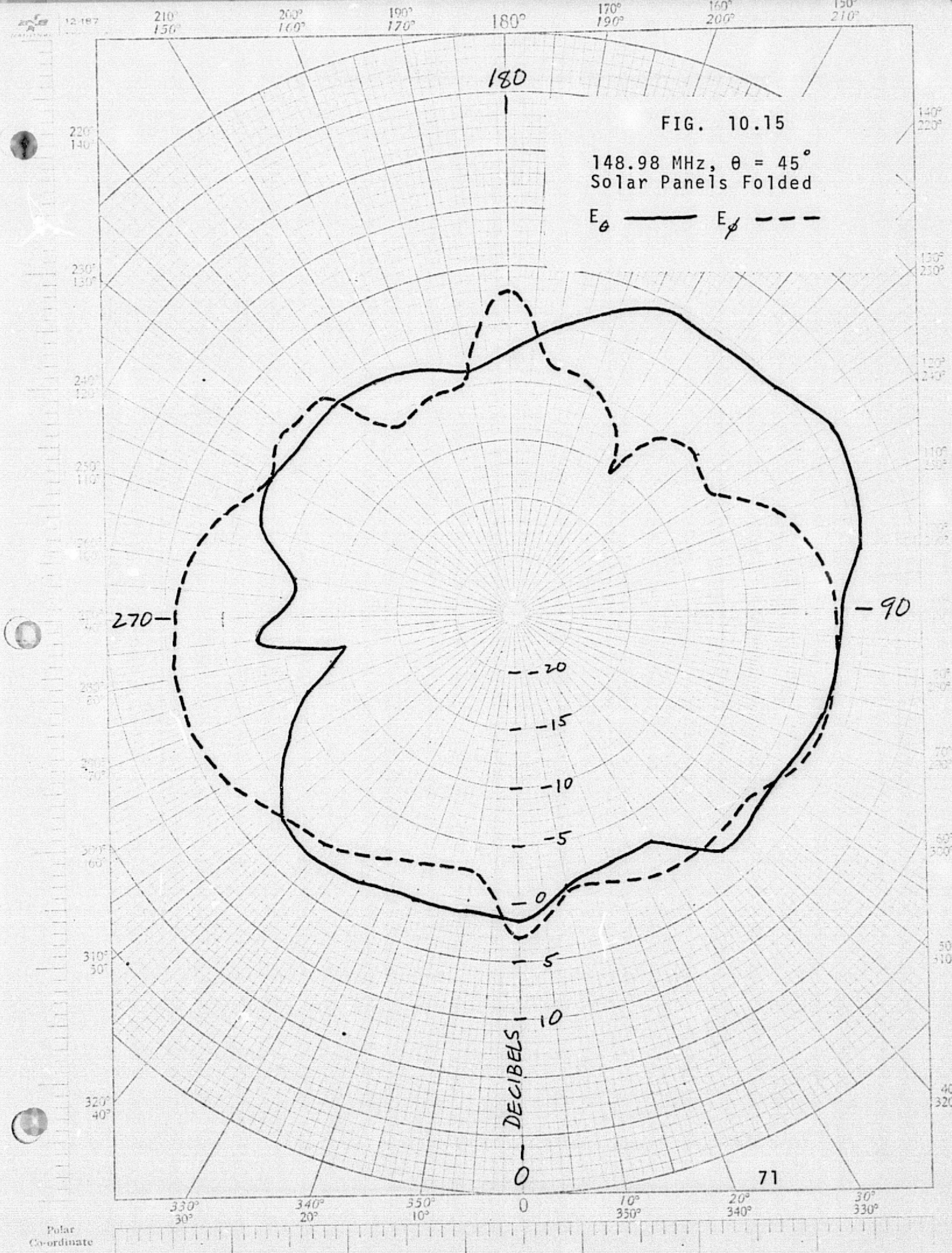
180
270
90
0
-20
-15
-10
-5
-0
5
10
DECIBELS
FIG. 10.15
148.98 MHz, θ = 45°
Solar Panels Folded
E_θ —— E_ϕ - - -
71

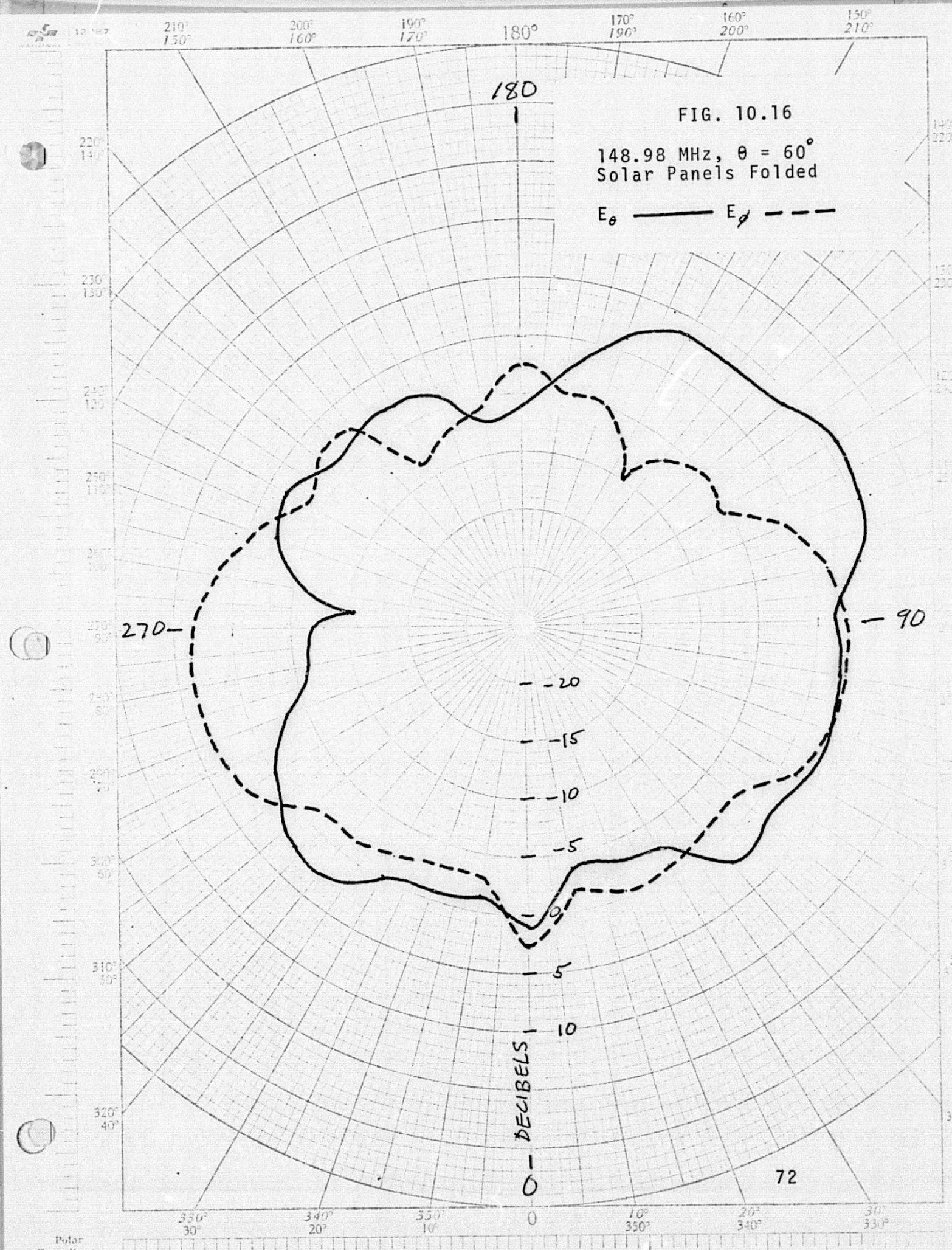

FIG. 10.16

148.98 MHz, θ = 60°
Solar Panels Folded

E_θ ——— E_ϕ - - -

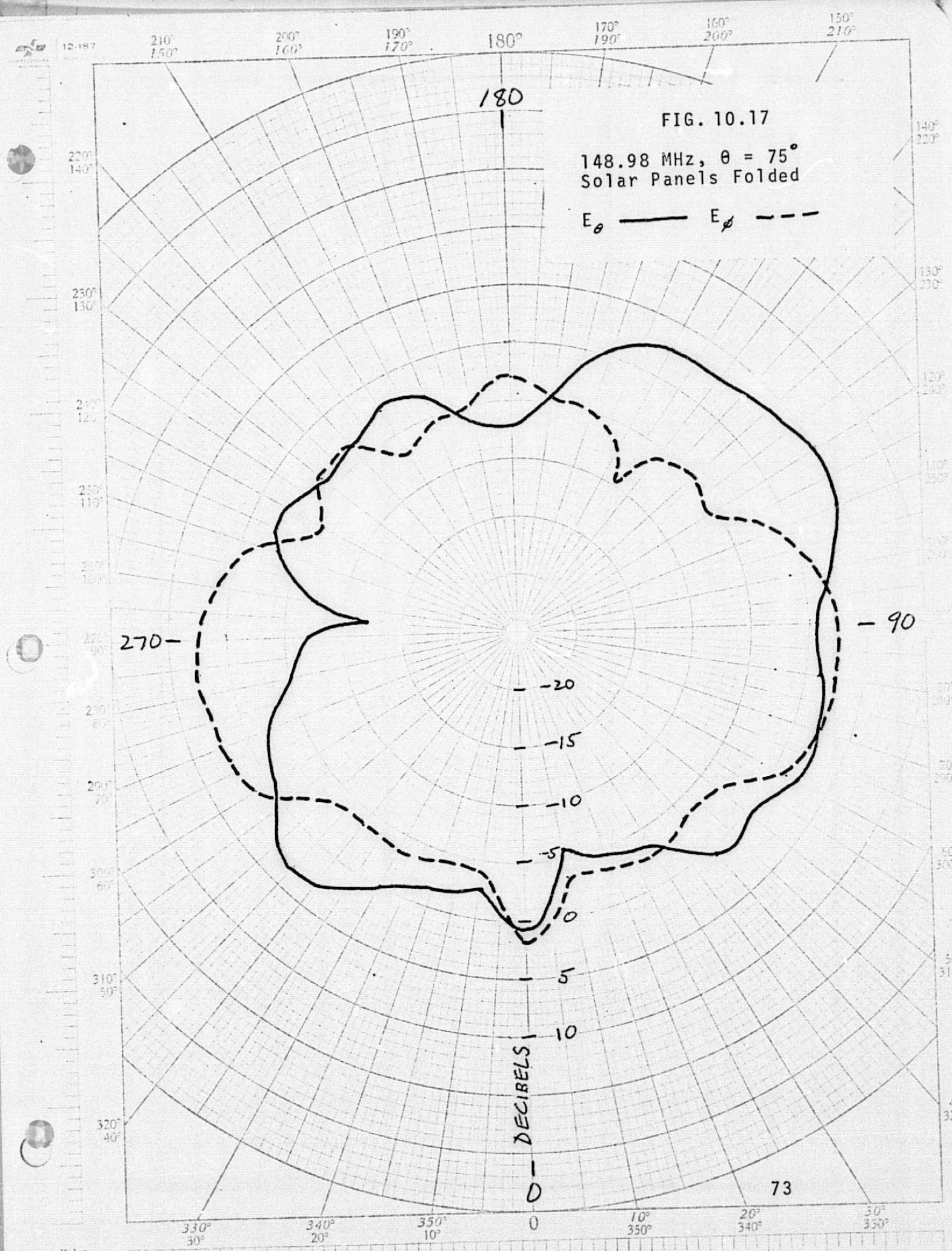

FIG. 10.17

148.98 MHz, θ = 75°
Solar Panels Folded

E_θ ——— E_ϕ - - -

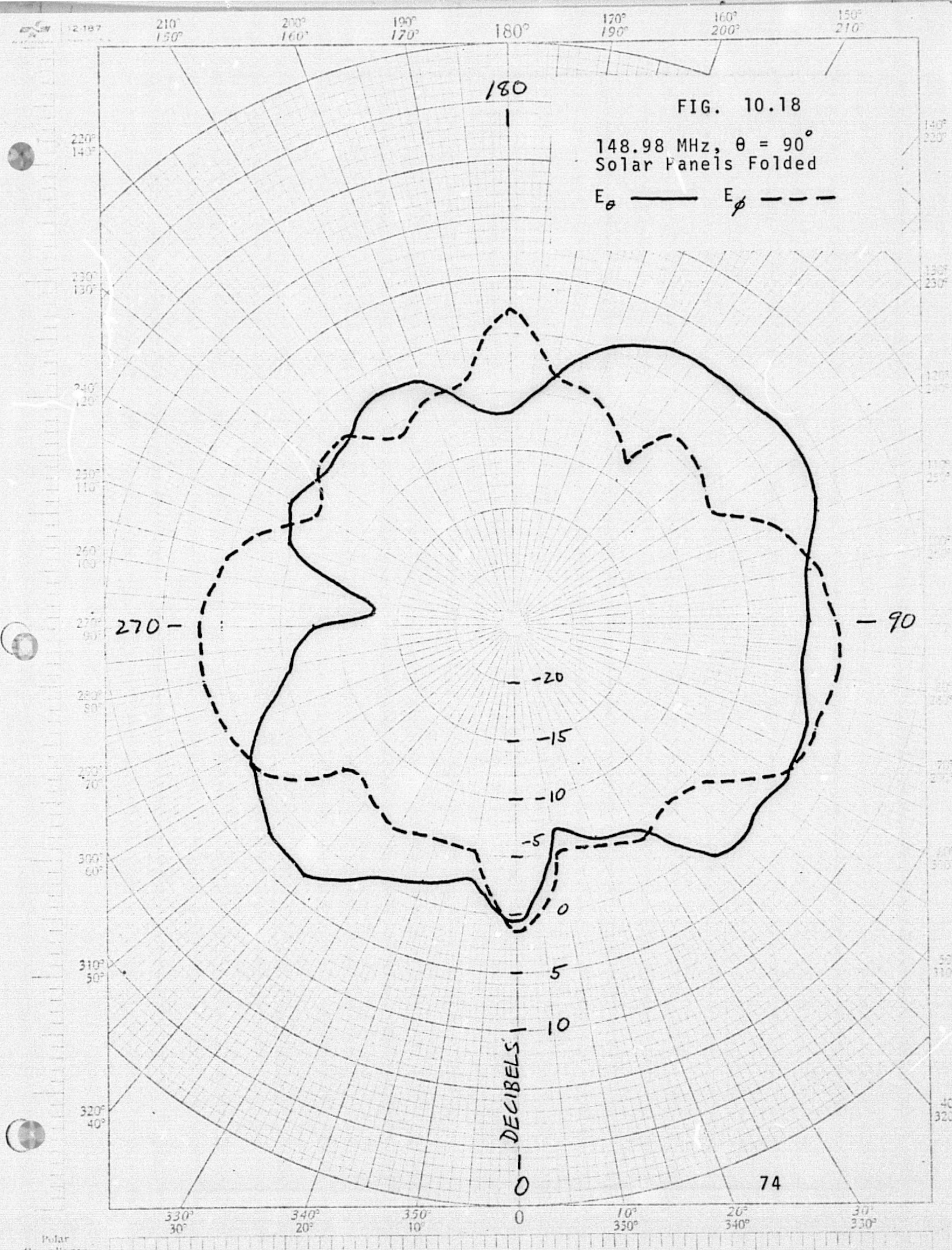

FIG. 10.18

148.98 MHz, θ = 90°
Solar Panels Folded

E_θ ——— E_ϕ - - -

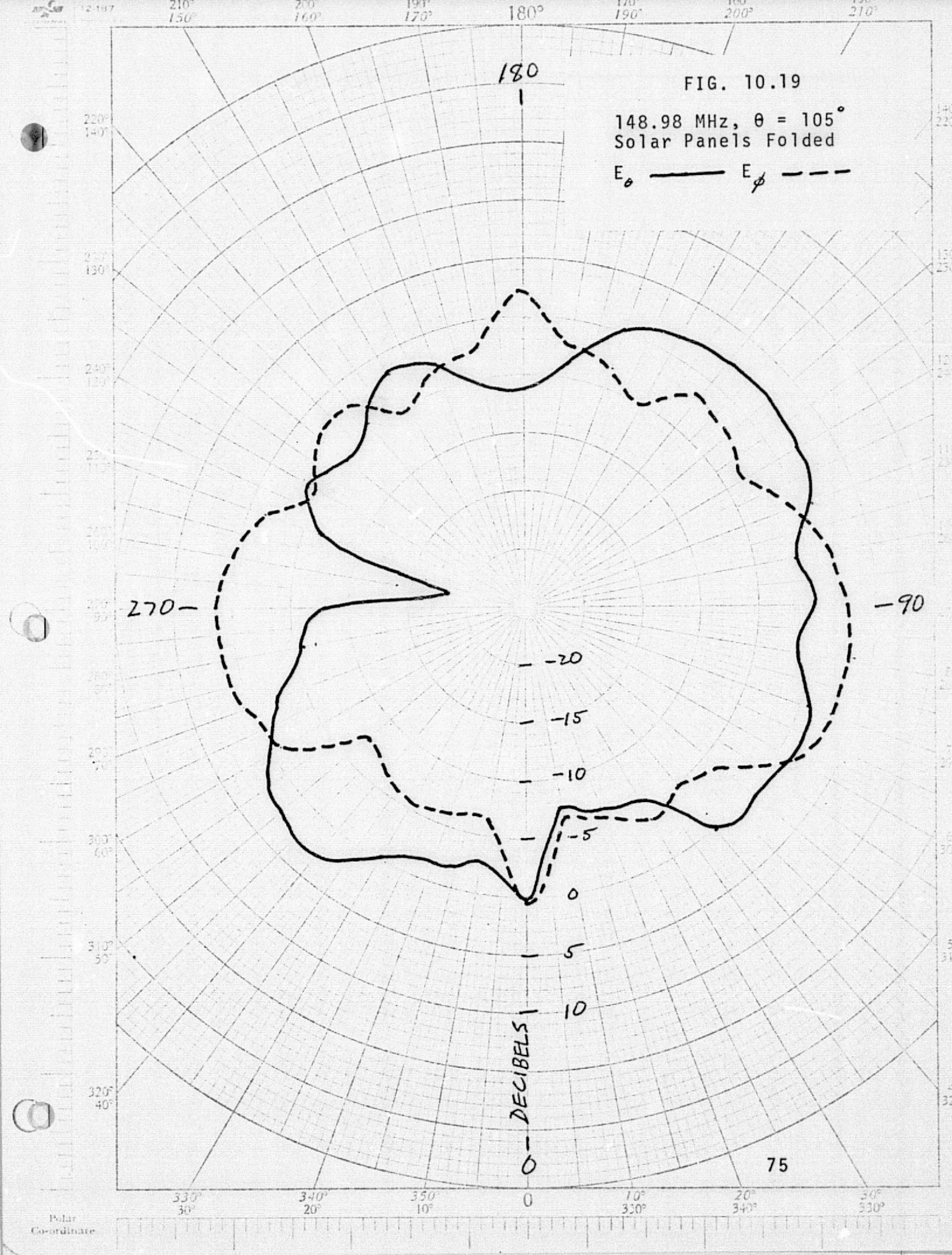

FIG. 10.19

148.98 MHz, θ = 105°
Solar Panels Folded

E_θ ——— E_ϕ - - -

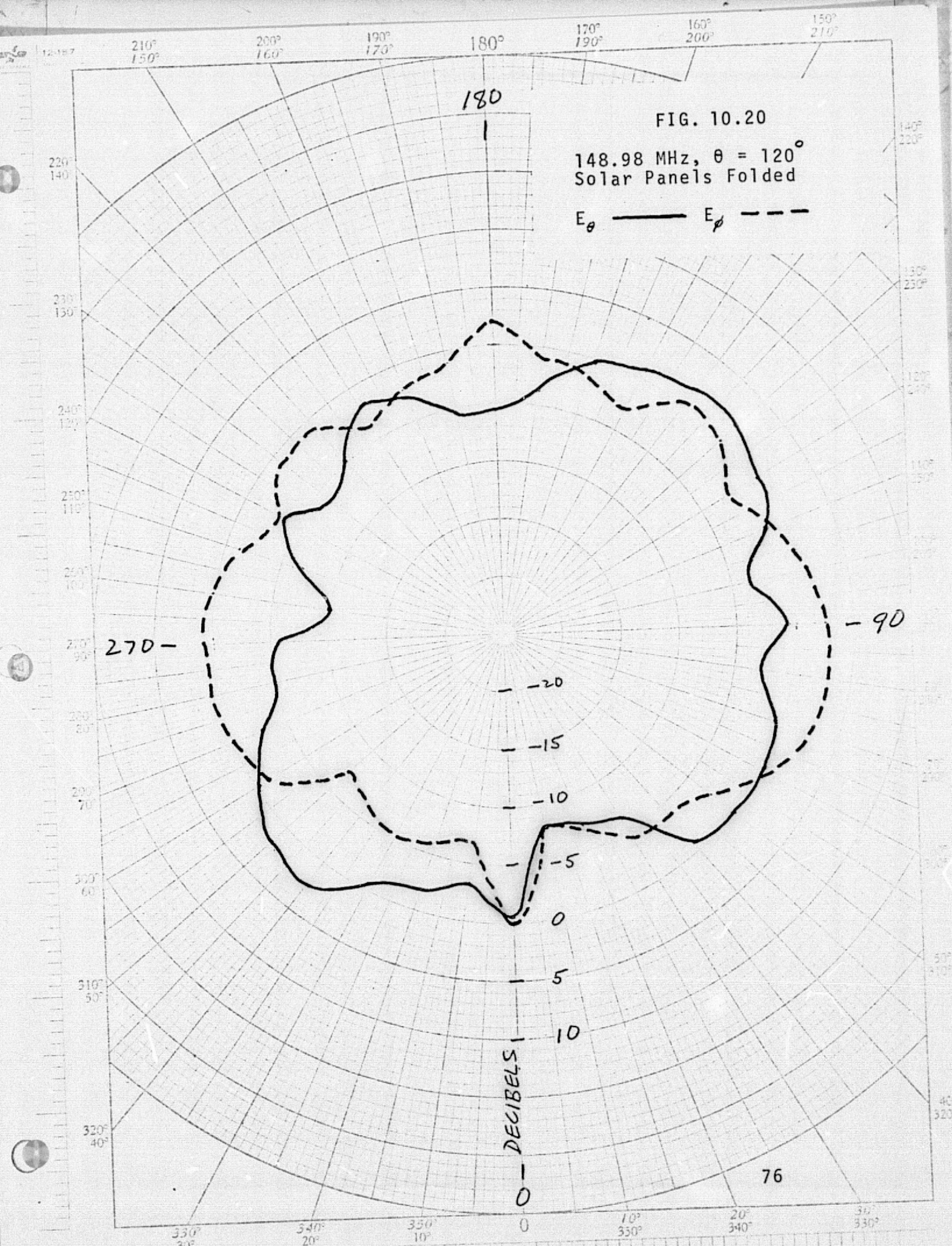

FIG. 10.20

148.98 MHz, θ = 120°
Solar Panels Folded

E_θ ——— E_ϕ - - -

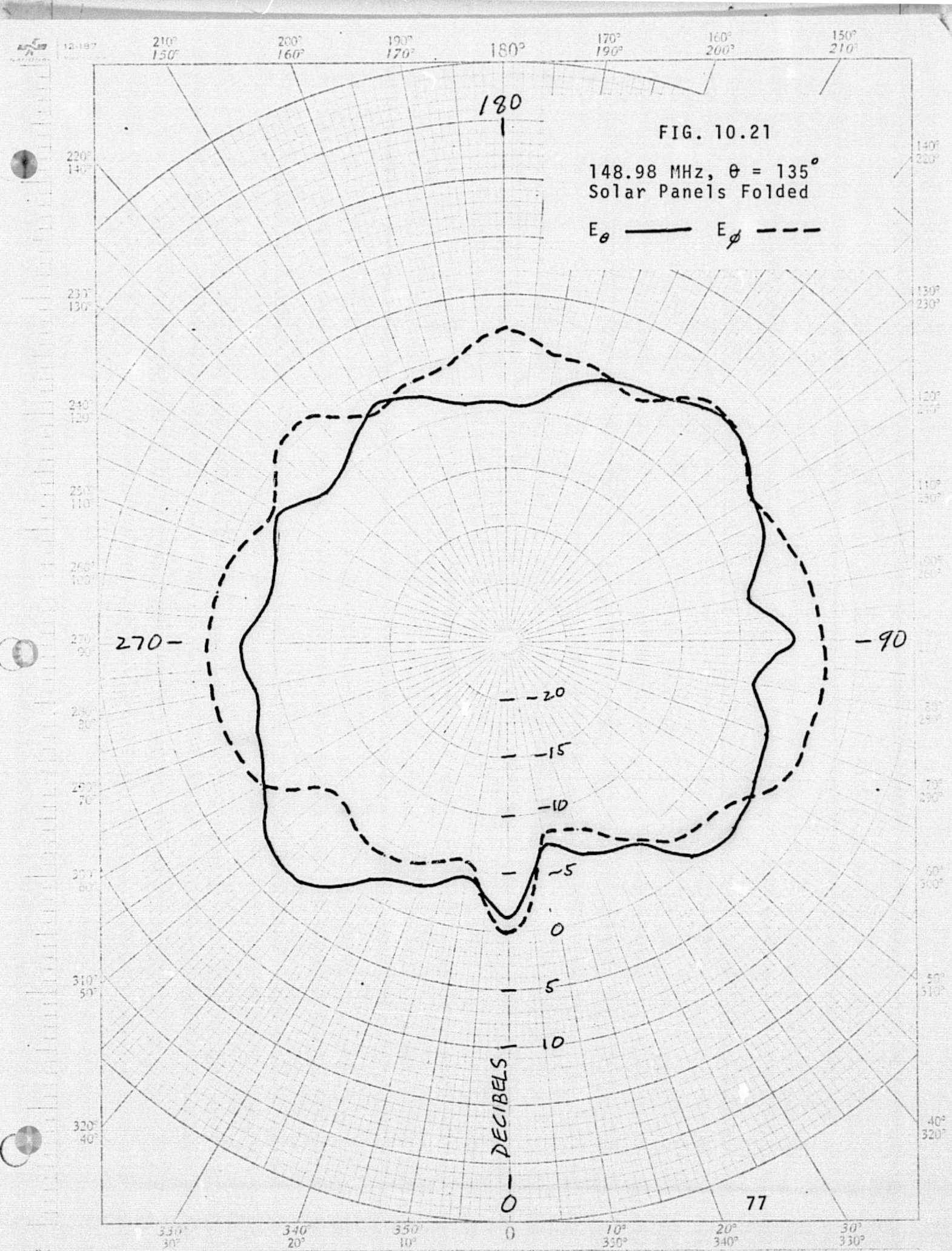

FIG. 10.21

148.98 MHz, $\theta = 135^{\circ}$
Solar Panels Folded

E_{θ} ——— E_{ϕ} - - -

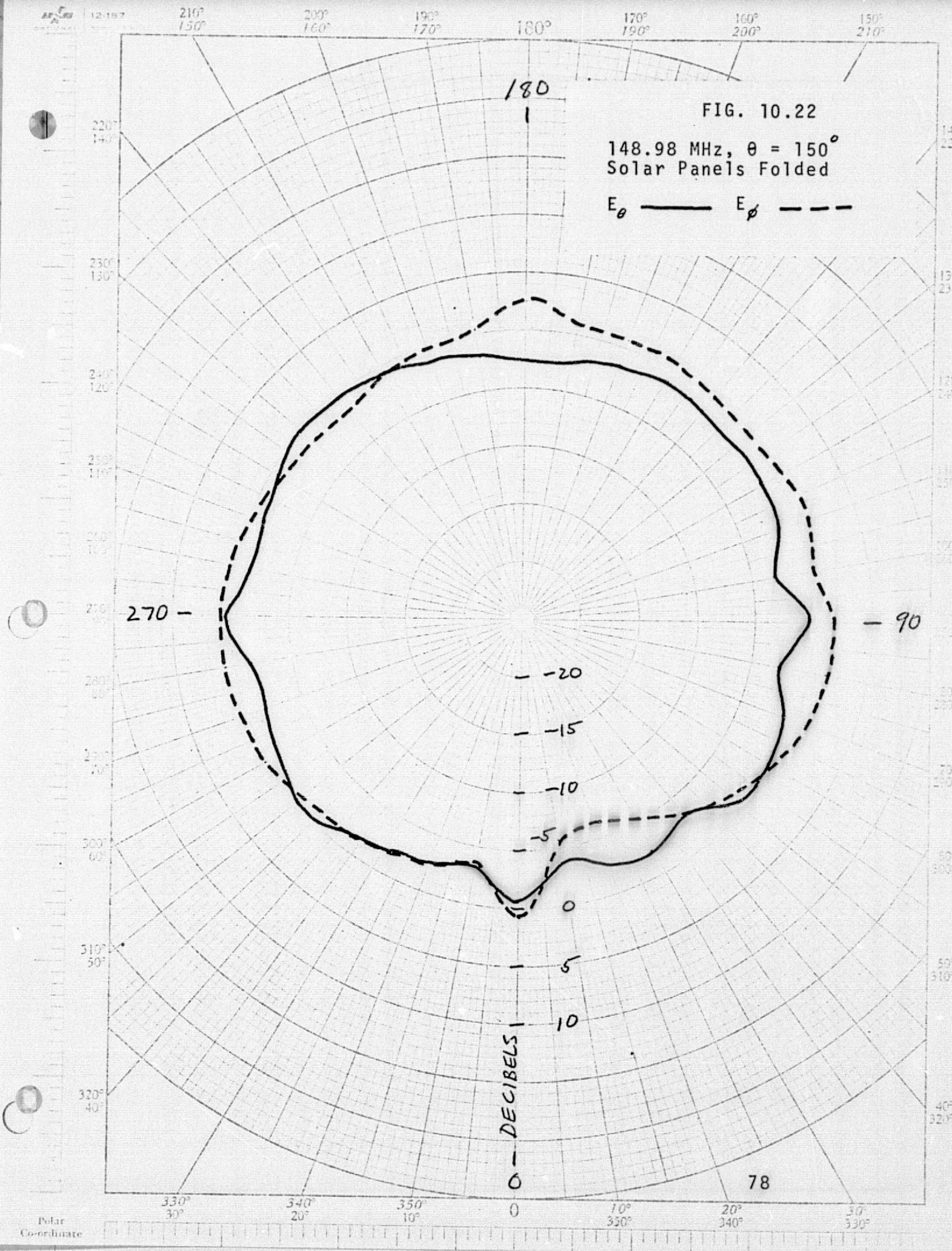
FIG. 10.22
148.98 MHz, θ = 150°
Solar Panels Folded
E_θ ——— E_ϕ – – –
180
270
90
0
-20
-15
-10
-5
0
5
10
DECIBELS
78

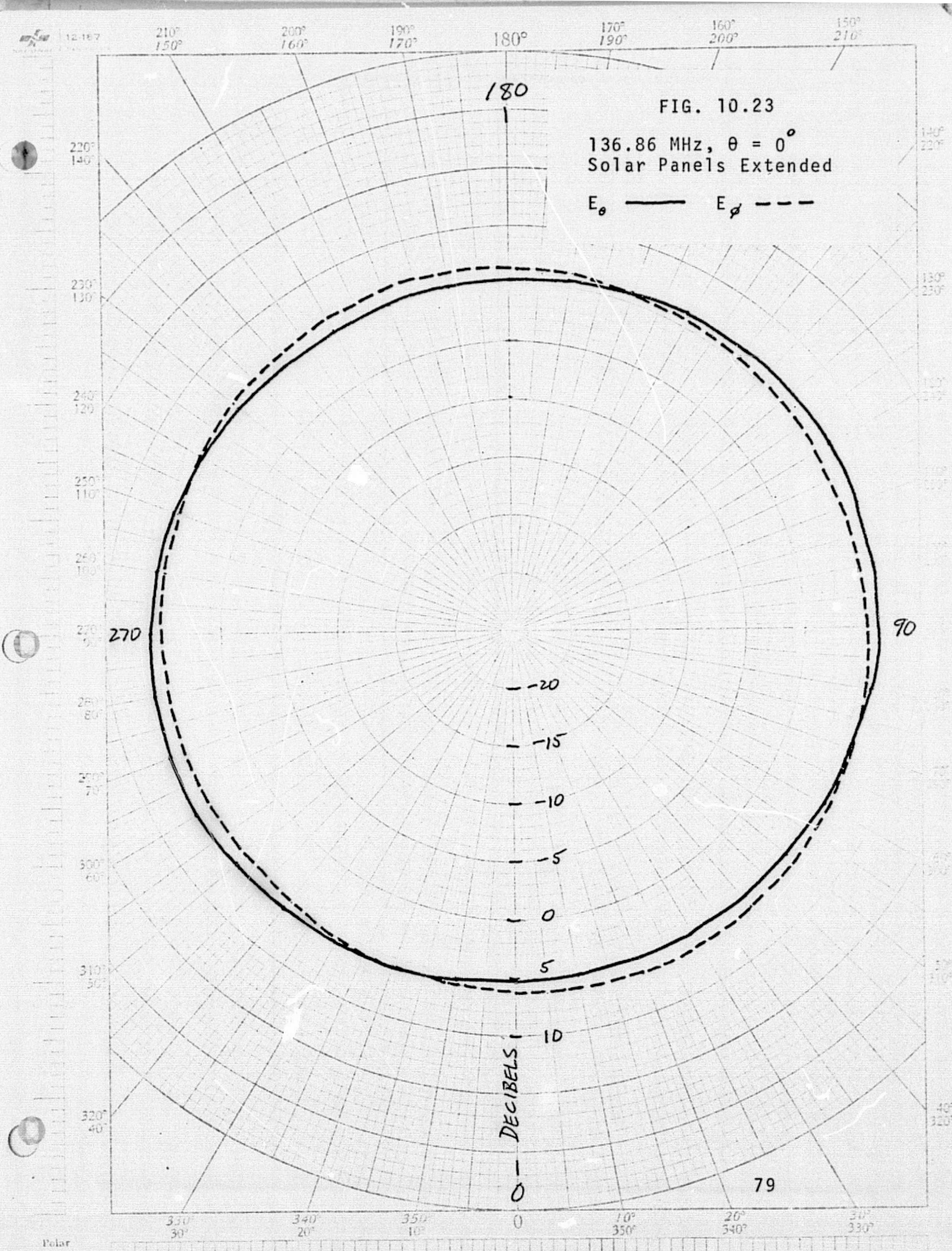
FIG. 10.23
136.86 MHz, θ = 0°
Solar Panels Extended
E_θ ——— E_ϕ - - -
180
270
90
0
-20
-15
-10
-5
0
5
10
DECIBELS
79

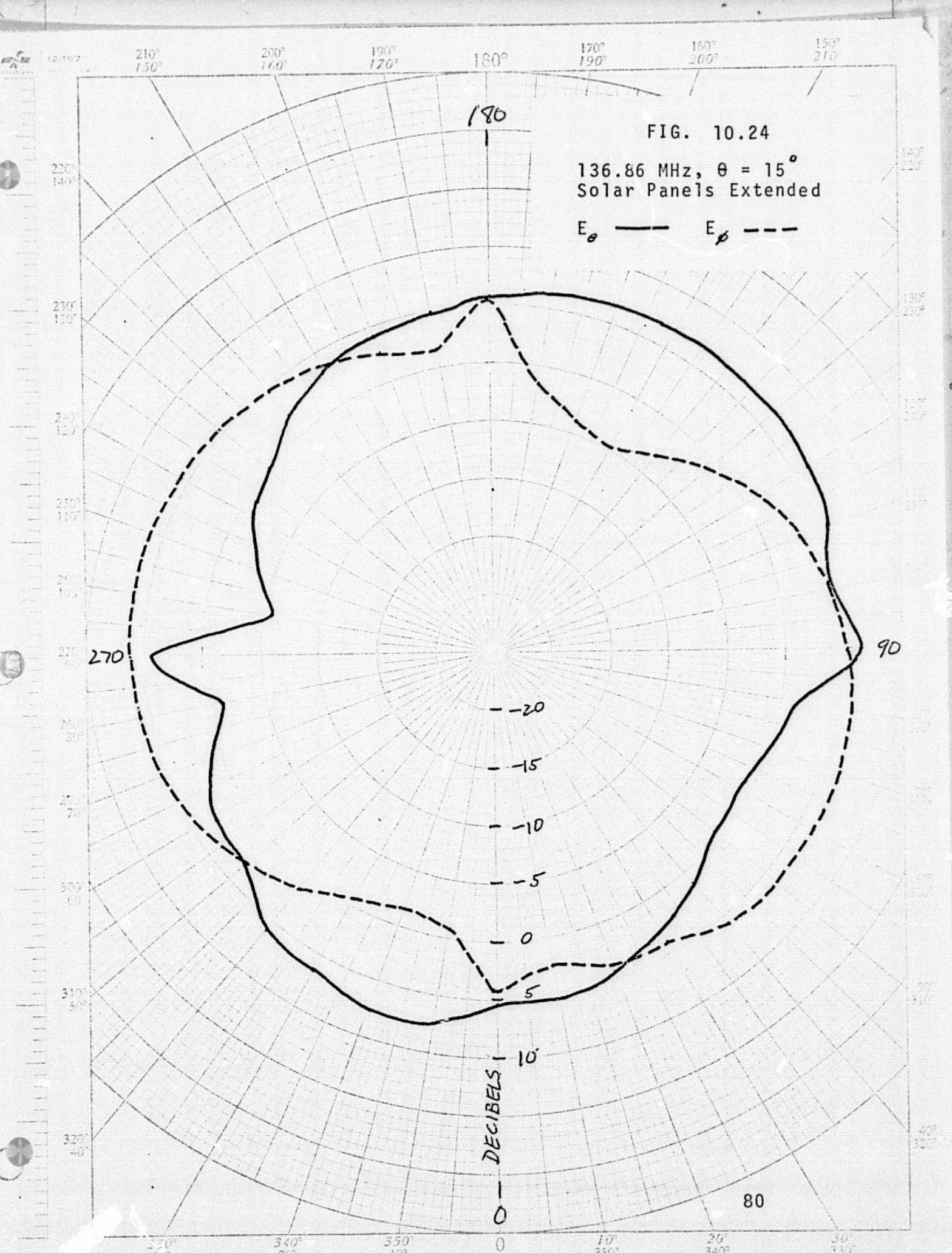

FIG. 10.24

136.86 MHz, $\theta = 15^{\circ}$
Solar Panels Extended

E_θ ——— E_ϕ - - -

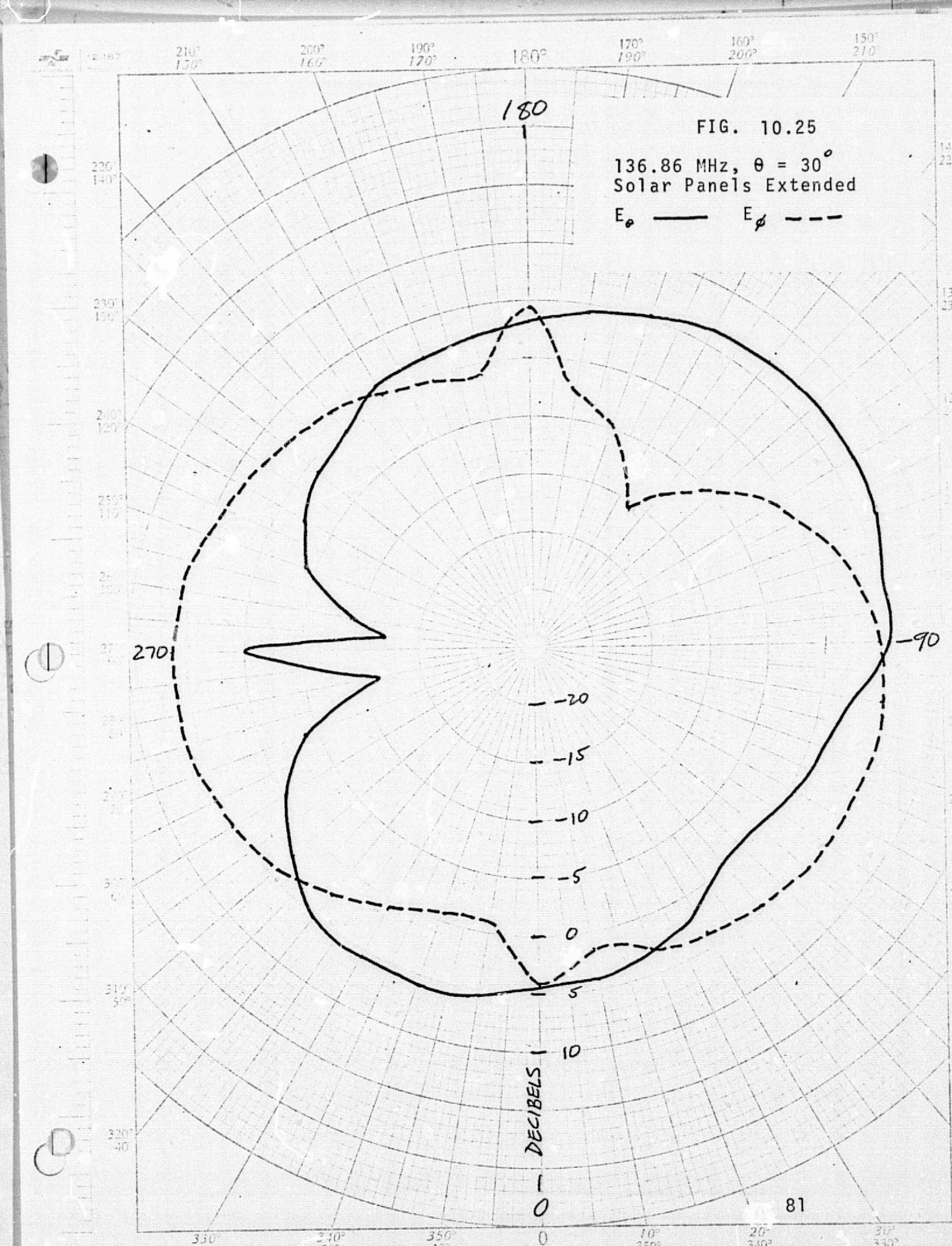

FIG. 10.25

136.86 MHz, $\theta = 30^{\circ}$
Solar Panels Extended

E_{θ} ——— E_{ϕ} - - -

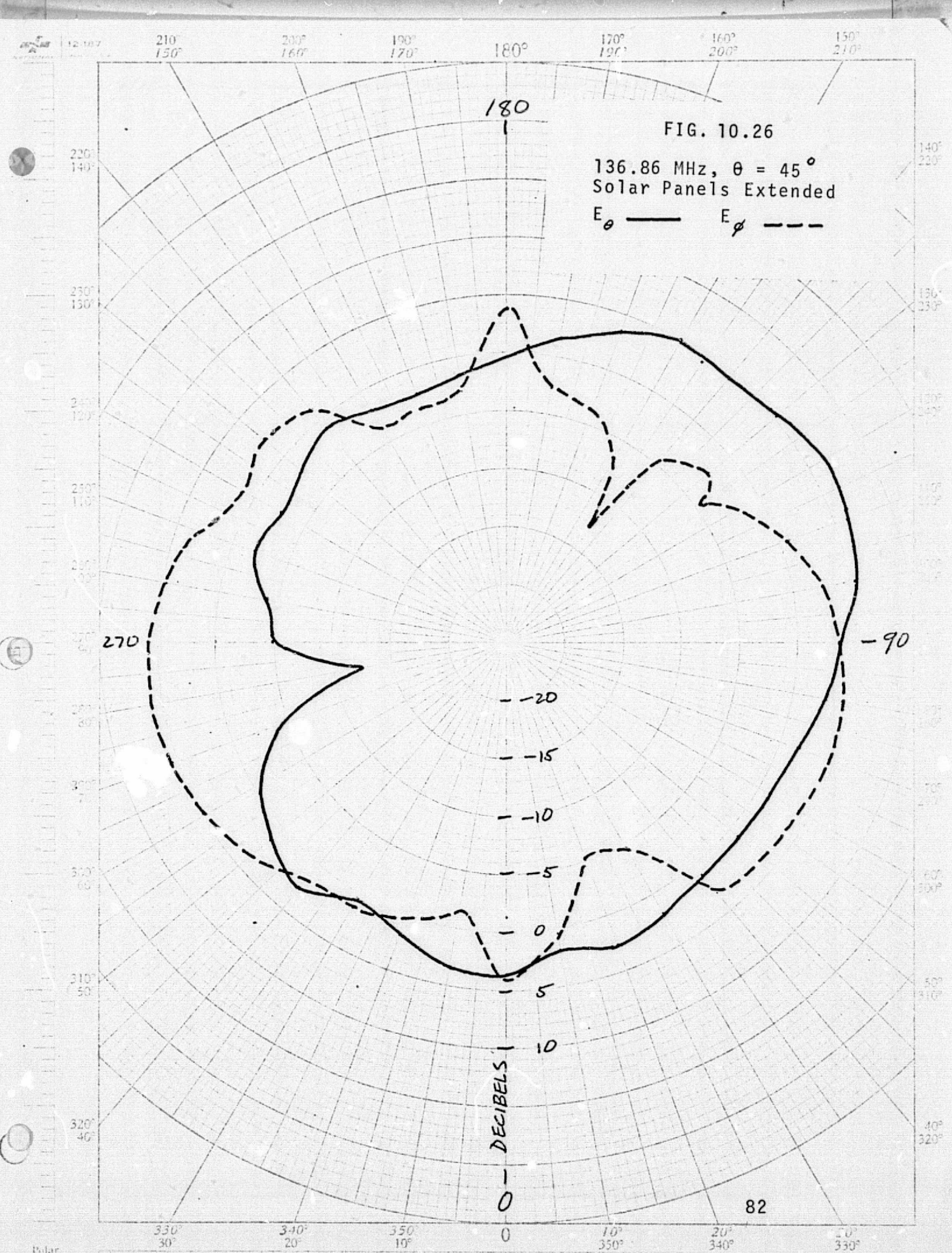

FIG. 10.26

136.86 MHz, $\theta = 45^\circ$
Solar Panels Extended
E_θ ——— E_ϕ – – –

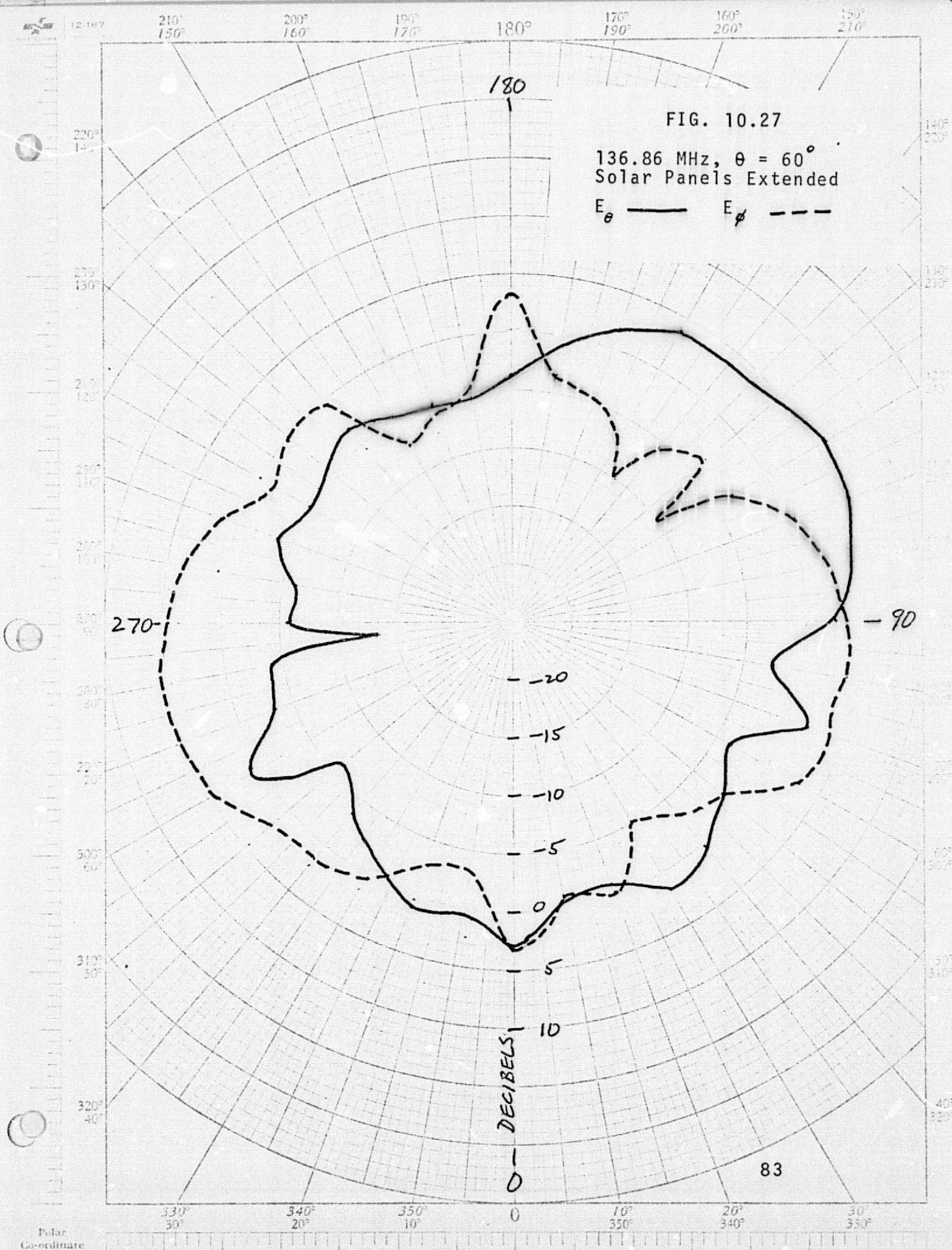

FIG. 10.27

136.86 MHz, $\theta = 60^\circ$
Solar Panels Extended

E_θ ——— E_ϕ - - -

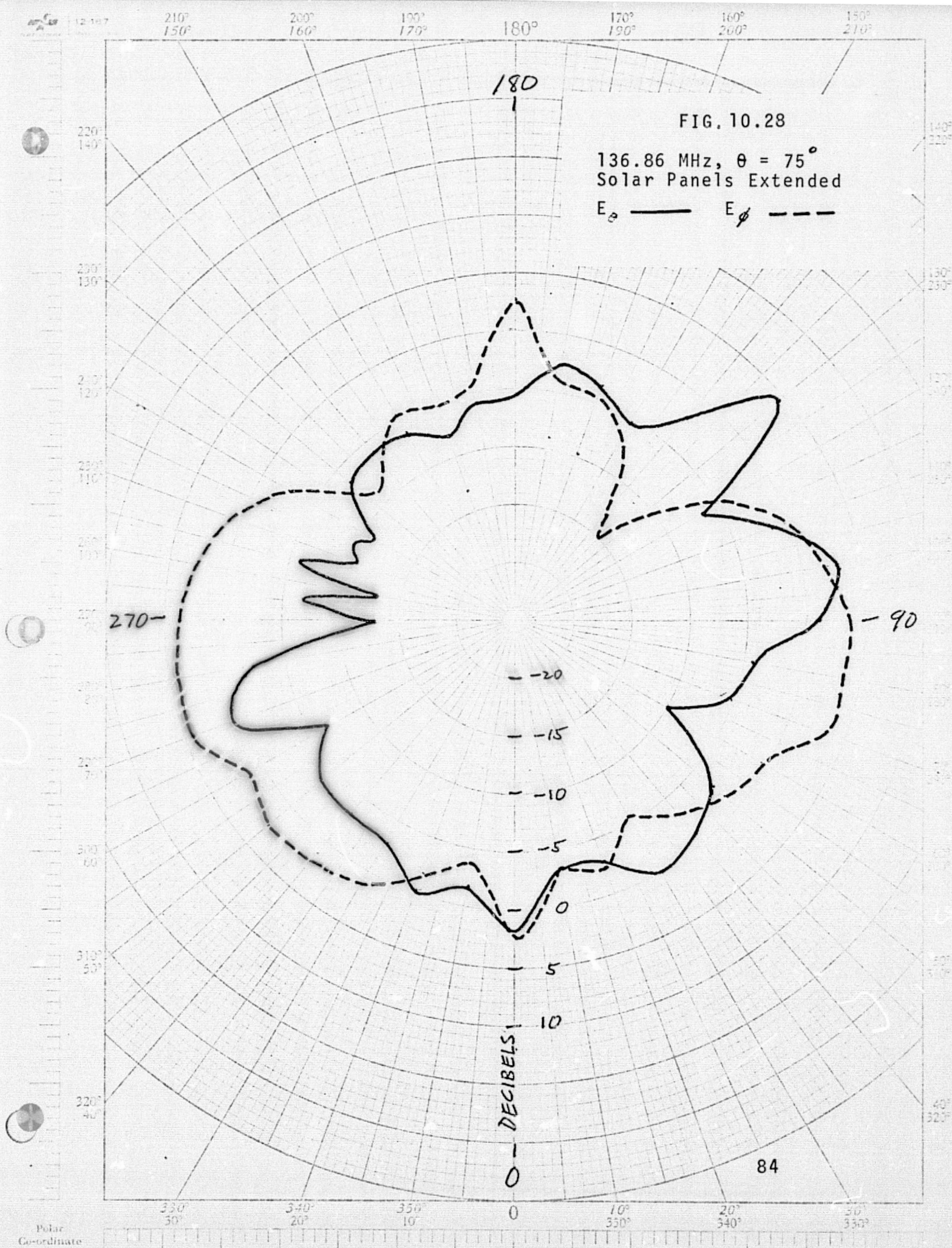

FIG. 10.28

136.86 MHz, $\theta = 75^{\circ}$
Solar Panels Extended

E_{θ} ——— E_{ϕ} - - -

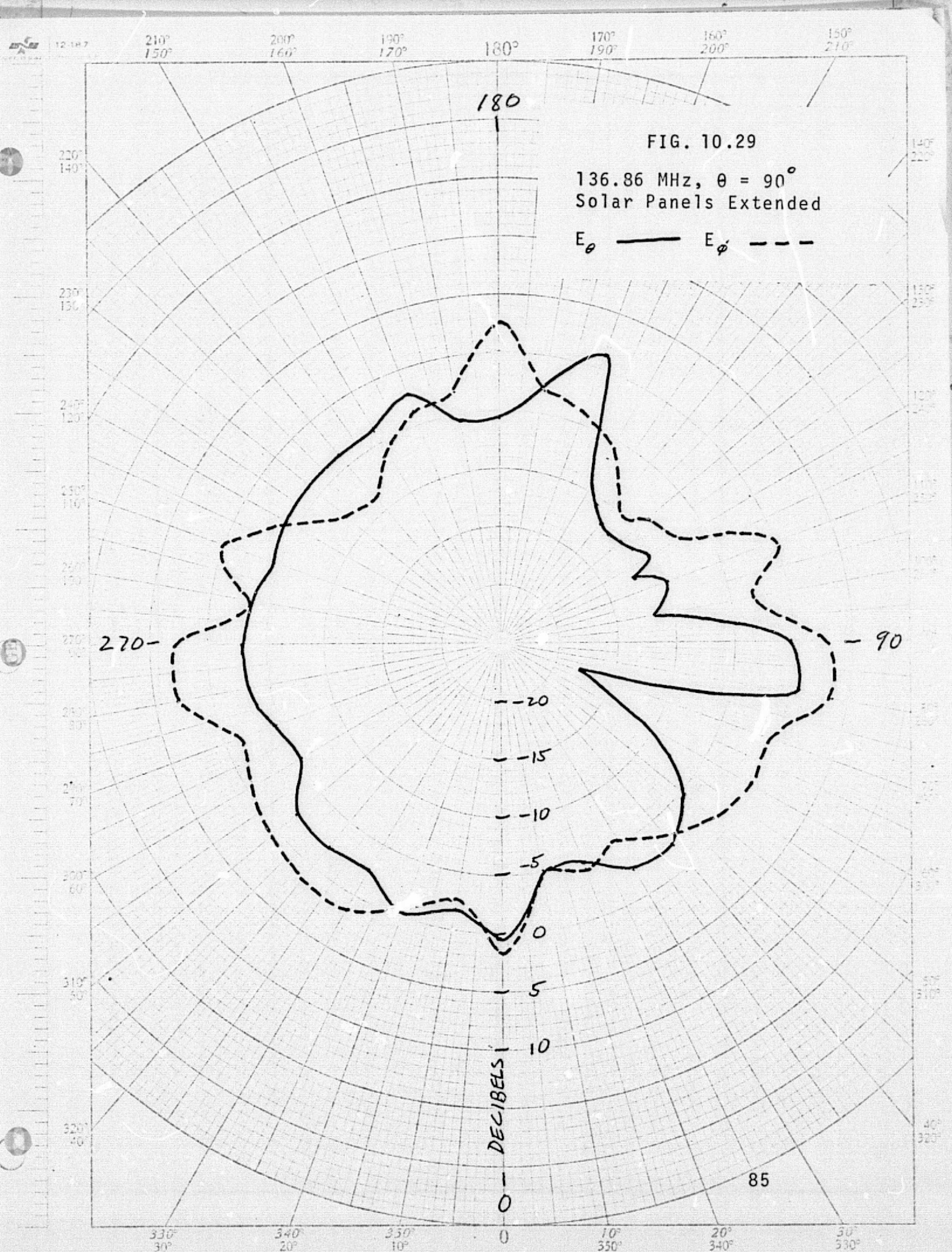
FIG. 10.29
136.86 MHz, θ = 90°
Solar Panels Extended
E_θ ——— E_ϕ - - -
180
270
90
0
-20
-15
-10
-5
0
5
10
DECIBELS
85

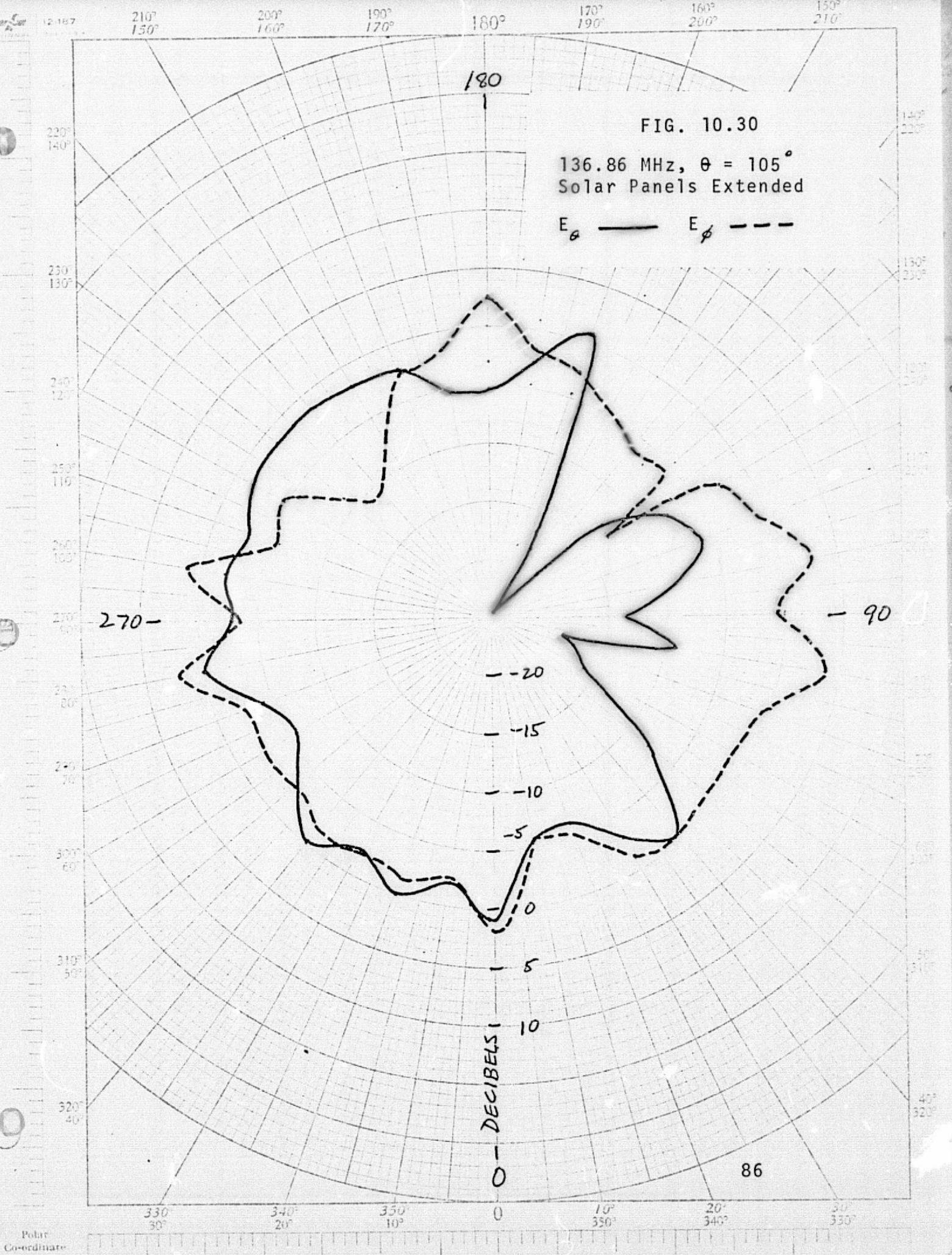

FIG. 10.30

136.86 MHz, θ = 105°
Solar Panels Extended

E_θ ——— E_ϕ - - -

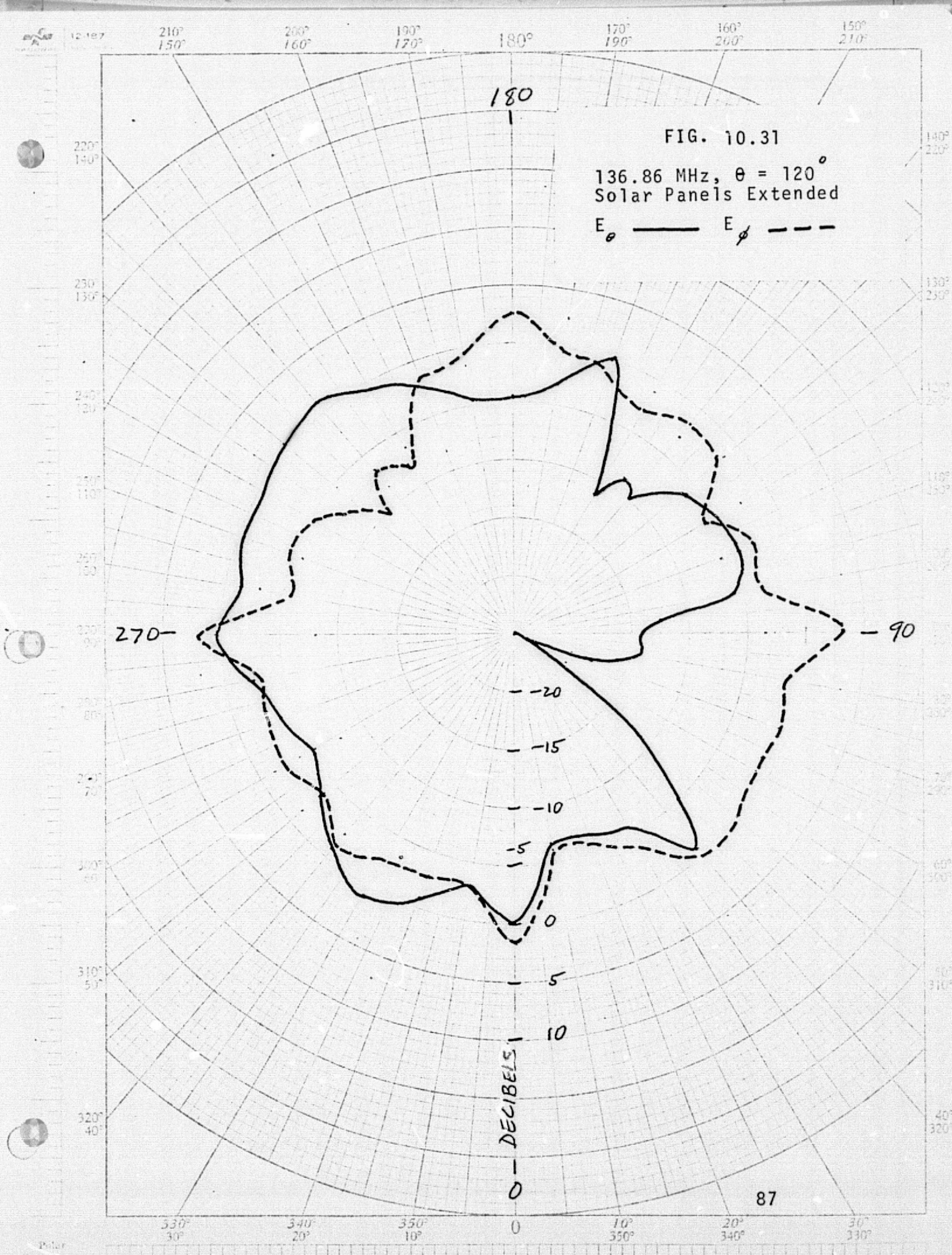

FIG. 10.31

136.86 MHz, $\theta = 120^{\circ}$
Solar Panels Extended

E_θ ——— E_ϕ - - -

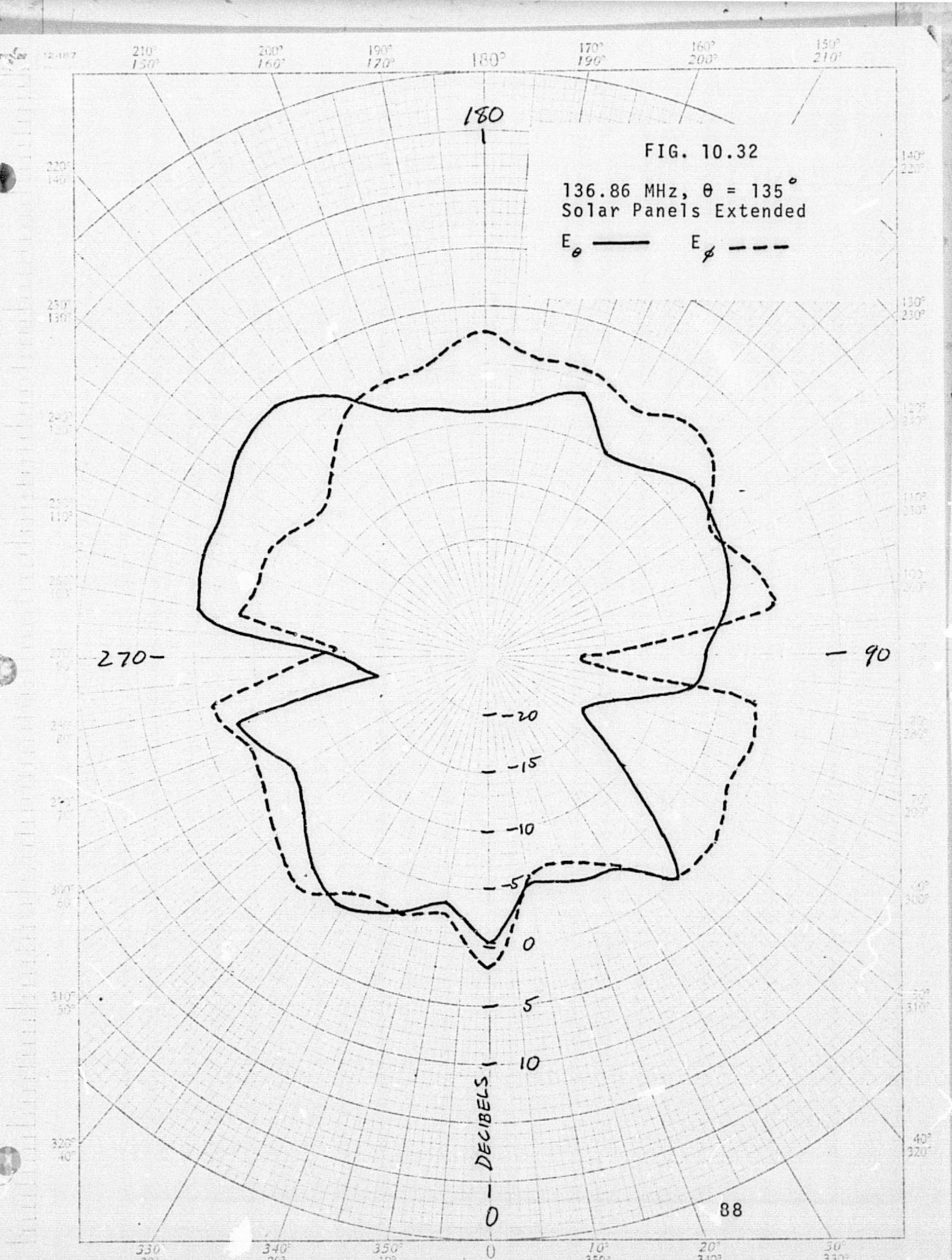

FIG. 10.32

136.86 MHz, θ = 135°
Solar Panels Extended

E_θ ——— E_ϕ - - -

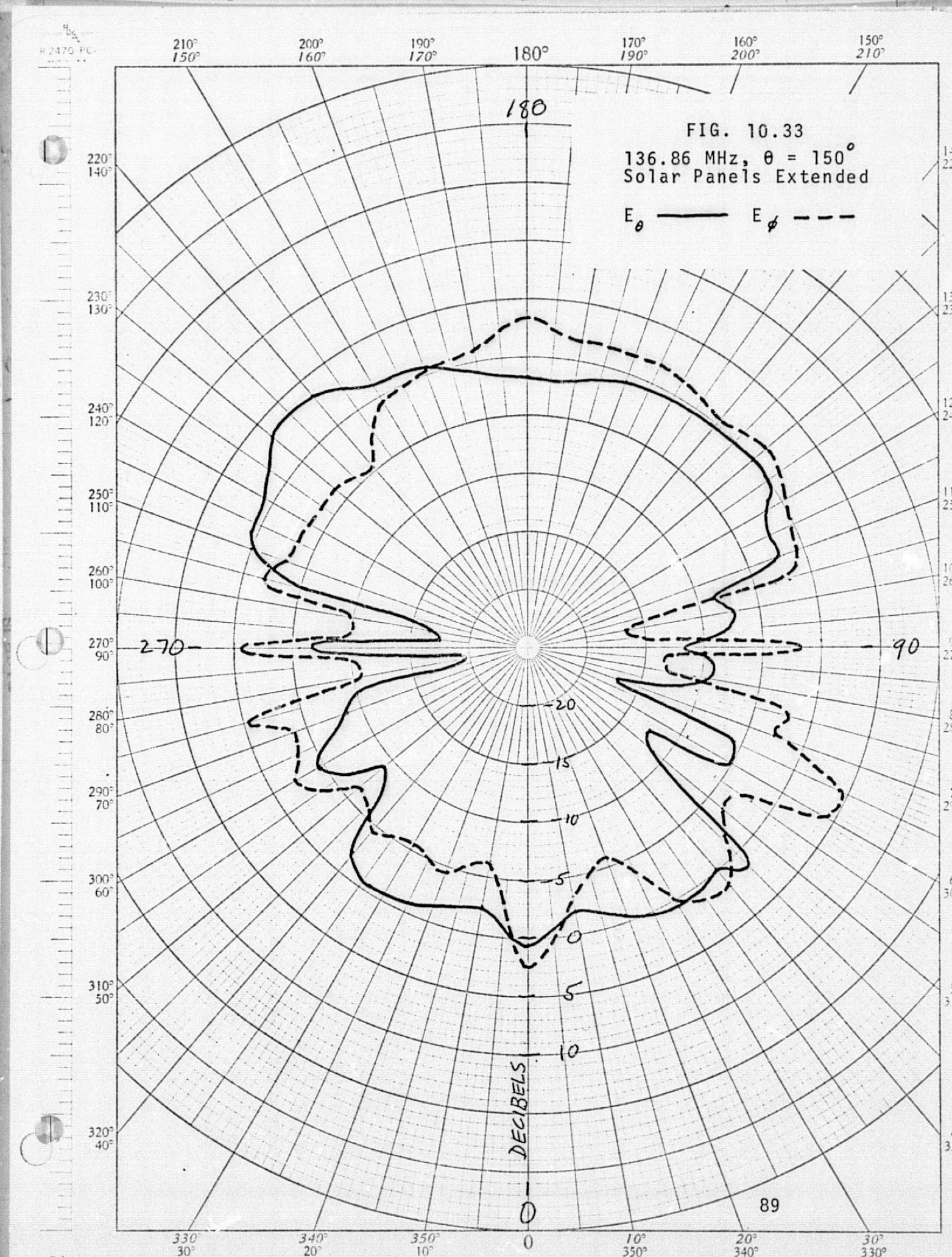
FIG. 10.33
136.86 MHz, θ = 150°
Solar Panels Extended
E_θ —— E_ϕ ---
180
270
90
0
-20
-15
-10
-5
0
5
10
DECIBELS
89

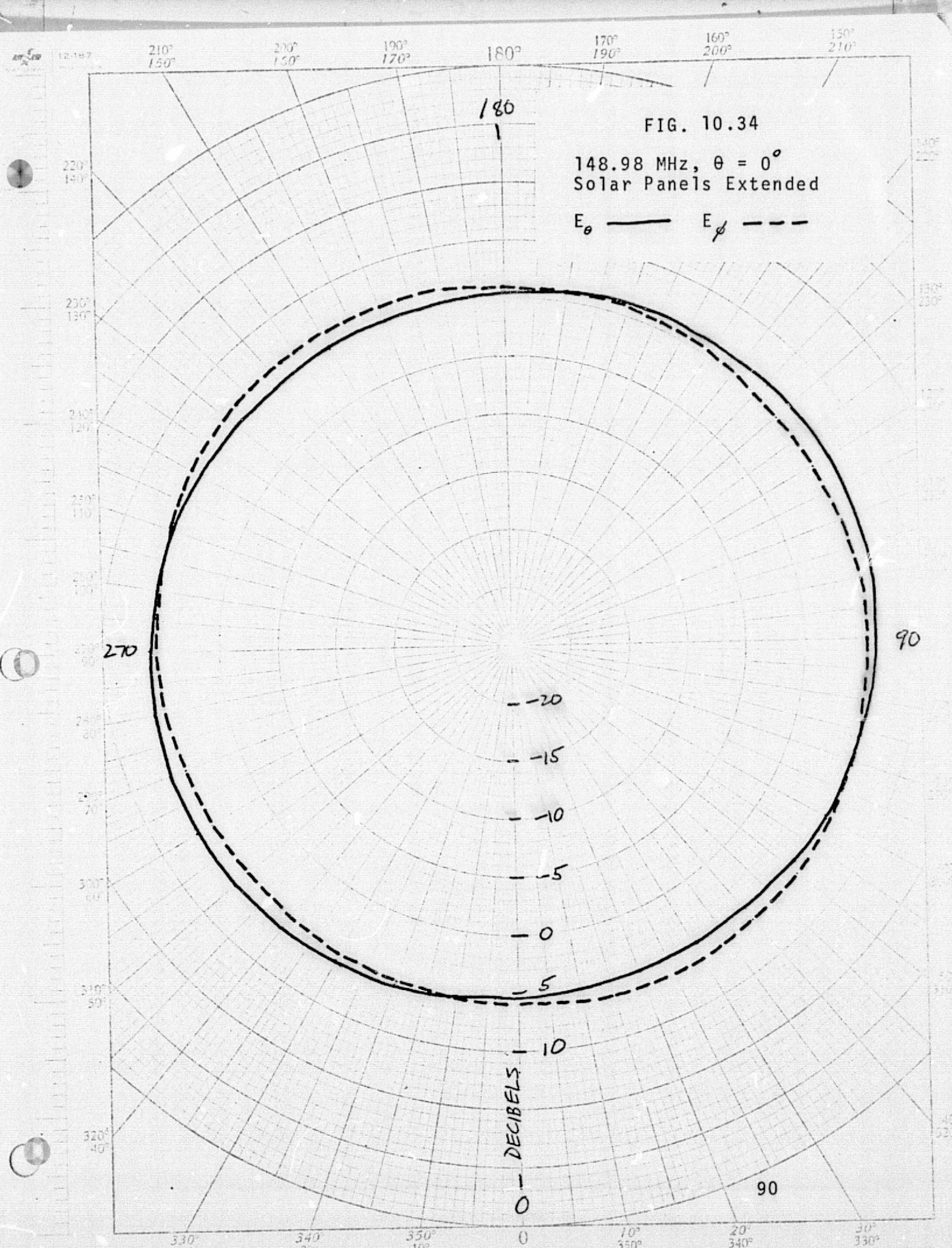

FIG. 10.34

148.98 MHz, $\theta = 0^{\circ}$
Solar Panels Extended

E_{θ} ——— E_{ϕ} - - -

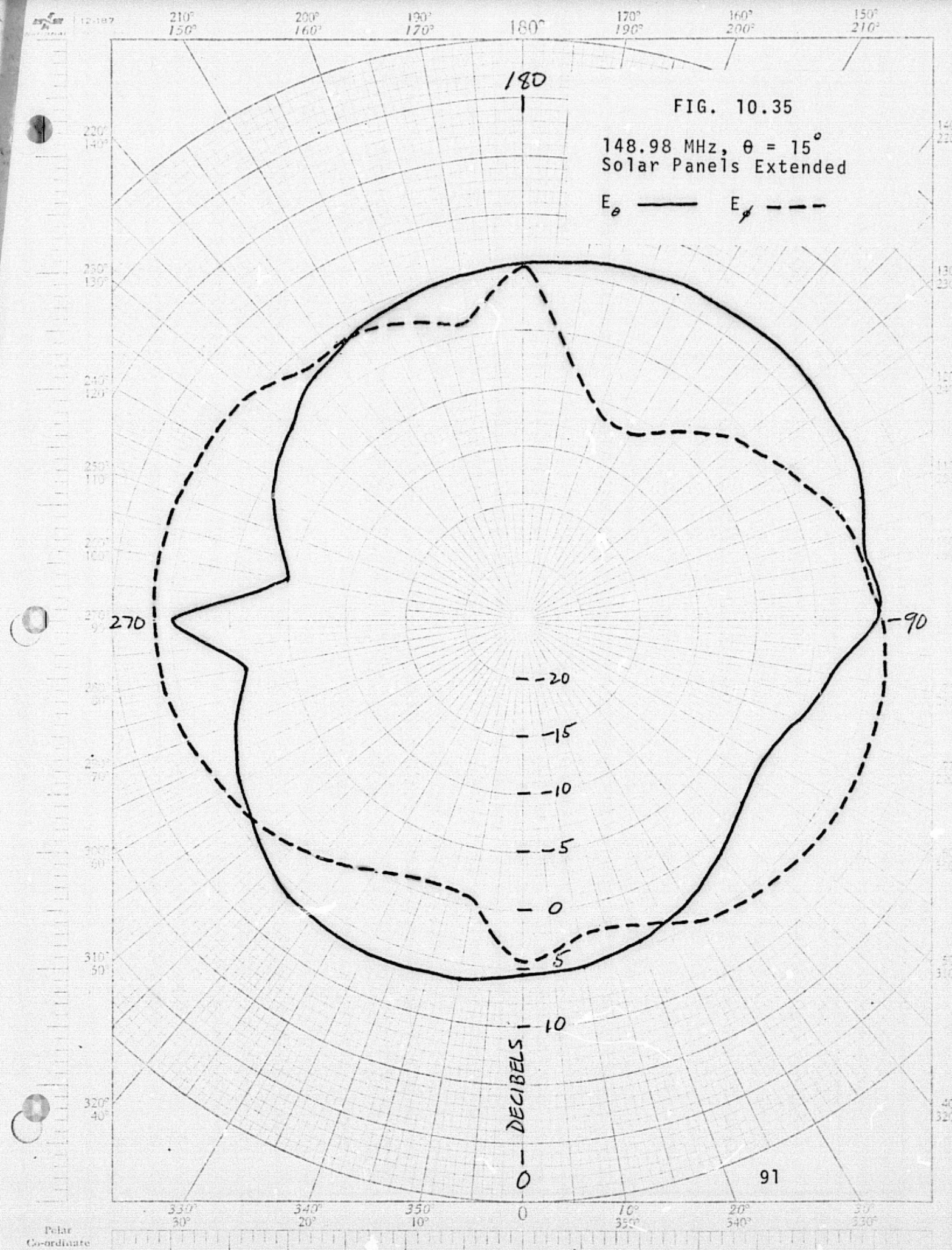

FIG. 10.35

148.98 MHz, θ = 15°
Solar Panels Extended

E_θ ——— E_ϕ - - -

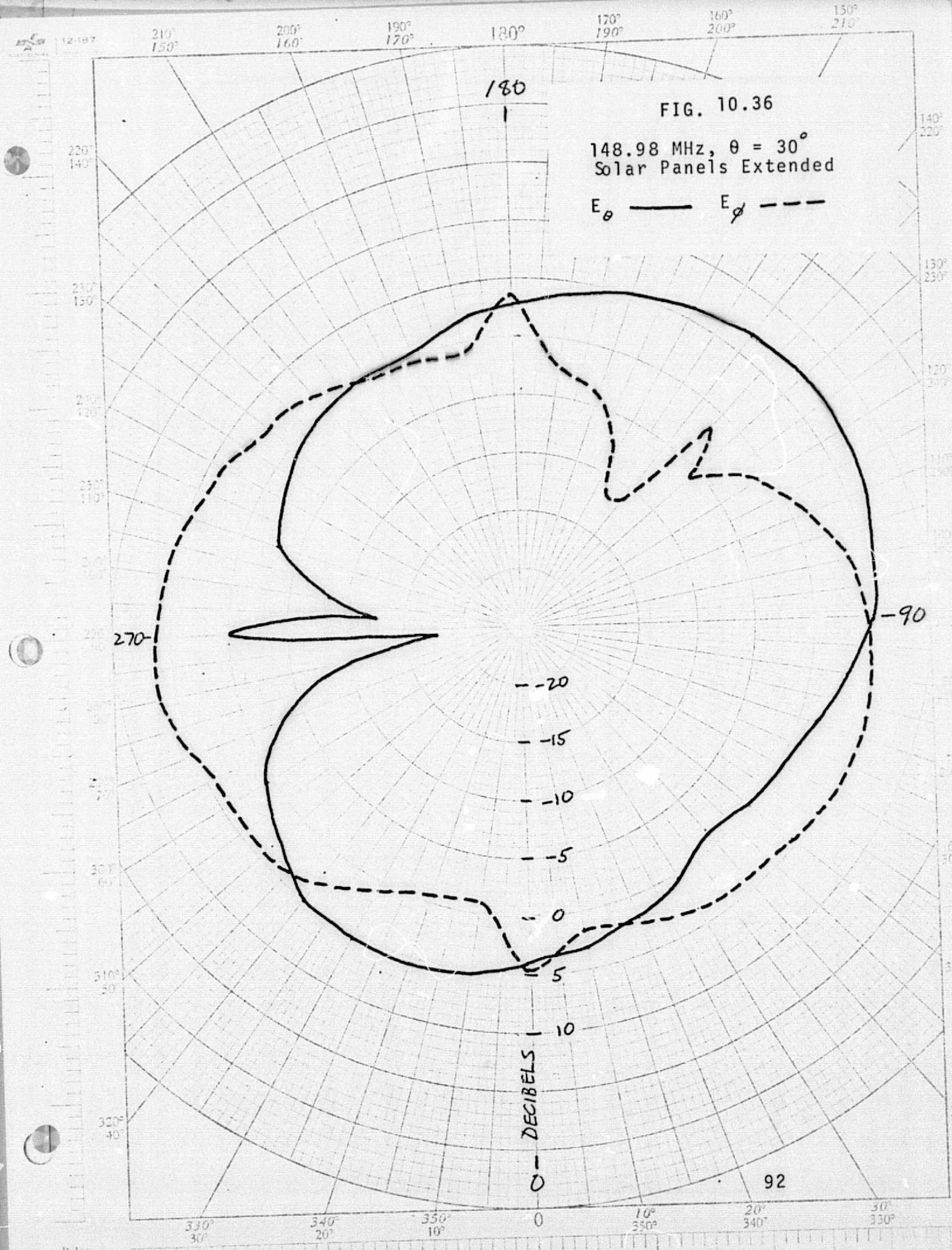
FIG. 10.36
148.98 MHz, θ = 30°
Solar Panels Extended
E_θ —— E_ϕ ---
180
270
90
0
-20
-15
-10
-5
0
5
10
DECIBELS
92

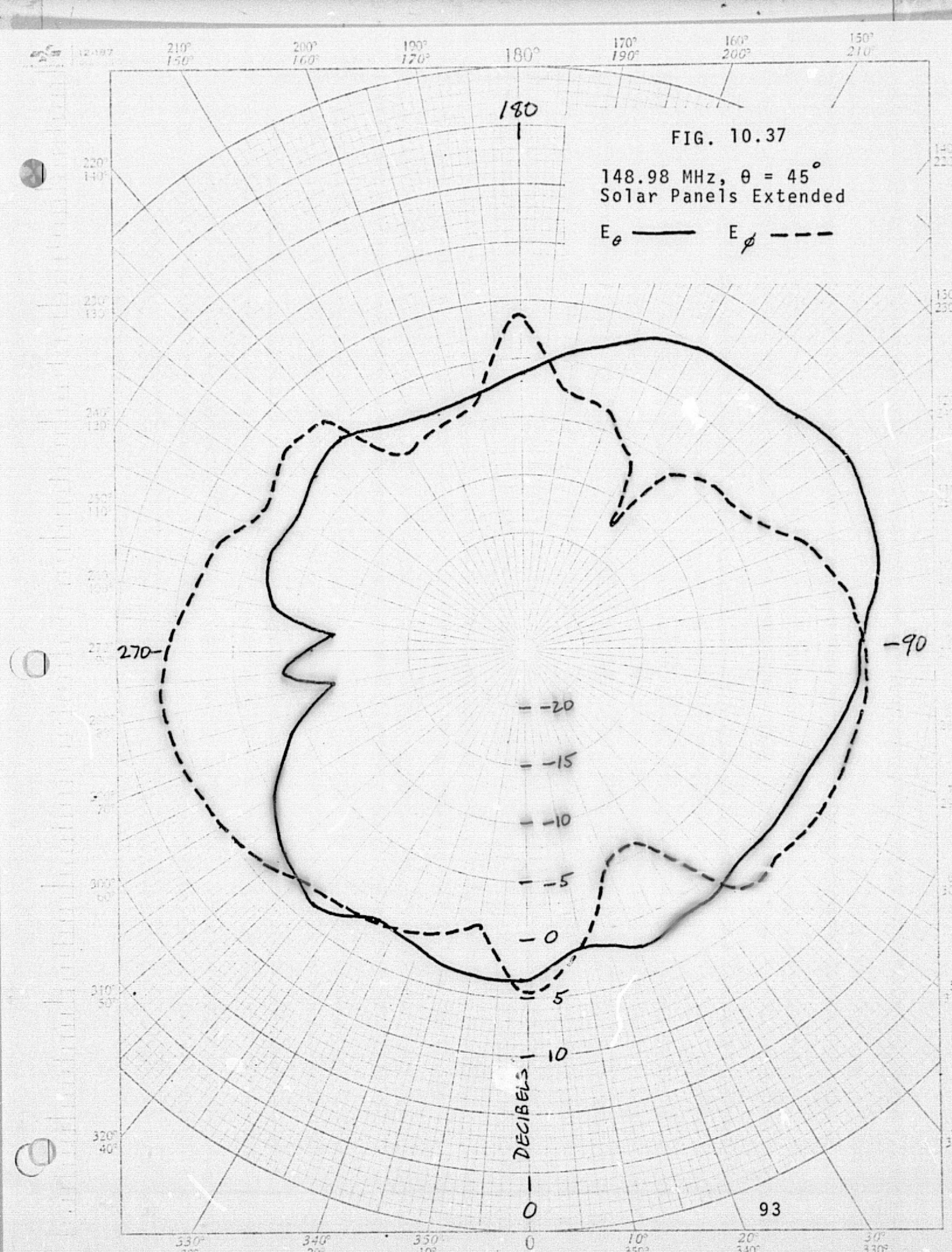

FIG. 10.37

148.98 MHz, $\theta = 45^\circ$
Solar Panels Extended

E_θ ——— E_ϕ - - -

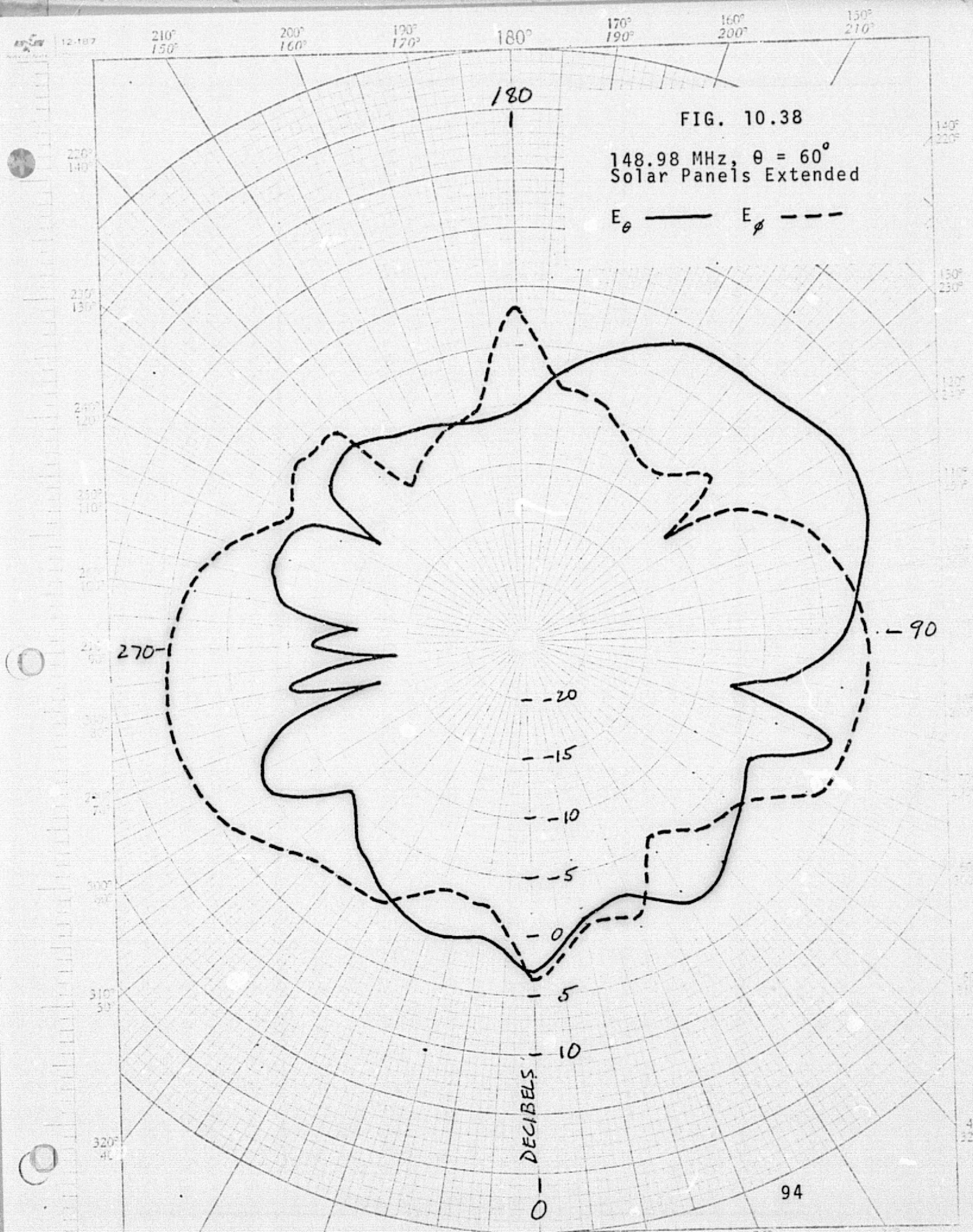

FIG. 10.38

148.98 MHz, $\theta = 60^{\circ}$
Solar Panels Extended

E_{θ} ——— E_{ϕ} - - -

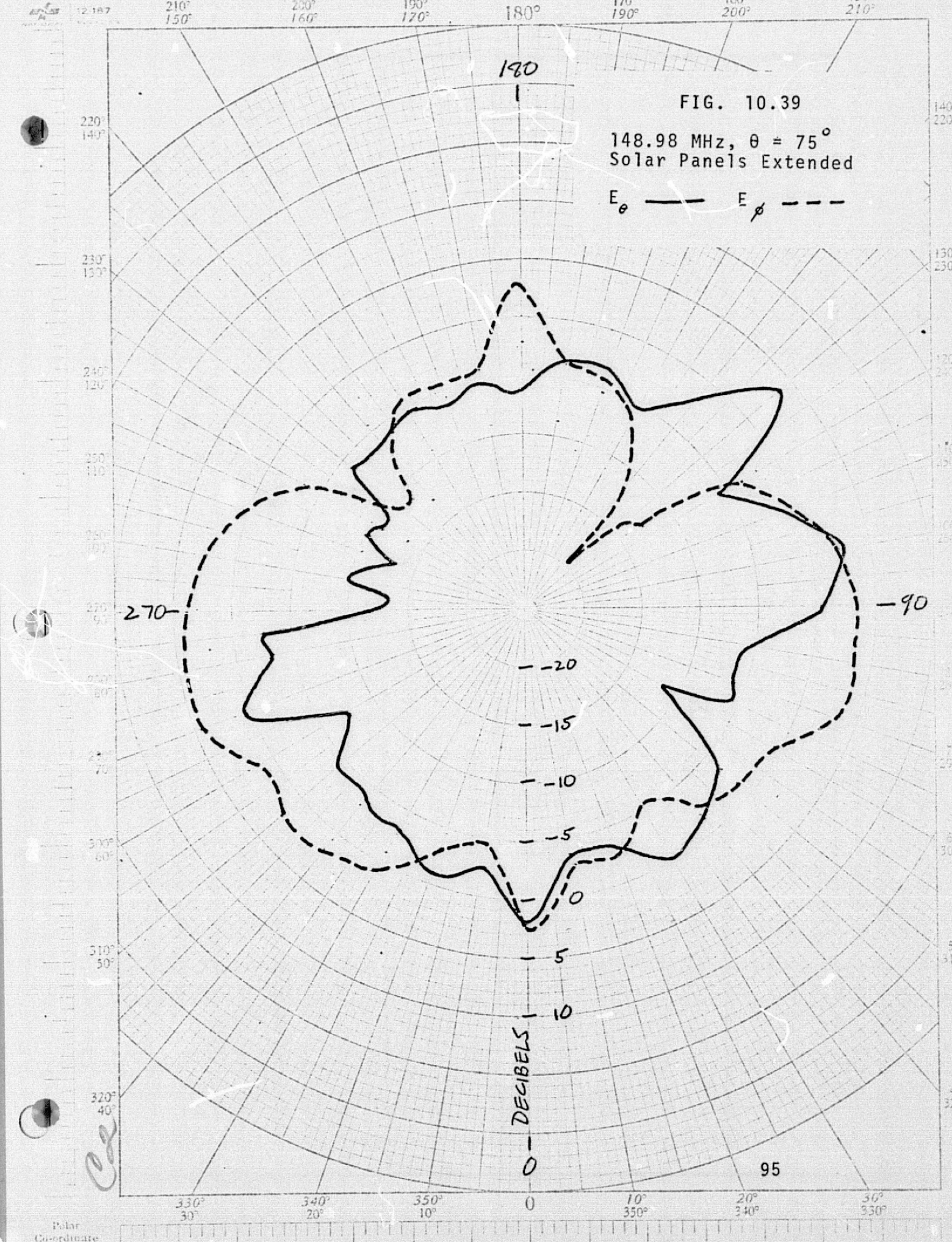

FIG. 10.39

148.98 MHz, $\theta = 75^\circ$
Solar Panels Extended

E_θ —— E_ϕ - - -

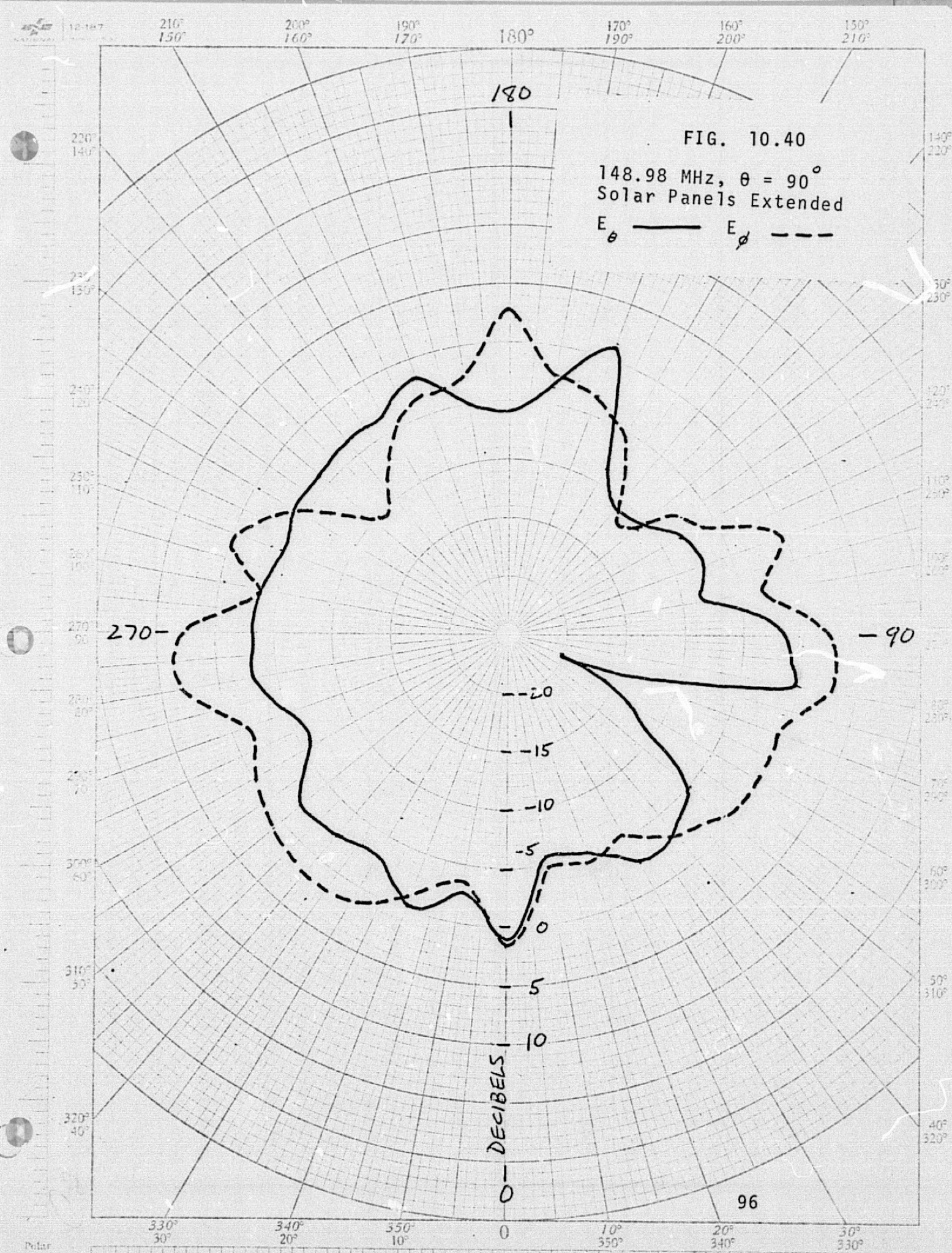

FIG. 10.40

148.98 MHz, $\theta = 90^{\circ}$
Solar Panels Extended
E_{θ} ——— E_{ϕ} - - -

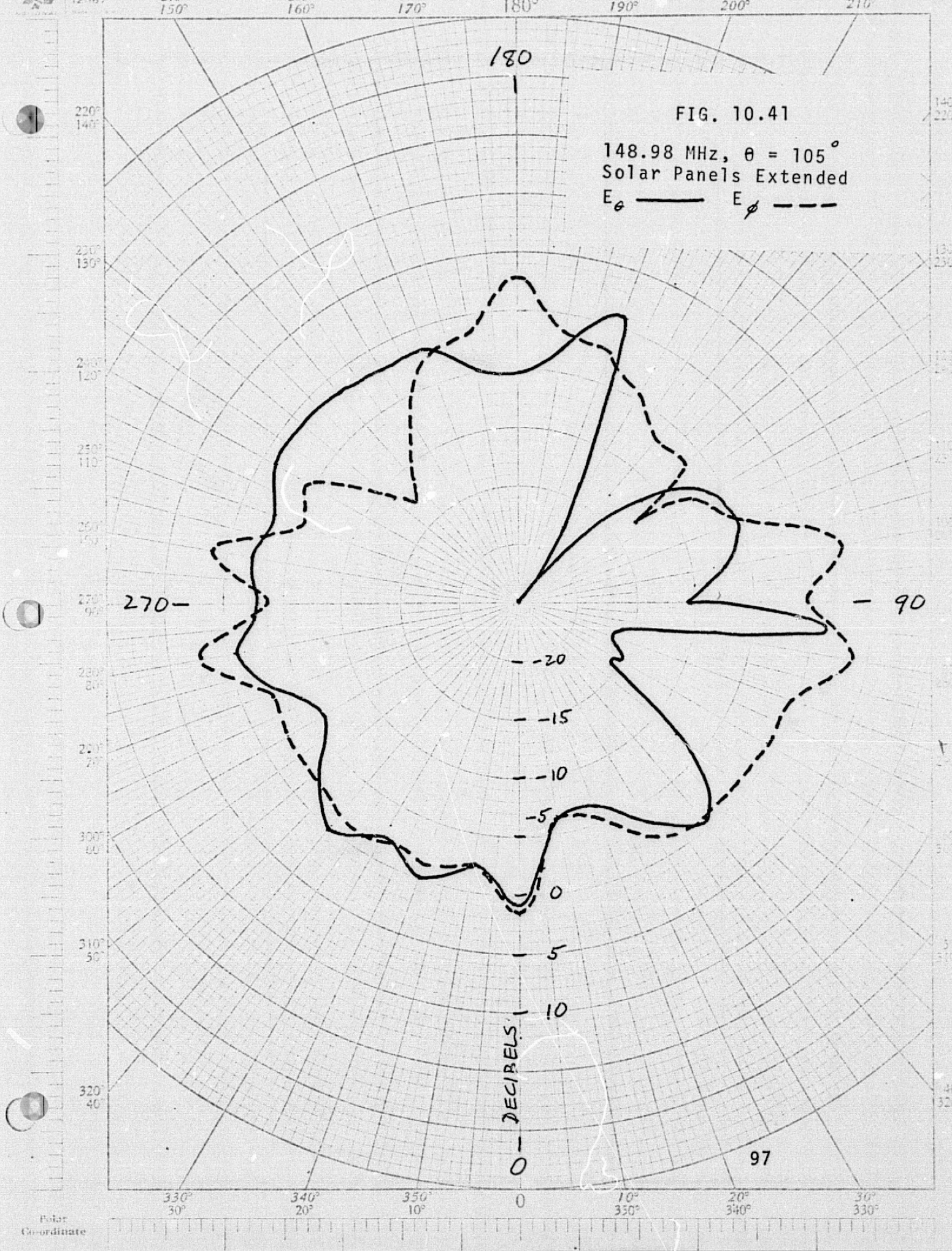
180
270
90
0
-20
-15
-10
-5
0
5
10
DECIBELS
FIG. 10.41
148.98 MHz, θ = 105°
Solar Panels Extended
E_θ ——— E_ϕ - - -
97
Polar Co-ordinate

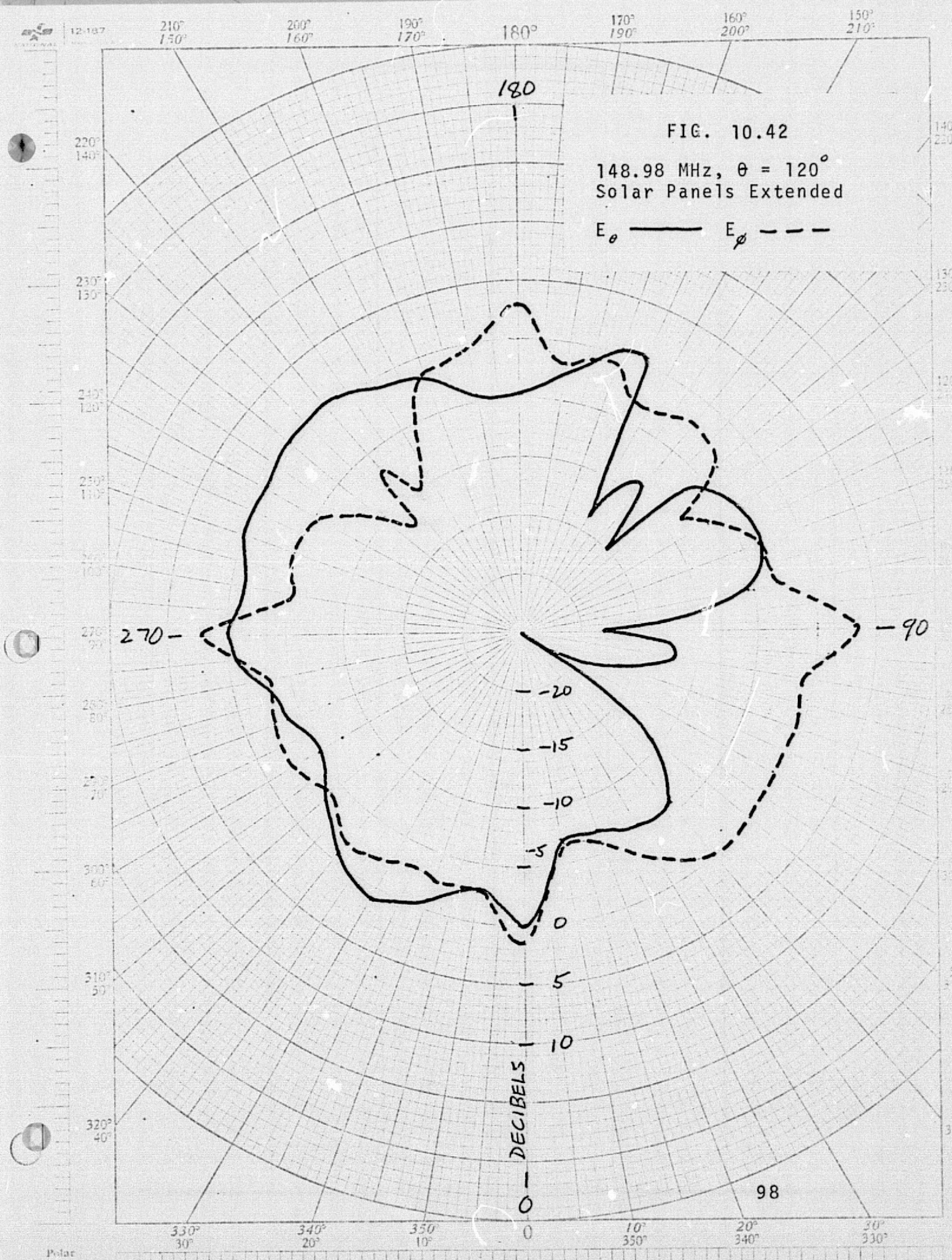
FIG. 10.42
148.98 MHz, θ = 120°
Solar Panels Extended
E_θ ——— E_ϕ - - -
180
270
90
0
-20
-15
-10
-5
0
5
10
DECIBELS
98

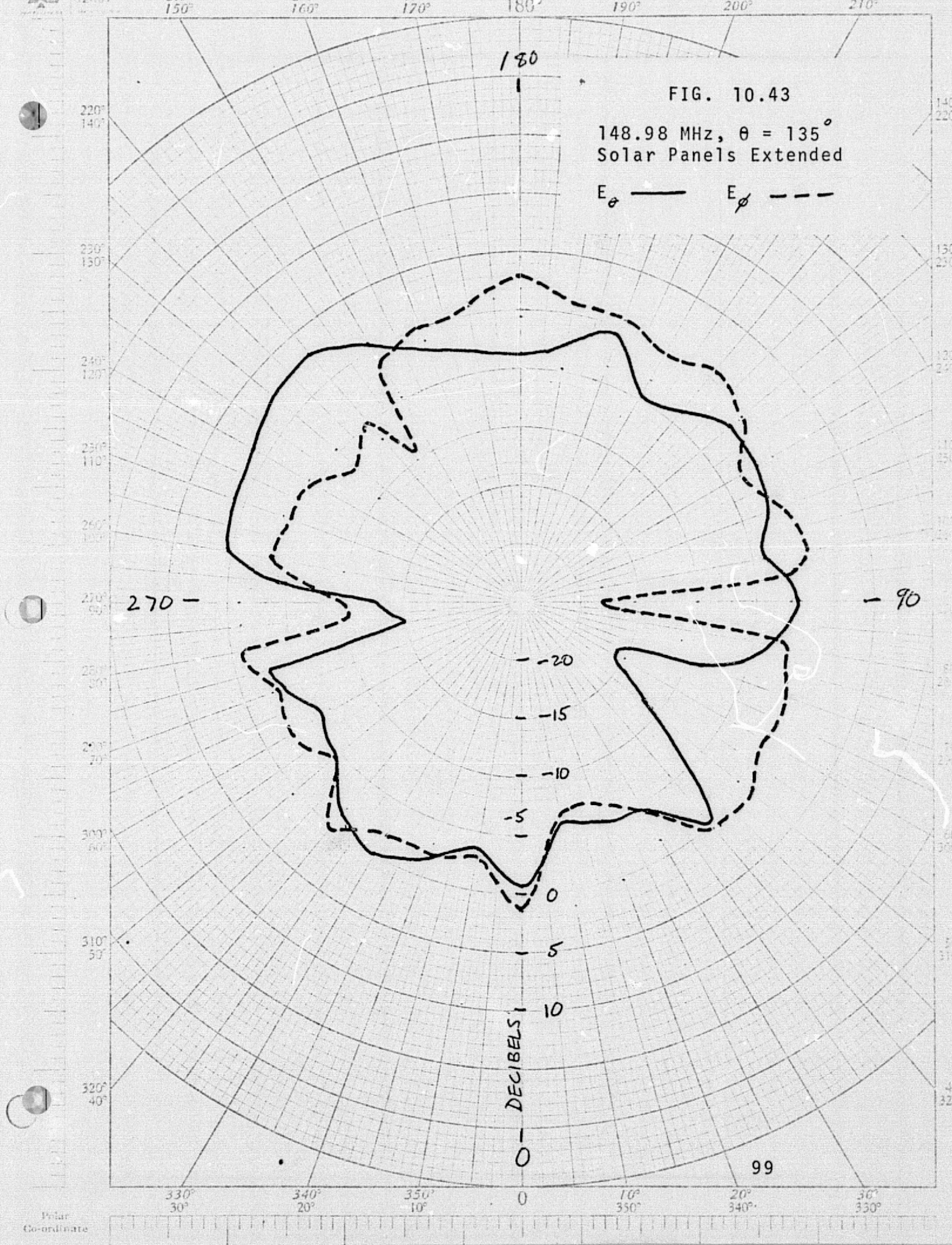

FIG. 10.43

148.98 MHz, θ = 135°
Solar Panels Extended

E_θ ——— E_ϕ - - -

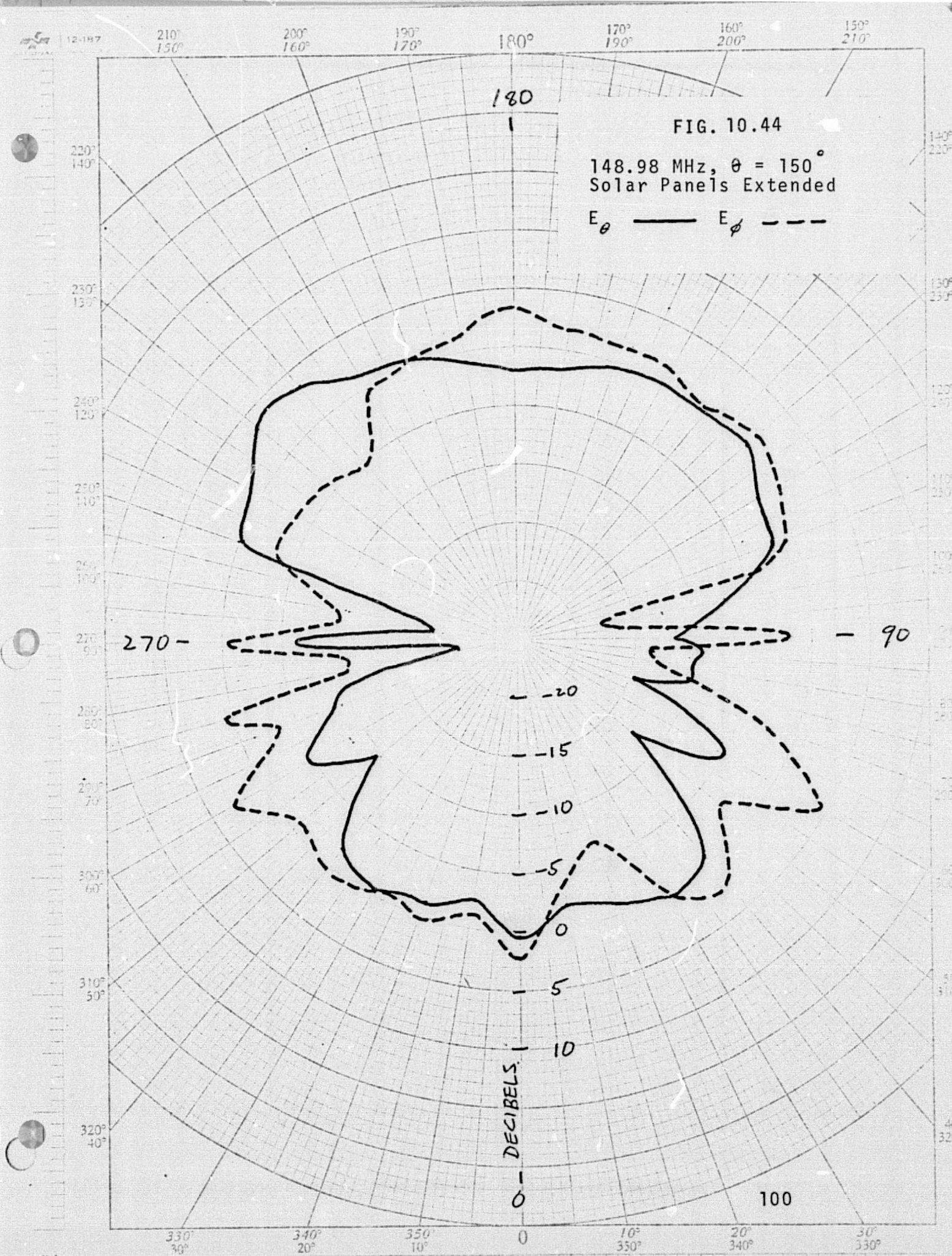
FIG. 10.44
148.98 MHz, θ = 150°
Solar Panels Extended
E_θ —— E_ϕ - - -
180
270
90
0
-20
-15
-10
-5
0
5
10
DECIBELS
100

11. References

1. Albertsen, N.C., Christiansen, P.L., Hansen, J.E., and Jensen, N.E. "Methods of Evaluating the Influence of Spacecraft Structures on Antenna Radiation Patterns." Tech. Univ. of Denmark Lab. of Electromagnetic Theory Rept. ESRO CR-51. (April, 1972) N72-30158.

2. Albertsen, N.C., Hansen,J.E., and Jensen, N.E. "Computation of Radiation from Wire Antennas on Conducting Bodies." IEEE Trans. Antennas and Propagation (March, 1974) pp. 200-6.

3. Carter, P.S. "Antenna Arrays Around Cylinders." Proc. IRE, 31, p. 671.

4. Chu, L.J. "Physical Limitations of Omnidirectional Antennas." J. Applied Physics. (December, 1948) pp. 1163-75.

5. Forgan, D.H. "Calculation of the Performance of HF Aerials Mounted on Aircraft." Royal Aircraft Establishment Rept. 74077. (June 10, 1974)

6. Green, K.A., Wood, J.R., Galindo, V. "Quasi Isotropic Spacecraft Antenna System." Dalmo Victor Rept. 65-430. (Nov. 5, 1964) N66-12183.

7. Gregorwich, W.S. "A Tangential Turnstile Antenna for Spacecraft." 1974 International IEEE/AP-S Symposium Record, pp. 207-9.

8. Jackson, R.B. "The Canted Turnstile as an Omnidirectional Spacecraft Antenna System." (1967) N67-37172.

9. Kravtsova, G.V. "Mutual Influence of Elementary Dipoles Lying Near Circular Ideally Conducting Intersecting Cylinders." Telecommunications and Radio Engineering (Sept., 1970) pp. 89-93.

10. Kravtsov, V.A. "The Field of a Radial Electric Dipole Located Close to an Ideally Conducting Circular Cylinder." Telecommunications and Radio Engineering (Aug., 1973) pp. 93-98.

11. Lucke, W.S. "Electric Dipoles in the Presence of Elliptic and Circular Cylinders." J. Applied Physics (Jan., 1951) pp. 14-19.

12. Mathis, H.F. "A Short Proof that an Isotropic Antenna is Impossible," Proc. IRE (Aug., 1951) p. 970.

13. Mathis, H.F. "On Isotropic Antennas." Proc. IRE (Dec., 1954) p. 1810.

14. Senior, T.B.A. "Analytical Studies of Relationships between Far Field Radiation Patterns and Near Field Current Distribution and Surface Configurations, including Consideration of the Effects of Small Vehicle on Antenna Performance." Univ. of Mich. Rad. Lab. Rept. CR-55191. N64-13336.

15. Woodward, O.M. "A Mode Analysis of Quasi-Isotropic Antennas." RCA Review (March, 1965) pp. 42-74.

16. Knight, B. A., "Methods of Calculating the Horizontal Radiation Patterns of Dipole Arrays Around a Support Mast." Proc. IEE (Nov., 1958) Part III, pp. 548-554.

17. Moullin, E.B., "On the Current Induced in a Conducting Ribbon by a Current Filament Parallel to It." Proc. IEE. (Aug., 1953) Part IV, p. 7.

18. Kouyoumijian, R.G. "The Geometrical Theory of Diffraction and Applications." Numerical Techniques for Antennas and Electromagnetics. Course offered at UCLA, June, 1973.

19. Schelkunoff, S.A. Advanced Antenna Theory. Wiley, 1952.